CHAPTER 4

Stratospheric Changes and Climate

Coordinating Lead Authors:
P.M. Forster
D.W.J. Thompson

Lead Authors:
M.P. Baldwin
M.P. Chipperfield
M. Dameris
J.D. Haigh
D.J. Karoly
P.J. Kushner
W.J. Randel
K.H. Rosenlof
D.J. Seidel
S. Solomon

Coauthors:
G. Beig
P. Braesicke
N. Butchart
N.P. Gillett
K.M. Grise
D.R. Marsh
C. McLandress
T.N. Rao
S.-W. Son
G.L. Stenchikov
S. Yoden

Contributors:
E.C. Cordero
M.P. Free
A.I. Jonsson
J. Logan
D. Stevenson

CHAPTER 4

STRATOSPHERIC CHANGES AND CLIMATE

Contents

SCIENTIFIC SUMMARY

- **Stratospheric climate trends since 1980 are better understood and characterized than in previous Assessments and continue to show the clear influence of both human and natural factors.**

  - **New analyses of both satellite and radiosonde data give increased confidence relative to previous Assessments of the complex time/space evolution of stratospheric temperatures between 1980 and 2009.** The global-mean lower stratosphere cooled by 1–2 K and the upper stratosphere cooled by 4–6 K from 1980 to about 1995. There have been no significant long-term trends in global-mean lower-stratospheric temperatures since about 1995. The global-mean lower-stratospheric cooling did not occur linearly but was manifested as downward steps in temperature in the early 1980s and the early 1990s. The cooling of the lower stratosphere included the tropics and was not limited to extratropical regions as previously thought.

  - **The complex evolution of lower-stratospheric temperature is influenced by a combination of natural and human factors that has varied over time.** Ozone decreases dominate the lower-stratospheric cooling over the long term (since 1980). Major volcanic eruptions and solar activity have clear shorter-term effects. Since the mid-1990s, slowing ozone loss has contributed to the lack of temperature trend. Models that consider all of these factors are able to reproduce this complex temperature time history.

  - **The largest lower-stratospheric cooling continues to be found in the Antarctic ozone hole region during austral spring and early summer.** The cooling due to the ozone hole strengthened the Southern Hemisphere polar stratospheric vortex compared with the pre-ozone hole period during these seasons.

  - **Tropical lower-stratospheric water vapor amounts decreased by roughly 0.5 parts per million by volume (ppmv) around 2000 and remained low through 2009.** This followed an apparent but uncertain increase in stratospheric water vapor amounts from 1980–2000. The mechanisms driving long-term changes in stratospheric water vapor are not well understood.

  - **Stratospheric aerosol concentrations increased by between 4 to 7% per year, depending on location, from the late 1990s to 2009.** The reasons for the increases in aerosol are not yet clear, but small volcanic eruptions and increased coal burning are possible contributing factors.

- **There is new and stronger evidence for radiative and dynamical linkages between stratospheric change and specific changes in surface climate.**

  - **Changes in stratospheric ozone, water vapor, and aerosols all radiatively affect surface temperature.** The radiative forcing of climate in 2008 due to stratospheric ozone depletion (-0.05 ± 0.1 Watts per square meter [W/m^2]) is much smaller than the positive radiative forcing due to the chlorofluorocarbons (CFCs) and hydrochlorofluorocarbons (HCFCs) largely responsible for that depletion ($+0.31 \pm 0.03$ W/m^2). Radiative calculations and climate modeling studies suggest that the radiative effects of variability in stratospheric water vapor (roughly ± 0.1 W/m^2 per decade) can contribute to decadal variability in globally averaged surface temperature. Climate models and observations show that the negative radiative forcing from a major volcanic eruption such as Mt. Pinatubo in 1991 (roughly -3 W/m^2) can lead to a surface cooling that persists for about two years.

  - **Observations and model simulations show that the Antarctic ozone hole caused much of the observed southward shift of the Southern Hemisphere middle latitude jet in the troposphere during summer since 1980.** The horizontal structure, seasonality, and amplitude of the observed trends in the Southern Hemisphere tropospheric jet are only reproducible in climate models forced with Antarctic ozone depletion. The southward shift in the tropospheric jet extends to the surface of the Earth and is linked dynamically to the ozone hole-induced strengthening of the Southern Hemisphere stratospheric polar vortex.

  - **The southward shift of the Southern Hemisphere tropospheric jet due to the ozone hole has been linked to a range of observed climate trends over Southern Hemisphere mid and high latitudes during summer.**

Because of this shift, the ozone hole has contributed to robust summertime trends in surface winds, warming over the Antarctic Peninsula, and cooling over the high plateau. Other impacts of the ozone hole on surface climate have been investigated but have yet to be fully quantified. These include observed increases in sea ice area averaged around Antarctica; a southward shift of the Southern Hemisphere storm track and associated precipitation; warming of the subsurface Southern Ocean at depths up to several hundred meters; and decreases of carbon uptake over the Southern Ocean.

- **In the Northern Hemisphere, robust linkages between Arctic stratospheric ozone depletion and the tropospheric and surface circulation have not been established, consistent with the comparatively small ozone losses there.**

- **The influence of stratospheric changes on climate will continue during and after stratospheric ozone recovery.**

  - **The global middle and upper stratosphere are expected to cool in the coming century, mainly due to carbon dioxide (CO_2) increases**. The cooling due to CO_2 will cause ozone levels to increase in the middle and upper stratosphere, which will slightly reduce the cooling. Stratospheric ozone recovery will also reduce the cooling. These ozone changes will contribute a positive radiative forcing of climate (roughly +0.1 W/m^2) compared to 2009 levels, adding slightly to the positive forcing from continued increases in atmospheric CO_2 abundances. Future hydrofluorocarbon (HFC) abundances in the atmosphere are expected to warm the tropical lower stratosphere and tropopause region by roughly 0.3 K per part per billion (ppb) and provide a positive radiative forcing of climate.

  - **Chemistry-climate models predict increases of stratospheric water vapor, but confidence in these predictions is low.** Confidence is low since these same models (1) have a poor representation of the seasonal cycle in tropical tropopause temperatures (which control global stratospheric water vapor abundances) and (2) cannot reproduce past changes in stratospheric water vapor abundances.

  - **Future recovery of the Antarctic ozone hole and increases in greenhouse gases are expected to have opposite effects on the Southern Hemisphere tropospheric middle latitude jet.** Over the next 50 years, the recovery of the ozone hole is expected to reverse the recent southward shift of the Southern Hemisphere tropospheric jet during summer. However, future increases in greenhouse gases are expected to drive a southward shift in the Southern Hemisphere tropospheric jet during all seasons. The net effect of these two forcings on the jet during summer is uncertain.

  - **Climate simulations forced with increasing greenhouse gases suggest a future acceleration of the stratospheric Brewer-Dobson circulation.** Such an acceleration would lead to decreases in column ozone in the tropics and increases in column ozone elsewhere by redistributing ozone within the stratosphere. The causal linkages between increasing greenhouse gases and the acceleration of the Brewer-Dobson circulation remain unclear.

  - **Future stratospheric climate change will affect tropospheric ozone abundances.** In chemistry-climate models, the projected acceleration of the Brewer-Dobson circulation and ozone recovery act together to increase the transport of stratospheric ozone into the troposphere. Stratospheric ozone redistribution will also affect tropospheric ozone by changing the penetration of ultraviolet radiation into the troposphere, thus affecting photolysis rates.

4.0 INTRODUCTION AND SCOPE

Climate is changing at all levels in the atmosphere. This chapter considers changes in the stratosphere and the related aspects of troposphere and surface climate. While covering some of the same aspects presented in Chapter 5 (Baldwin and Dameris et al., 2007) of the previous Ozone Assessment (WMO, 2007), the current chapter is broader in scope and also addresses aspects of climate change beyond those associated with stratospheric ozone.

It is evident that the 1987 Montreal Protocol and its subsequent Amendments and Adjustments have led to reduced emissions of ozone-destroying halocarbons, many of which are greenhouse gases. The current chapter helps to place the Protocol's climate impact within a wider context by critically assessing the effect of stratospheric climate changes on the troposphere and surface climate, following a formal request for this information by the Parties to the Montreal Protocol. As requested, the current chapter also considers the effects on stratospheric climate of some emissions that are not addressed by the Montreal Protocol, but are included in the 1997 Kyoto protocol. Hence, the chapter covers some of the issues assessed in past Intergovernmental Panel on Climate Change (IPCC) reports (IPCC, 2007; IPCC/TEAP, 2005). The current chapter is designed to provide useful input to future IPCC assessments.

The troposphere and surface climate are affected by many types of stratospheric change. Ozone plays a key role in such stratospheric climate change, but other physical factors play important roles as well. For this reason, we consider here the effects on the stratosphere of not only emissions of ozone-depleting substances (ODSs), but also of emissions of greenhouse gases, natural phenomena (e.g., solar variability and volcanic eruptions), and chemical, radiative, and dynamical stratosphere/troposphere coupling (Figure 4-1).

First, the chapter combines information about past trace gas emissions (from Chapter 1) and past ozone concentrations (from Chapter 2) with a new assessment of other relevant emissions (Section 4.1). It then draws on the assessed changes in emissions (Section 4.1) and observed stratospheric change (Section 4.2) to assess the nature and drivers of stratospheric climate change (Section 4.3). The chapter subsequently assesses the physical linkages between stratospheric climate change and climate change at Earth's surface (Section 4.4). The chapter closes with a discussion of future stratospheric climate change and its influence on the troposphere and surface climate (Section 4.5), which links to the Chapter 3 discussion of future

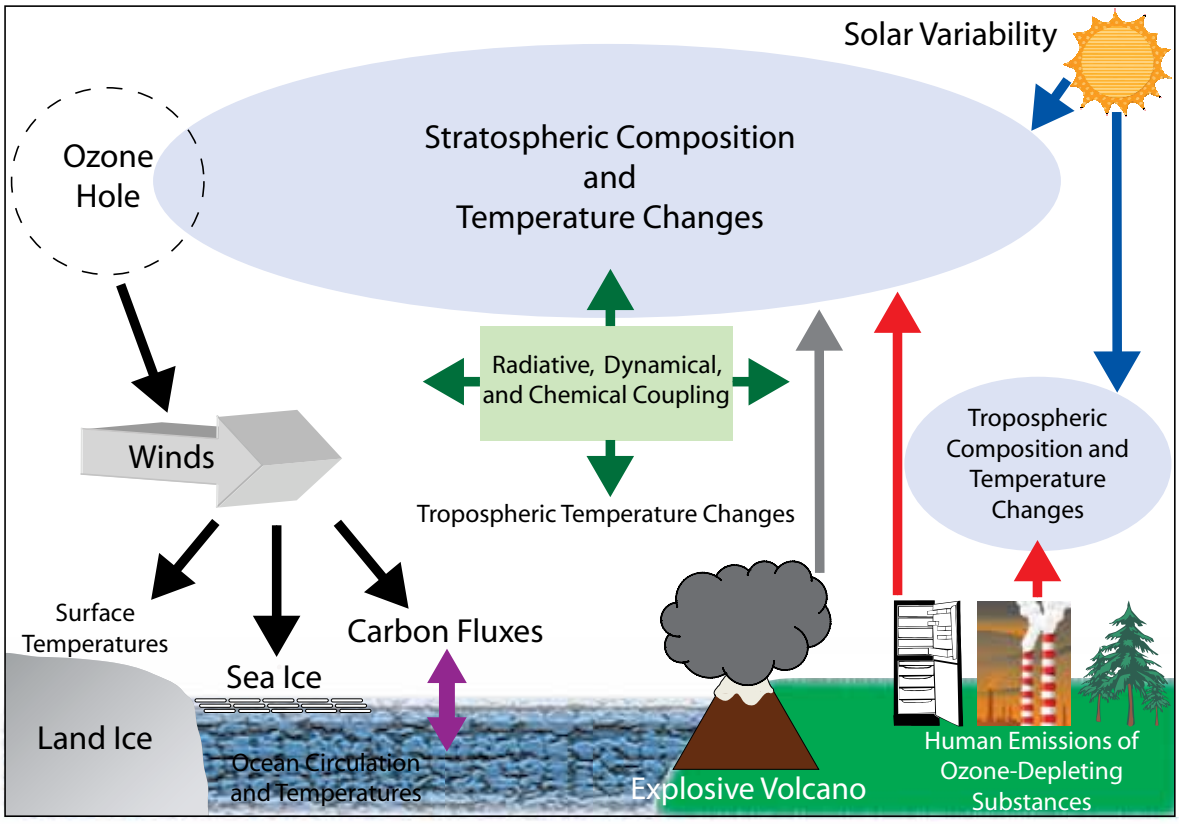

Figure 4-1. Schematic of the drivers and mechanisms considered in this chapter.

ozone trends. Section 4.5 also provides input into discussions of future scenarios in Chapter 5.

4.1 OBSERVED VARIATIONS IN STRATOSPHERIC CONSTITUENTS THAT RELATE TO CLIMATE

In this section we assess our current understanding of stratospheric composition changes. The mechanisms whereby such composition changes affect climate are reviewed briefly in Box 4-1.

4.1.1 Long-Lived Greenhouse Gases and Ozone-Depleting Substances

ODSs, carbon dioxide (CO_2), nitrous oxide (N_2O), and methane (CH_4) are all gases of tropospheric origin that impact climate and stratospheric ozone amounts. ODSs and N_2O directly impact ozone chemistry. Changes in atmospheric concentrations of CH_4 will lead to changes in stratospheric water vapor that in turn impact ozone chemistry and climate. Such gases also affect ozone indirectly via their effects on climate. Recent measurements and growth rates for these gases are covered in Chapter 1 of this report, with a summary of recent growth rates shown in Table 1-1 for the ODSs and Table 1-15 for other greenhouse gases. Atmospheric concentrations of CO_2, N_2O, CH_4, and ODS replacements are projected to increase in the future, as discussed in more detail in Section 4.5.

4.1.2 Ozone

Variations and trends in stratospheric ozone influence climate via direct radiative effects and the resulting temperature and circulation changes. Past changes in stratospheric ozone are reviewed in Chapter 2, and the key points are summarized here as they relate to climate.

Column ozone for the recent past (2006–2008) is approximately 2.5% and 3.5% lower than pre-1980 values for 60°N–60°S and the globe, respectively. Time series of global ozone anomalies show a relative minimum during the middle 1990s, followed by an increase and relatively constant values since 1999 (Chapter 2). Locally, the largest losses have occurred in the Antarctic ozone hole, which is associated with a near-total loss of ozone in the lower stratosphere (~15–22 km) during Southern Hemisphere spring. The Antarctic ozone hole has led to large changes in temperature and circulation in the Southern Hemisphere polar stratosphere, as assessed in WMO (2007) and Section 4.2 of this chapter. The ozone hole has also led to changes at the Southern Hemisphere surface, as assessed here in Section 4.4.2. In contrast to the Antarctic, the Arctic is marked by smaller long-term trends and larger year-to-year variance in ozone during winter and spring (the variance is linked to meteorological variability). Observed changes in profile ozone (see Section 2.1.4.2 of Chapter 2) show relatively large percentage decreases across the globe in the upper stratosphere (~35–47 km), with net changes of over 10% between 1980 and 2009. For the same period, relatively small decreases of ozone concentrations have been observed for the altitude range ~24–32 km.

Significant long-term changes in ozone concentrations are found in the lower stratosphere (below 24 km), although the observational record in this region of the stratosphere is more uncertain due to the dearth of high vertical resolution ozone measurements, including a lack of global long-term sampling from ozonesondes and continuous observations from high vertical resolution satellite instruments. Despite this uncertainty, high-vertical resolution Stratospheric Aerosol and Gas Experiment (SAGE)-based ozone trends will be used in the climate simulations run for the IPCC Fifth Assessment Report. The long-term global observations from the SAGE I and II satellite data (covering 1979–2005) show net lower-stratospheric ozone concentration decreases of ~5–10% near 20 km, with the largest percentage decreases in the tropics (over 30°N-30°S) (Randel and Wu, 2007; see also Figure 2-27 in Chapter 2 of this Assessment). The decreases in lower tropical stratospheric ozone are uncertain (see discussion in Chapter 2), but are consistent with decreases in tropical stratospheric temperatures (Thompson and Solomon, 2005; Randel et al., 2009), and if robust provide possible observational evidence of increased upwelling in the lower tropical stratosphere (see Sections 4.2.2 and 4.3.2). Updated estimates of lower-stratospheric variations and trends are a topic of current research.

Changes in the amount of ozone since 1980 have caused a cooling of the lower and upper stratosphere (Section 4.3) and have likely contributed a negative radiative forcing of the surface climate (Section 4.4). They have also affected stratospheric circulation (Section 4.3) and caused significant changes to the surface-troposphere climate of the Southern Hemisphere (Section 4.4). Stratospheric ozone concentrations will continue to change in response to changes in ODSs and chemical feedbacks associated with stratospheric temperatures and composition, and these changes will continue to affect the climate of the stratosphere, troposphere, and surface (Section 4.5).

4.1.3 Stratospheric Water Vapor

Water vapor is the principal greenhouse gas and plays a key role in tropospheric and stratospheric chemistry. Throughout the atmosphere, water vapor plays both a radiative and chemical role. An increase in stratospheric

Box 4-1. How Do Stratospheric Composition Changes Affect Stratospheric Climate?

The vertical temperature structure of Earth's stratosphere is primarily driven by radiative processes (Figure 1). Solar radiation is principally absorbed by ozone, stratospheric aerosols, and molecular oxygen, and this absorption warms the stratosphere. Outgoing longwave (thermal infrared) radiation from the surface/troposphere is absorbed and re-emitted by greenhouse gases. Prime greenhouse gases in the atmosphere are water vapor (H_2O), ozone (O_3), carbon dioxide (CO_2), methane (CH_4), and nitrous oxide (N_2O). Additionally, halocarbons (i.e., chlorofluorocarbons (CFCs), hydrochlorofluorocarbons (HCFCs) and brominated chlorofluorocarbons (halons)) not only affect atmospheric chemistry, but are also significant greenhouse gases. Aerosols can also emit in the longwave range.

Whether a change of greenhouse gas concentration warms or cools the stratosphere depends on the strength of the absorption bands of the gas and the opacity of the troposphere at the wavelength of absorption (e.g., Clough and Iacono, 1995). In high opacity regions of the spectrum, where powerful greenhouse gases such as CO_2 and H_2O absorb, there is little transmission from the surface to the stratosphere. These gases in the stratosphere therefore receive upwelling radiation from the generally cooler tropopause region below and emit longwave radiation at the stratosphere's generally higher temperature. As this layer in the stratosphere emits more than it absorbed, the stratosphere cools if greenhouse gas concentrations are increasing. This is in contrast to their warming effect on the troposphere-surface region. CFCs, hydrofluorocarbons (HFCs), and other gases that absorb weakly in the "window" regions of the spectrum warm both the lower stratosphere and troposphere (e.g., Forster and Joshi, 2005) as they receive upwelling radiation from near the generally warmer surface and emit their radiation at a lower temperature. For strong absorbers the cooling effect in the stratosphere increases with altitude as these gases cool to space, maximizing at the stratopause near 50 km altitude where temperature is highest. For weaker absorbers their warming effect is maximized at the tropopause region, where the temperature contrast with the surface is largest.

The solar forcing of the Earth's atmosphere is modulated by the 11-year activity cycle of the sun that is reflected in fluctuations in the intensity of solar radiation at different wavelengths. 11-year solar UV irradiance variations have a direct impact on the radiation and ozone budget of the stratosphere (e.g., Haigh, 1994). During years with high solar activity the solar UV irradiance is clearly enhanced, leading to additional ozone production and heating in the stratosphere and above (e.g., Lee and Smith, 2003).

The feedbacks operating between temperature and ozone are determined not only by radiative processes but also by chemical processes (Figure 1). Stratospheric composition is intimately related to the absorption of incoming solar (shortwave) radiation. Solar ultraviolet (UV) radiation is involved in both the creation and destruction of ozone resulting in a maximum ozone concentration near 25 km. The dominant ozone loss cycles in the middle and upper stratosphere (via the catalytic cycles of nitrogen oxides (NO_x), chlorine radicals (ClO_x), and odd hydrogen (HO_x)) slow with decreasing temperatures (e.g., Haigh and Pyle, 1982), leading to higher ozone concentrations. The situation is even more complicated in the polar lower stratosphere in late winter and spring. In addition to the gas-phase ozone loss cycles, as described above, there is an offset by chlorine- and bromine-containing reservoir species (Zeng and Pyle, 2003). These chemical substances are activated via heterogeneous processes on surfaces of polar stratospheric clouds. The rate of chlorine and bromine activation that determines the rate of ozone depletion is strongly dependent on stratospheric temperatures, increasing significantly below approximately 195 K due to enhanced particle formation. The amount of stratospheric ozone is also affected by heterogeneous chemical reactions acting on the surfaces of stratospheric aerosol particles. The injection of sulfate aerosols into the stratosphere leads to transformation of inactive chlorine compounds to active forms that destroy ozone.

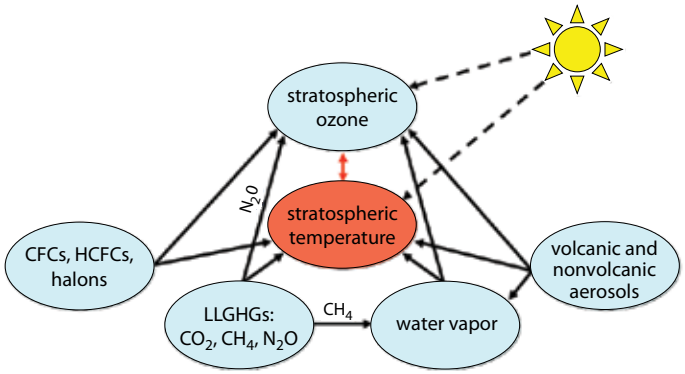

Box 4-1, Figure 1. Schematic of ozone-temperature feedbacks due to changes in stratospheric chemical composition. Stratospheric temperature is determined directly by concentrations of radiatively active gases (e.g., long-lived greenhouse gases, LLGHGs) and aerosols (both emitted by explosive volcanic eruptions and human activities) via the absorption and emission of short- and longwave radiation. Moreover, the amount of stratospheric ozone is defined by transport via winds (i.e., dynamics) and chemical processes, which on its own part depends on concentrations of other greenhouse gases and aerosols. The picture is even more complex since stratospheric temperature influences net ozone production due to temperature-dependent reactions rates. The sun drives radiative, dynamical, and chemical processes affecting ozone and stratospheric temperature.

water vapor will radiatively cool the lower stratosphere and also affect the frequency of occurrence of polar stratospheric clouds, thereby impacting stratospheric ozone chemistry (Kirk-Davidoff et al., 1999; Feck et al., 2008). Enhanced levels of stratospheric water vapor strengthen ozone loss in the presence of ODSs. Hence, a climate with increased stratospheric water vapor will have a delayed ozone recovery even while ODSs are reduced (Shindell, 2001; Shindell and Grewe, 2002; Tian et al., 2009). Changes in stratospheric water vapor also can be a significant radiative forcing for surface climate (see Section 4.4.1).

The principal sources of stratospheric water vapor are entry through the tropical tropopause (Brewer, 1949) and oxidation of methane within the stratosphere (Jones et al., 1986; le Texier et al., 1988). Oxidation of molecular hydrogen (H_2) is another source of stratospheric water vapor, albeit currently small, but with the potential to grow in the future if hydrogen fuel cells come into common use (Tromp et al., 2003; Schultz et al., 2003).

Each source of stratospheric water vapor is associated with a distinct timescale. The input of water vapor into the stratosphere by an individual air parcel in the tropics is largely a function of the lowest temperature a parcel encounters on its transit into the stratosphere, as originally noted by Brewer (1949) and more recently discussed in Schiller et al. (2009). The actual trajectory a parcel takes does need to be considered (Fueglistaler et al., 2009), but a simple model of horizontal processing of air by passage through the Western Pacific cold point tropopause reasonably reproduces observed stratospheric humidity (Holton and Gettelman, 2001; Geller et al., 2002; Scaife et al., 2003). Variability in stratospheric water vapor on seasonal and interannual timescales has been well reproduced by climatological trajectory studies using saturation mixing ratios calculated from global temperature analyses (Jensen and Pfister, 2004; Fueglistaler and Haynes, 2005), demonstrating that to first order, variability in the entry of water vapor into the stratosphere is controlled by variability in tropical cold point temperatures. Convection overshooting into the stratosphere has been observed on limited occasions, and when it occurs likely hydrates the stratosphere locally (Khaykin et al., 2009; Nielsen et al., 2007). However, evidence for a global impact of this phenomenon is lacking at this time (Schiller et al., 2009). Because there is a relatively short turnover time for air in the lowermost stratosphere, on the order of months (Rosenlof and Holton, 1993), changes in the entry value of water vapor to the stratosphere due to tropical cold point temperature changes will be seen almost immediately throughout the lowermost stratosphere. However, there will be a time lag before the signal reaches the middle and upper stratosphere on the order of years. As noted in Engel et al. (2009) (and references therein), the mean age of air in the middle stratosphere at northern midlatitudes (between 20 and 40 km) is approximately 4 years, hence the multiyear time lag before seeing a signal in the middle stratosphere.

Measurement of stratospheric water vapor concentrations is highly challenging and uncertain. There are significant discrepancies noted between coincident measurements of stratospheric water vapor concentrations using different in situ and satellite techniques (Vömel et al., 2007; Kley et al., 2000; Lambert et al., 2007; Weinstock et al., 2009). These discrepancies range from 10% to 50% or even greater in some cases and preclude combining data sets for trend analysis without extreme care. However, data quality is sufficient to examine annual and interannual variations of water vapor in the tropical lower stratosphere. Such variations have been noted to be in quantitative agreement with the idea that observed variations in tropical tropopause temperatures control the entry value of stratospheric water vapor (Randel et al., 2004; Fueglistaler and Haynes, 2005). Chapter 7 in SPARC CCMVal (2010) notes that most chemistry-climate models are able to reproduce the general sense of the annual cycle of water vapor in the tropical lower stratosphere with a minimum in Northern Hemisphere spring and a maximum in Northern Hemisphere fall and winter. There is a wide spread in the stratospheric entry value of water vapor in the models ranging from 2–6 parts per million by volume (ppmv). Kley et al. (2000) presented observationally based estimates ranging from 2.0–4.1 ppmv for the stratospheric entry value, and noted differences between measurement systems larger than the stated uncertainties for those instruments. Assessing the exact mechanism for the amount of dehydration of air entering the stratosphere requires better accuracy than currently exists. As concluded in Weinstock et al. (2009), the differences using coincident measurement noted between independent in situ instruments are sufficiently large that different conclusions can be reached with regard to the impact of convective processes in the tropical tropopause layer, and the degree of supersaturation that is plausible (Peter et al., 2006).

Global water vapor trend determination from the historical record is difficult. There are differences in trends noted between measurement systems covering the same time period (for example the Northern Hemisphere frost point balloon as compared with the Upper Atmosphere Research Satellite (UARS) Halogen Occultation Experiment (HALOE) satellite instrument, as noted in Randel et al., 2004). The multidecadal stratospheric water vapor record is limited to Northern Hemisphere midlatitudes. The longest continuous record of stratospheric water vapor data is from frost point balloon measurements taken at 40°N from Boulder, Colorado. At present, the longest satellite records are from SAGE II and HALOE instruments. Both of these instruments ceased operation in 2005, and there are a number of newer satellite instruments currently mea-

suring stratospheric water vapor concentrations, including Aura Microwave Limb Sounder (MLS), which has extensive spatial coverage. Using overlap periods between instruments, it may be possible to continue estimation of global trends; however, this is a current research endeavor and there is no relevant literature to assess at this time.

From the historic record of the amount of stratospheric water vapor, an increase based on midlatitude frost point balloon measurements below 30 km in Washington, D.C., and Boulder, Colorado, on the order of 0.05 ± 0.01 ppmv/yr for the period from 1964–2000 was reported by Oltmans et al. (2000). Corrections to the Boulder frost point data were reported by Scherer et al. (2008), which reduced the trend for the period from 1980–2000 to 0.03 ± 0.005 ppmv/yr. The time series of the revised Boulder data is shown in Figure 4-2 as well as the comparable time series from HALOE, SAGE II, and Aura MLS. Independent data from a variety of remote sounding and in situ sources show an average trend for the period from 1960–2000 of 0.045 ppmv/yr at Northern Hemisphere midlatitudes at levels below 30 kilometers (km) (Rosenlof et al., 2001). Analyses by Rohs et al. (2006) using in situ balloon measurements show that changes in methane mixing ratio can account for a midlatitude trend below 30 km of .0132 ± 0.002 ppmv/yr of the Boulder increase. The exact mechanism for the remainder of the observed increase of water vapor concentration for the period ending in 2000 is in question, with circulation changes postulated related to the width of the tropics (Zhou et al., 2001; Rosenlof, 2002), as well as changes in aerosol processes near the tropical tropopause (Notholt et al., 2005; Sherwood, 2002). As shown in Figure 4-2 (lower stratosphere midlatitudes) and Figure 4-3 (tropics), since the end of 2000, a decrease in the mixing ratio of water vapor entering the tropical stratosphere occurred (Randel et al., 2006; Rosenlof and Reid, 2008), coincident with a drop in tropical tropopause temperatures that has occurred during a period without an increase of methane concentration (Dlugokencky et al., 2009). The drop in tropical water vapor entry values estimated using HALOE data at 82 hectoPascals (hPa) is ~0.5 ppmv, or approximately 10% of average stratospheric water vapor values (Solomon et al., 2010), and 25% of the nominal maximum-to-minimum difference in the annual cycle of 82 hPa tropical water vapor as estimated from HALOE measurements. The drops in tropical tropopause temperature and entry of water vapor into the stratosphere at the end of 2000 appear to be associated with an increase in the rate of tropical upwelling (Randel et al., 2006; Rosenlof and Reid, 2008) and associated changes in eddy wave driving (Dhomse et al., 2008). There is not agreement in the literature as to the reason for the strengthening of tropical upwelling near the tropical tropopause; both tropical

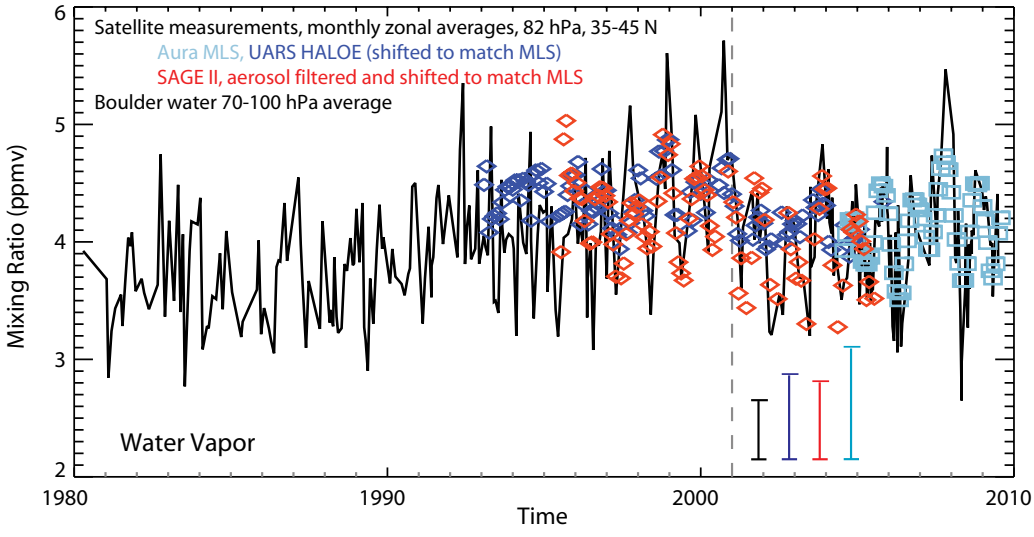

Figure 4-2. Observed changes in stratospheric water vapor. Time series of stratospheric water vapor mixing ratio (ppmv) averaged from 70 to 100 hPa near Boulder Colorado (40°N, 105.25°W) from a balloonborne frost point hygrometer covering the period 1981 through 2009; satellite measurements are monthly averages, balloon data plotted are from individual flights. Also plotted are zonally averaged satellite measurements in the 35°N–45°N latitude range at 82 hPa from the Aura MLS (turquoise squares), UARS HALOE (blue diamonds) and SAGE II instruments (red diamonds). The SAGE II and HALOE data have been adjusted to match MLS during the overlap period from mid-2004 to the end of 2005, as there are known biases (Lambert et al., 2007). Representative uncertainties are given by the colored bars; for the satellite data sets these show the uncertainty as indicated by the monthly standard deviations, while for the balloon dataset this is the estimated uncertainty provided in the Boulder data files. Figure adapted from Solomon et al. (2010).

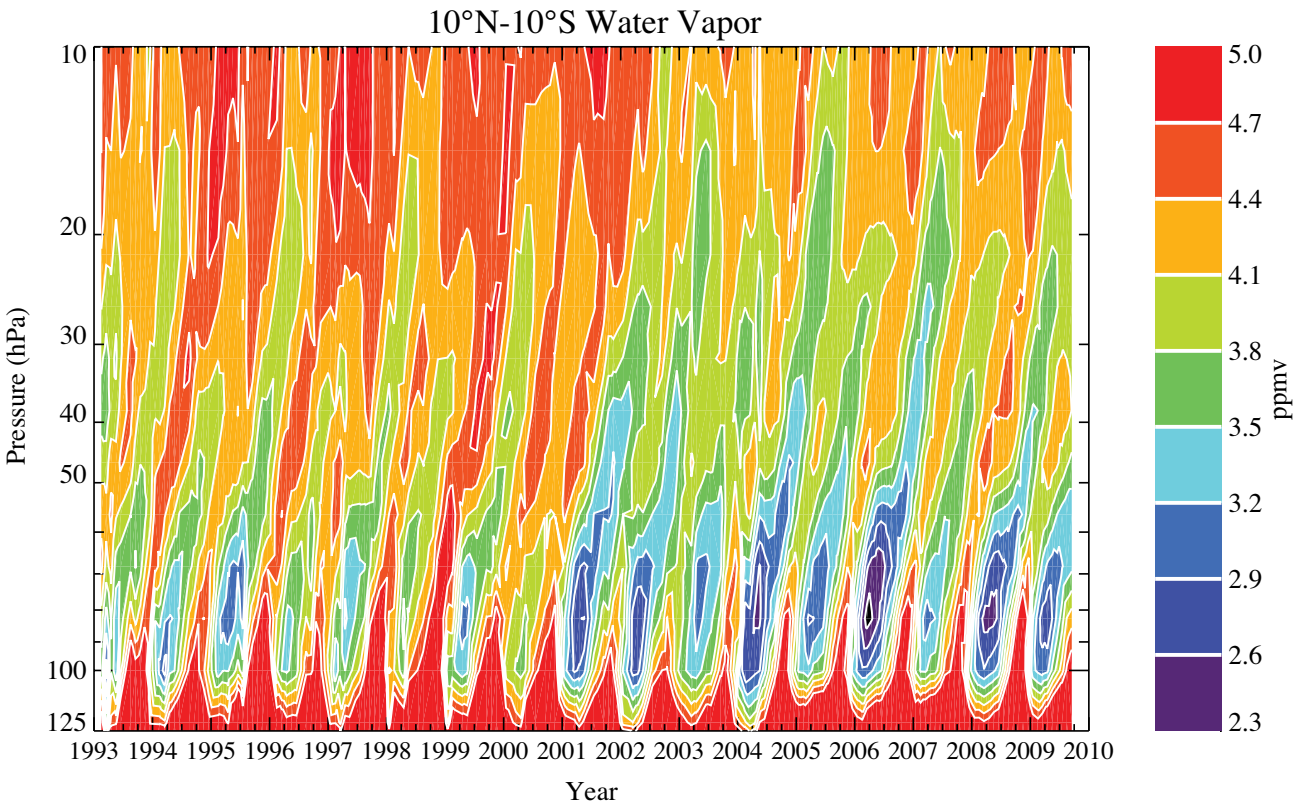

Figure 4-3. Tropical water vapor (ppmv, 10°N–10°S, monthly averages) plotted versus time, showing upward propagation of the water vapor tape recorder (Mote et al., 1996). This is a combination of UARS HALOE and Aura MLS measurements. During the period of data overlap (from mid-2004 through the end of 2005), differences were computed for matching profiles at each pressure level. That average shift was applied to the HALOE measurements at each level; for 82 hPa it is on the order of 0.5 ppmv. The key feature to note here is the change to lower values of the water vapor minimum (hygropause) at the end of 2000, and upward propagation of those lower values in subsequent years. Update of Figure 10 from Rosenlof and Reid (2008).

sea surface temperature changes (Deckert and Dameris, 2008) and changes in high-latitude wave forcing (Ueyama and Wallace, 2010) have been suggested.

There is a good understanding of the annual cycle of water vapor entering the stratosphere (Figure 4-3). The amplitude of the annual cycle is 50% to 60% of the mean and well explained by the known annual cycle in tropical tropopause temperatures (Reed and Vleck, 1969). In contrast, the trend in stratospheric water vapor is not well understood. Over the period 1950–2000 there was an increase in entry-level stratospheric water vapor on the order of 1%/yr (Rosenlof et al., 2001) during a period of increasing tropospheric methane and decreasing tropopause temperatures (Zhou et al., 2001). At the end of 2000 there was a decrease in stratospheric entry-level water vapor coincident with a step-like drop in tropical tropopause temperatures (Randel et al., 2006; Rosenlof and Reid, 2008). The observed long-term increase in stratospheric water vapor over the 1950–2000 period cannot be explained through tropical tropopause temperature trends, although some aspects of interannual variability can be. The more recent decrease in stratospheric water vapor can be explained by tropical tropopause temperature changes, although the mechanism driving that temperature change is not well understood. Given the uncertainties in our understanding and modeling of past water vapor changes, it is difficult to predict changes expected in a future climate.

4.1.4 Stratospheric Aerosols

The stratospheric aerosol layer has often been characterized as a "background" punctuated by volcanic enhancements. The composition of these aerosols is largely sulfuric acid/water solutions, and hence is strongly dependent on sources of stratospheric sulfur. Carbonyl sulfide (OCS) is an important source of sulfur to the stratosphere (Crutzen, 1976). However, the observed abundance of background stratospheric aerosol is many times larger

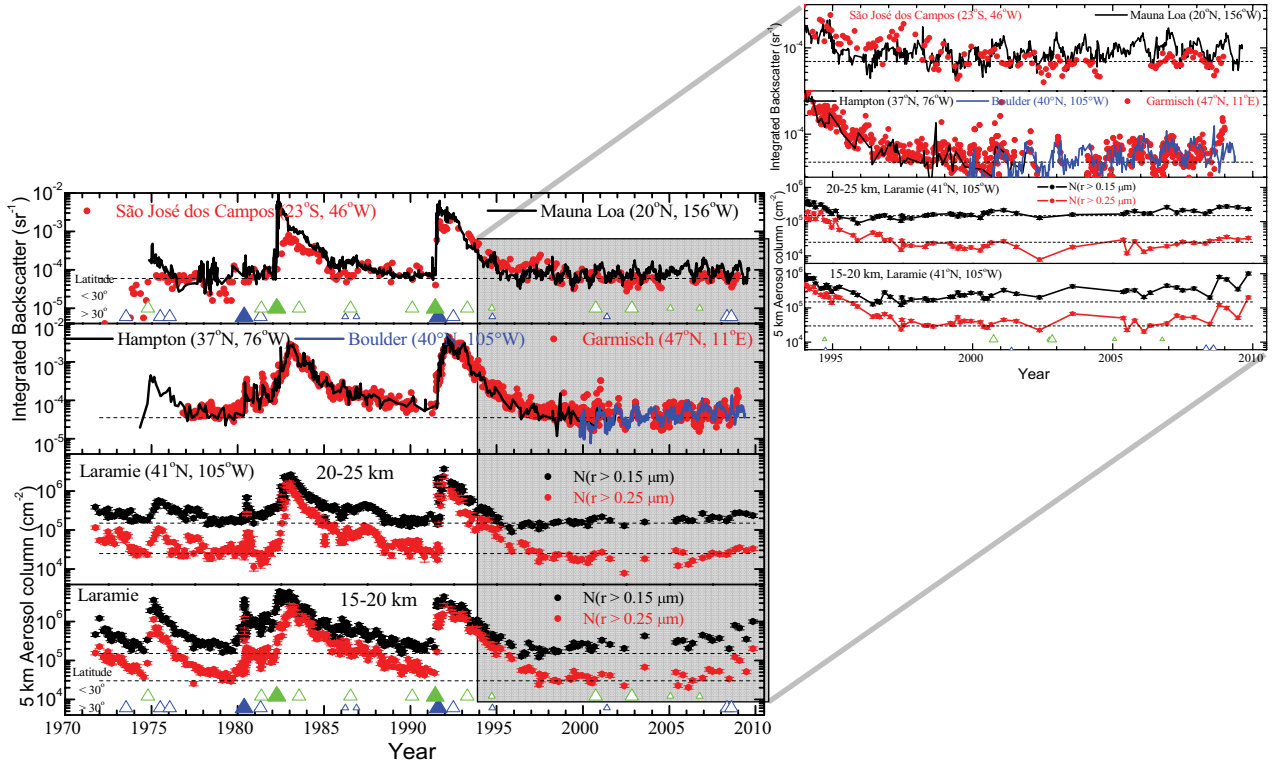

Figure 4-4. History of stratospheric integrated optical backscatter (sr^{-1}) at 694 nm from lidar measurements at five locations (top two panels) and 5 km aerosol column concentration (cm^{-2}) from in situ measurements over two altitude intervals above the tropopause at Laramie, Wyoming, USA (bottom two panels). Top panel shows measurements from São José dos Campos, Brazil, integration 17–35 km, and Mauna Loa, Hawaii, USA, integration 15.8–33 km. Second panel show measurements from Hampton, Virginia, USA, integration tropopause to 30 km, Boulder, Colorado, USA, integration 20–33 km, and Garmisch-Partenkirchen, Germany, integration tropopause +1 km - layer top. The measurements from São José dos Campos (589 nm), Boulder (532 nm), and Mauna Loa (532 nm since 1999) are scaled to 694 nm using a wavelength exponent of –1.4. The times of volcanic eruptions are indicated in the top and bottom panels with triangles, separated into eruptions at latitudes less (green upper symbols) and greater (blue lower symbols) than 30 degrees. Eruptions with volcanic explosivity indices of 5 (large closed symbols), 4 (small open symbols), and 4 with some uncertainty (tiny open symbols) are shown. This figure extends that presented by Deshler (2008) and Hofmann et al. (2009). The Hampton measurements have been discontinued. Right multipanel plot is an expansion of the data since 1994.

than can be explained using OCS alone (Chin and Davis, 1995; Weisenstein et al., 1997; Pitari et al., 2002), which suggests an important role for other sources—such as sulfur dioxide (SO_2)—in pollution. Explosive volcanic eruptions that occurred in the past several decades include Mt. Pinatubo in 1991 and El Chichón in 1982, and these eruptions increased the integrated stratospheric aerosol abundance by more than a factor of ten, as shown in Figure 4-4. Volcanic aerosols directly affect stratospheric temperatures (as discussed in this chapter), as well as mid-latitude and polar surface chemistry and thus stratospheric ozone depletion (as discussed in Chapters 2 and 3). Large explosive eruptions also cause episodic cooling of global average surface temperatures for a few years and other climate effects (see Section 4.4.1). There is presently no systematic global monitoring system to document long-term future changes in stratospheric aerosol that could affect ozone and climate.

Stratospheric aerosols have been measured at a few key sites using balloonborne optical counters and laser ranging (lidar) methods, beginning at some stations in the early to mid-1970s (e.g., Hofmann, 1990; Jäger, 2005; Deshler, 2008). Systematic global satellite measurements using visible spectroscopy (SAGE) began in the mid-1980s (Thomason et al., 1997) but were terminated in 2005. The data sets, methods used, their intercomparison, and the range of available records were recently reviewed under the auspices of SPARC (SPARC, 2006) and by Deshler (2008).

Hofmann (1990) noted an apparent increase in stratospheric aerosols between the late 1970s and the late 1980s, which are two periods with little volcanic influence (Figure 4-4); he suggested a positive trend in the nonvolcanic aerosol background of about 5%/yr over that decade. However, following the major eruption of Mt. Pinatubo in June 1991, stratospheric aerosol declined to the lowest values observed in at least two decades. Taken over the period 1970–2005, there has been no significant trend in background aerosols (Deshler, 2008), raising questions about the origin of the positive trend in the earlier data. However, while recent data remain close to that of the 1970s, they also reveal trends over limited time intervals. A closer look at the most recent data from numerous sites reveals increases of about 4%/yr to 7%/yr in backscatter from 20–30 km since the late 1990s (see Hofmann et al., 2009 and insets in Figure 4-4).

Hofmann et al. (2009) suggested that these recent increases could be linked to sulfur emissions from coal burning in China, which has dramatically increased in the past decade. Notholt et al. (2005) noted the importance of the Asian summer monsoon for transport of SO_2 to the tropical upper troposphere and for cross-tropopause transport, which they suggest could affect stratospheric water vapor transport. Such transport has the potential to influence the source of sulfur to the stratosphere as well. However, input from volcanoes, including from some less explosive eruptions previously thought to be small, may be more important than previously thought. For example, spaceborne laser ranging (lidar) observations at high resolution show evidence for substantial volcanic inputs to stratospheric aerosol associated with the eruption of Soufriere on Montserrat in mid-2006 (Vernier et al., 2009). The conclusion is that decadal variability in stratospheric aerosol is larger than previously anticipated. The relative contribution of recent anthropogenic versus natural emissions to changes in stratospheric aerosol loading remains an area of active research.

4.2 OBSERVED VARIATIONS IN STRATOSPHERIC CLIMATE

4.2.1 Observations of Long-Term Changes in Stratospheric Temperature

Substantial progress has been made since the 2006 Assessment (WMO, 2007) in the evaluation of past stratospheric temperature changes. As a result of this recent work, we have increased confidence relative to previous assessments of the magnitude and meridional structure of temperature trends in the lower stratosphere. We also have a better understanding of the errors inherent in measurements of temperature changes in the middle and upper stratosphere. Three factors contribute to the changes in our understanding:

1. Improved knowledge of the inherent uncertainties in stratospheric data derived from space-borne instruments (e.g., CCSP, 2006; Mears and Wentz, 2009; Shine et al., 2008) and radiosondes (e.g., Lanzante et al., 2003; Free et al., 2005; Sherwood et al., 2005; Thorne et al., 2005; CCSP, 2006; Free and Seidel, 2007; Randel et al., 2009), and in stratospheric products available from reanalysis products (e.g., Randel et al., 2009; Section 2.4 in Chapter 2 of this Assessment);

2. The emergence of several independent analyses of satellite and radiosonde data sets, with distinct approaches to homogeneity adjustments (e.g., Free et al., 2005; Haimberger, 2007; Haimberger et al., 2008; Thorne et al., 2005; Randel and Wu, 2006; Sherwood et al., 2008); and

3. The lengthening of data records with the passing of time.

There are now six global lower-stratospheric temperature data sets specifically developed for climate studies based on radiosonde data: RATPAC (Free et al., 2005); HadAT (Thorne et al., 2005); RATPAC-lite (an abridged version of the RATPAC data set; Randel and Wu, 2006); RAOBCORE (Haimberger, 2007); RICH (Haimberger et al., 2008); and IUK (Sherwood et al., 2008) (see Appendix C for definitions of these acronyms). The radiosonde data sets are not fully independent, but their different approaches to identifying and adjusting temporal inhomogeneities that can affect trends (particularly in the stratosphere) help us to characterize the overall uncertainty in estimates of long-term stratospheric temperature change since the late 1950s. There are now three lower-stratospheric temperature data sets derived from Microwave Sounding Unit (MSU) and Advanced MSU (AMSU) observations from polar-orbiting satellites since 1979 (University of Alabama-Huntsville (UAH), Christy et al., 2003; Remote Sensing Systems (RSS), Mears and Wentz, 2009; Center for Satellite Applications and Research (STAR), Zou et al., 2009). The lower-stratospheric MSU/AMSU temperature data are derived by blending MSU Channel 4 with AMSU Channel 9 data (see the discussion in Randel et al., 2009). The blended data are hereafter referred to simply as MSU4.

Figure 4-5 (from Thorne, 2009) presents time series of global-mean lower-stratospheric temperatures from five radiosonde and three MSU4 data sets. The radiosonde data have been vertically weighted as per the

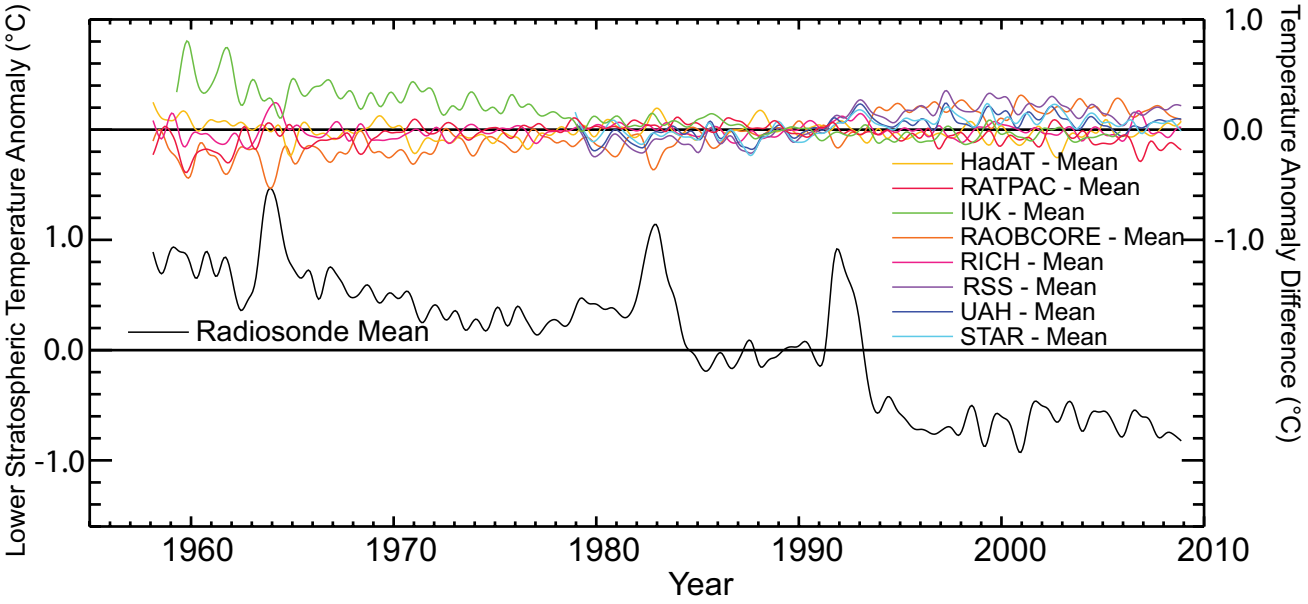

Figure 4-5. Global-mean lower-stratospheric temperature anomalies (1958–2008) from multiple data sets, including five radiosonde data sets (HadAT, IUK, RAOBCORE, RATPAC, and RICH) and three satellite MSU data sets (RSS, UAH, and STAR). Acronyms are defined in Appendix C of this Assessment. All time series are for the layer sampled by MSU channel 4, spanning 10–25 km in altitude, with a peak near 18 km. Black curve is the average of all available radiosonde data sets, and the colored curves show differences between individual data sets and this average. (Based on Thorne, 2009.)

MSU4 weighting function (the general time evolution of lower-stratospheric temperatures shown in Figure 4-5 is mirrored in time series based on global-mean radiosonde data at individual standard pressure levels between 100 and 30 hPa; not shown). The figure is an updated and extended version of the global-mean time series shown in, for example, Ramaswamy et al. (2001; 2006), Seidel and Lanzante (2004), CCSP (2006), and Thompson and Solomon (2009). Three key aspects of global-mean lower-stratospheric temperature changes are evidenced in all data sets:

1. In the global mean, the lower stratosphere has cooled by ~0.5 K/decade since 1980 (~0.35 K/decade in RAwinsonde OBservation (RAOB) data extended back to 1958). The robustness of the global-mean lower-stratospheric cooling has been documented in numerous recent studies (e.g., see the recent review by Randel et al., 2009), but varies slightly from data set to data set. For example, the cooling during 1980–2008 is 0.33 to 0.42 K/decade for the three MSU4 data sets but 0.50 ± 0.16 K/decade for the (vertically weighted) radiosonde data sets (Thorne, 2009; Figure 4-5).

2. The global-mean lower-stratospheric cooling has not occurred linearly but rather appears to be manifested as two downward steps in temperature coincident with the end of the transient warming associated with explosive volcanic eruptions. The steps are most pronounced after the eruptions of El Chichón (1982) and Mt. Pinatubo (1991) and have been emphasized in numerous studies (Pawson et al., 1998; Seidel and Lanzante, 2004; Ramaswamy, et al., 2006; Eyring et al., 2006; Free and Lanzante, 2009; Thompson and Solomon, 2009). Thompson and Solomon (2009) argue that the steps are consistent with the superposition of (i) long-term stratospheric cooling; (ii) transient warming due to volcanic aerosols loading; and (iii) transient cooling due to volcanically induced ozone depletion.

3. In the global mean, the lower stratosphere has not cooled noticeably since 1995. Global-mean lower-stratospheric temperatures during the period following 1995 are significantly lower than they were during the decades prior to 1980, but have not dropped further since 1995.

Another key aspect of recent stratospheric temperature trends is the near uniformity of the cooling at all latitudes outside of the polar regions since 1980. Trends based on lower-stratospheric data from multiple radiosonde data sets show cooling of ~0.4 K/decade (from RATPAC-lite data; Randel and Wu, 2006) to ~0.8

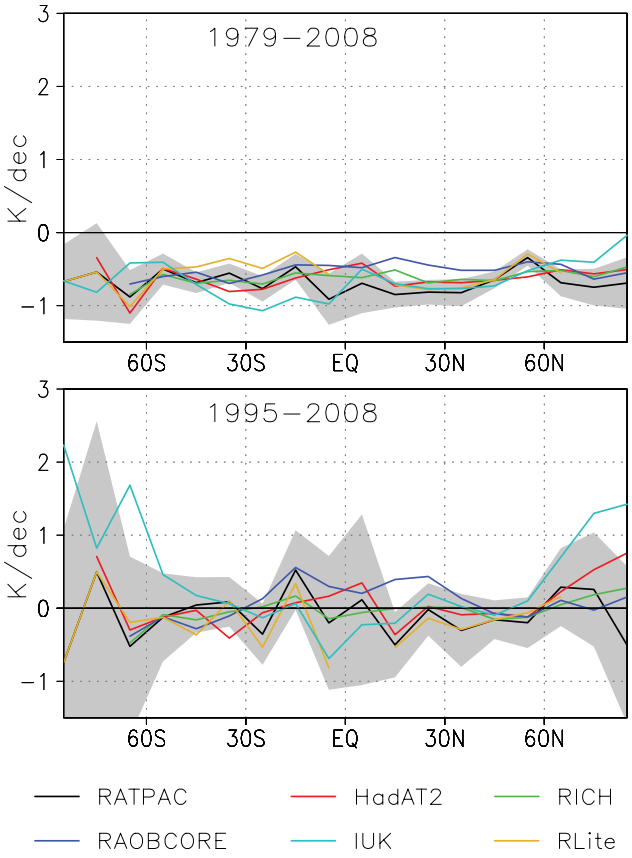

Figure 4-6. Zonal-mean temperature trends (K/decade) at 50 hPa from six adjusted radiosonde data sets for the periods 1979–2008 (top) and 1995–2008 (bottom). Gray shading indicates the 2-sigma trend confidence interval from the RATPAC data set (others are comparable). Trends are computed from temperature anomaly time series, omitting data for two years after the El Chichón and Mt. Pinatubo volcanic eruptions.

K/decade (from RATPAC data; Free et al., 2005) for 1980–2008 for zonal bands within about 45 degrees north and south of the equator (Figure 4-6 top; Thompson and Solomon, 2005; Free et al., 2005). The presence of significant lower-stratospheric cooling at tropical latitudes (Thompson and Solomon, 2005) has implications for the attribution of changes in stratospheric circulation, as discussed in Sections 4.2.2 and 4.3. The structure and amplitude of the lower-stratospheric cooling also has implications for the interpretation of tropospheric temperature trends estimated from the MSU2 satellite, since the MSU2 weighting function samples the lowermost stratosphere (e.g., Fu et al., 2004).

In the annual mean, the cooling of the tropical and middle latitudes since 1980 occurred primarily before 1995 (compare the top and bottom panels of Figure 4-6). Since 1995, annual-mean lower-stratospheric temperatures have remained steady over much of globe, albeit with significant rises over the polar regions in one but not all data sets (the IUK data; Figure 4-6 bottom). The drop in tropical tropopause temperatures circa 2001 highlighted in Section 4.1.3 is centered on a very narrow layer about the tropical tropopause (Randel et al., 2006) and is not apparent in trends at 50 hPa (which are shown in Figure 4-6 bottom).

Lower-stratospheric temperature trends also exhibit considerable seasonal variability. The top panel in Figure 4-7 (from Fu et al., 2010; see also Figure 11 in Randel et al., 2009) shows updated trends in the RSS MSU4 data as a function of latitude and calendar month. Regions of 90% significance are denoted by hatching. The bottom panel in Figure 4-7 shows time series of polar stratospheric temperatures averaged over the seasons indicated based on radiosonde data (from Randel et al., 2009). The tropical cooling evident in the annual-mean is largest between June and January (Figure 4-7, top). Between 1979 and 2007, the Southern Hemisphere polar regions are marked by significant (at the 90% level) cooling between November and March. During the same period, the Northern Hemisphere polar regions are marked by significant cooling during March/April and June–September. The polar warming in August-September in the Southern Hemisphere and December-January in the Northern Hemisphere are not statistically significant at the 90% level in the zonal mean (Figure 4-7, top).

Time series of 100 hPa polar temperature anomalies from radiosonde data confirm visually the following aspects of lower-stratospheric temperature trends (Figure 4-7, bottom): (1) the robust cooling of the polar regions during the spring and summer seasons in both hemispheres (with notably larger cooling observed in the Antarctic), and (2) the absence of significant temperature trends during the winter season in both hemispheres.

In contrast to the lower stratosphere, temperature changes in the middle and upper stratosphere are relatively uncertain due to the limited availability of long-term temperature data there. Radiosonde data are generally available only up to about 20 hPa, and the quality of radiosonde data diminishes with height. There is currently only one satellite data record (from the Stratospheric Sounding Unit) and one corresponding analysis (the analysis combines the available SSU zonal temperature anomaly data from ten separate satellites and is available through 2005; see Randel et al., 2009). Temperature trends based on lidar measurements have large sampling limitations and are only available at limited locations throughout the globe (see discussions in Randel et al., 2009, and Funatsu et al., 2008).

The Stratospheric Sounding Unit senses emissions from carbon dioxide and thus is sensitive to the increases in CO_2 over the past few decades (Shine et al., 2008). For this reason, trends derived from Stratospheric Sounding

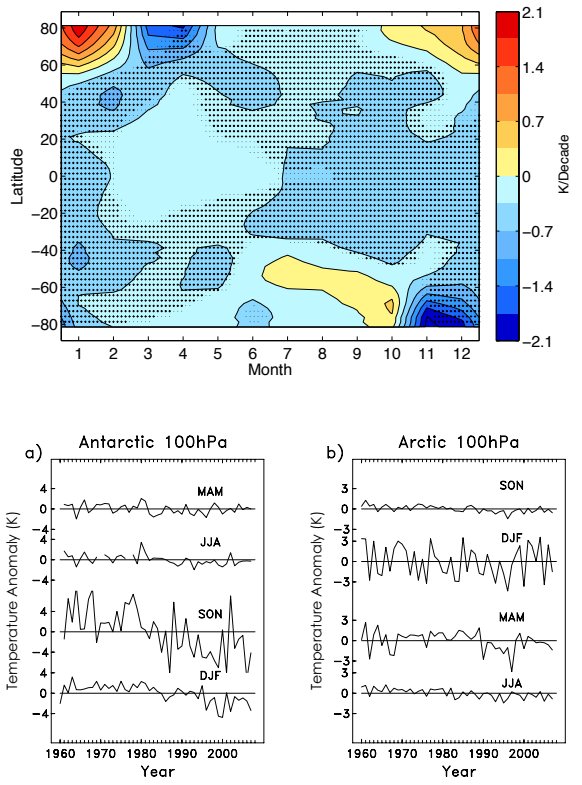

Figure 4-7. (top) Zonal-mean lower-stratospheric temperature trends (K/decade) for 1979–2007 for each calendar month from MSU4 observations (MSU4 spans roughly 10–25 km in altitude, with a peak near 18 km). The color contour interval is 0.35 K/decade. Warm colors indicate warming; cool colors indicate cooling. Hatching indicates where the trends are significant at the 90% confidence level. Results reproduced from Fu et al. (2010). (bottom) Time series of 100 hPa temperature anomalies (K) averaged over the polar regions based on radiosonde measurements (adapted from Randel et al., 2009).

Unit data that are not treated for the influence of increasing CO_2 (i.e., all Stratospheric Sounding Unit trends published prior to 2008) are affected by uncorrected changes in the retrieval weighting function. The principal effect of correcting the Stratospheric Sounding Unit weighting function for increasing CO_2 is to increase the cooling trends by as much as ~0.2–0.4 K/decade throughout much of the stratosphere (see Figure 4 in Shine et al., 2008). Recent analyses of Stratospheric Sounding Unit temperature data corrected for the increases in atmospheric CO_2 are summarized in Randel et al. (2009; compare Figures 18 and 19), and the updated figures of 60°S-60°N mean Stratospheric Sounding Unit temperatures are shown in Figure 4-8. The Stratospheric Sounding Unit temperature data suggest that (1) the middle and upper stratosphere cooled more rapidly than the lower stratosphere (~1.5 K/decade for 1980–2005 for channels centered ~40–50 km) and (2) stratospheric temperatures remained steady from ~1995–2005 from the lower stratosphere up to ~1 hPa.

The outlook for evaluation of future changes in stratospheric temperature is mixed. It appears likely that multiple radiosonde and MSU/AMSU lower-stratospheric temperature analyses will continue to be available from several research teams. The recent initiation of a reference upper-air observing network (Seidel et al., 2009) bodes well for the eventual availability of high quality temperature (and water vapor and other) observations to calibrate and evaluate satellite and radiosonde data. Other data sets that will likely prove useful for future analyses of stratospheric temperatures include lidar deployed within the Network for the Detection of Atmospheric Composi-

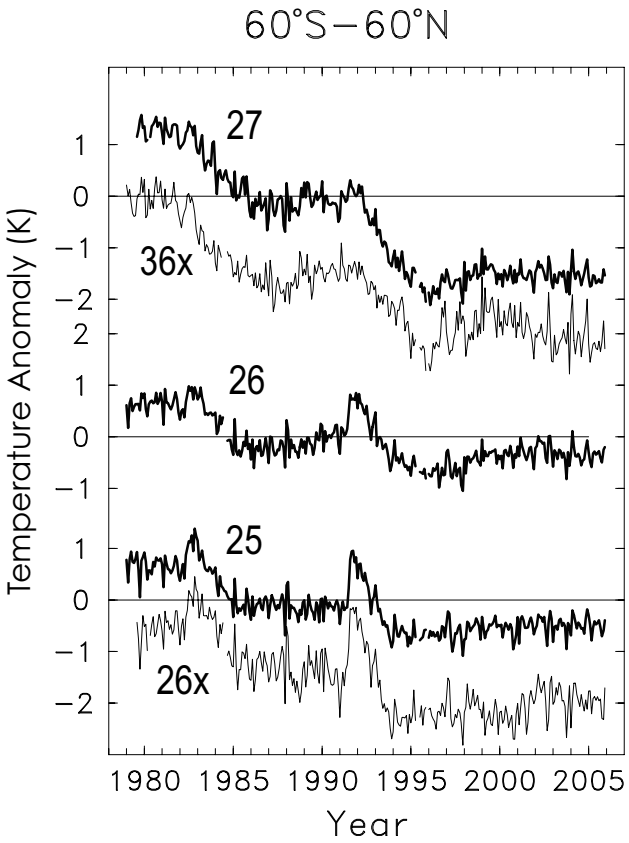

Figure 4-8. Time series of SSU temperature anomalies (K) for channels indicated (Figure 18 from Randel et al., 2009). Data for channels 26x and 36x are shifted for clarity. Exact weighting functions for the SSU satellite instrument can be found in Figure 1 of Randel et al. (2009). Channel 27 corresponds to ~34–52 km altitude, channel 36x to ~38–52 km, channel 26 to ~26–46 km, channel 25 to ~20–38 km, and channel 26x to ~21–39 km.

tion Change and the Global Positioning System radio occultation temperature profiles (the latter are available continuously starting in 2001). For the upper stratosphere, Stratospheric Sounding Unit data could be merged with AMSU observations to extend the record past 2005, but the lack of multiple analyses will continue to limit our understanding of temperature changes in the middle and upper stratosphere.

4.2.2 Observations of Long-Term Changes in the Stratospheric Circulation

4.2.2.1 Stratospheric Zonal Flow

Assessment of long-term trends in the stratospheric circulation is more difficult than it is for temperature because

1. Observations of horizontal stratospheric winds from rawinsondes are sparse and, in general, have not been homogenized for changes in instrumentation.

2. Estimates of the meridional overturning (i.e., the Brewer-Dobson) circulation based on chemical and age-of-air measurements are very noisy and have error bars that exceed the amplitude of the observed trends (Baldwin and Dameris et al., 2007; Engel et al., 2009).

Observed trends in the stratospheric horizontal wind field must be inferred indirectly from measurements of atmospheric temperature (derived from both radiosonde and spaceborne instruments) and atmospheric geopotential height (derived from radiosonde measurements through application of the hypsometric equation).

The trends in the Southern Hemisphere stratospheric vortex during austral spring are well established and were assessed in the 2006 Ozone Assessment (Baldwin and Dameris et al., 2007). They are revisited briefly here since they provide important context for the tropospheric trends assessed in Section 4.4.2. As assessed in the 2006 Assessment, temperatures and geopotential heights both dropped throughout the Southern Hemisphere polar stratosphere from ~1970 to the late 1990s (Thompson and Solomon, 2002). Figure 4-9 shows such trends extended to 2003 (from Thompson and Solomon, 2005). More recent updates of trends in polar geopotential height are not available. Since the trends in geopotential height are relatively small at middle latitudes (not shown), the polar trends in geopotential height shown in Figure 4-9 are consistent with an anomalous eastward acceleration of the Southern Hemisphere stratospheric polar vortex. The eastward acceleration of the Southern Hemisphere stratospheric vortex between November and January is consistent with diabatic cooling associated with the Antarctic ozone hole (Waugh et al., 1999; Thompson and Solomon, 2002) and is reflected in a delay in the dynamical breakdown of the Southern Hemisphere stratospheric vortex (Waugh et al., 1999; Zhou et al., 2000; Karpetchko et al., 2005; Haigh and Roscoe, 2009).

The Northern Hemisphere polar stratosphere cooled markedly during winter and spring between the 1960s and the late 1990s (e.g., WMO, 2003), but exhibited a string of warm winters during the 2000s (Section 4.2.1; Randel et al., 2009). Hence, winter and springtime trends in Northern Hemisphere stratospheric zonal-flow are less significant and more difficult to interpret than those in the Southern Hemisphere. As evidenced in the time series in Figure 4-7 (bottom), the Northern Hemisphere polar stratospheric temperature trends are not significant during December-February. The statistically significant cooling and geopotential height decreases in the Northern Hemisphere polar stratosphere during summer (Figure 4-7; Figure 4-9) are not associated with marked meridional gradients, and thus do not imply changes in the stratospheric thermal wind.

4.2.2.2 Brewer-Dobson Circulation

The Brewer-Dobson circulation model is a simple circulation suggested by Brewer (1949) and Dobson (1956), and consists of three basic parts. The first part is the rising tropical motion of air from the troposphere into the stratosphere. The second part is poleward transport of air in the stratosphere. The third part is descending motion of air in both the stratospheric middle and polar latitudes. This seemingly simple picture leaves a number of possible ambiguities. For instance, the distribution of the tropical air rising through the tropical tropopause is important in that air rising in the inner tropics (near the Equator) encounters lower tropopause temperatures than air rising in the outer tropics. The latitudinal distribution of the descending air is also important since middle latitude descending air is transported back into the troposphere (as a result of isentropic mixing), while the polar latitude descending air is transported into the polar lower stratosphere (via diabatic descent). The Brewer-Dobson circulation is driven primarily by the dissipation of Rossby and gravity waves that have propagated upward from the troposphere. Convective overshooting may also play a role in the vertical transport of trace species in the tropical lower stratosphere, but the role of convective overshooting is less understood than the role of stratospheric wave drag (e.g., Fueglistaler et al., 2009).

Measures of the Brewer-Dobson circulation include the upward flux of tropical air, but if this air descends elsewhere in the tropics, it should not be considered a part of the Brewer-Dobson circulation. The net upward mass

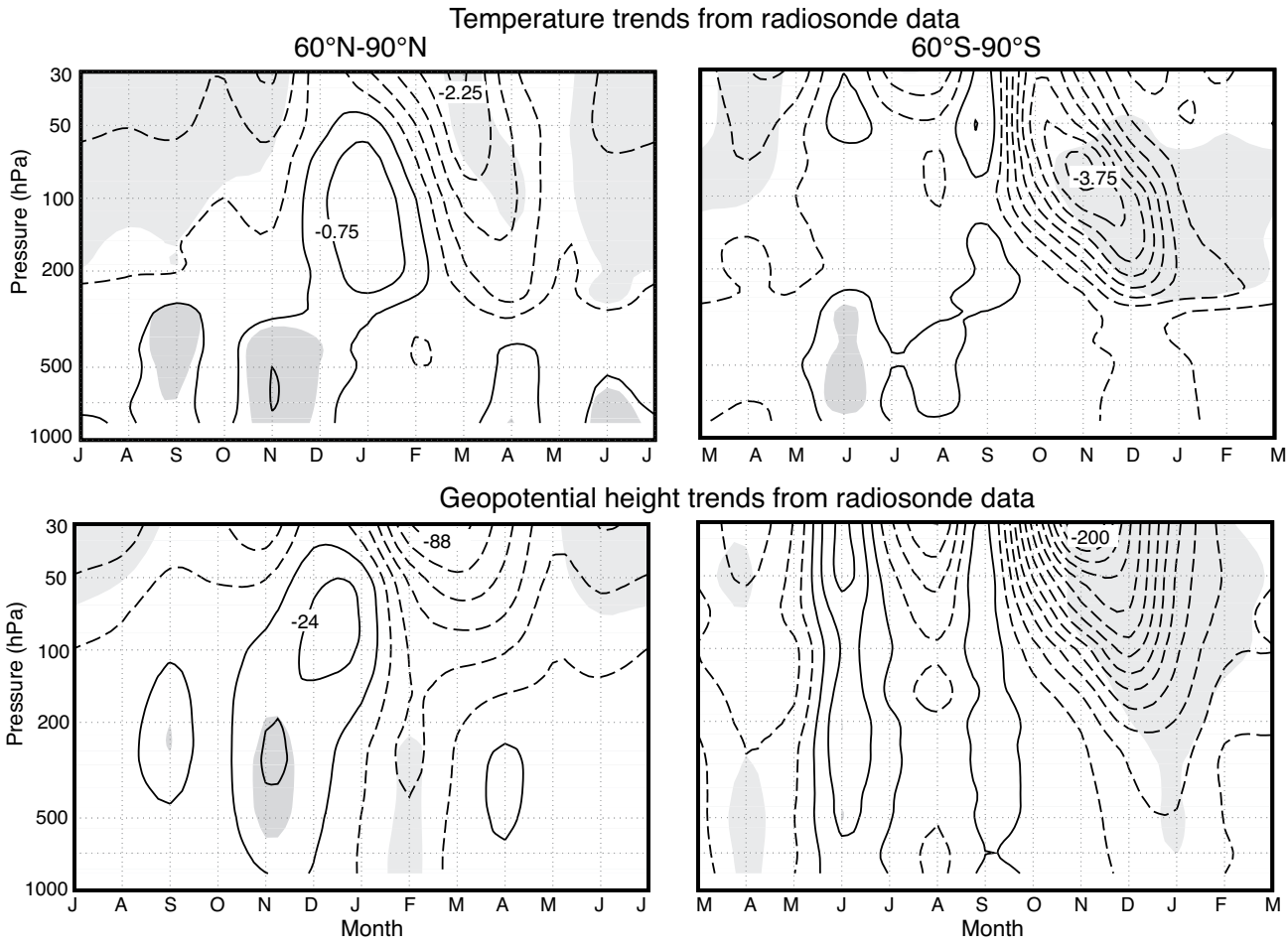

Figure 4-9. Trends in (top) temperature (K/decade) and (bottom) geopotential height (m/decade) averaged over (left) 60°N–90°N and (right) 60°S–90°S for 1979–2003. Trends are shown as a function of month and pressure level. Shading denotes trends that exceed the 95% confidence level. Tick marks on the abscissa denote the center of the respective month. Note that the calendar months on the abscissa are shifted between the Northern and Southern Hemisphere. Trends based on radiosonde data from the Integrated Global Radiosonde Archive (IGRA). Units: K/decade (–0.25, 0.25, 0.75…) and m/decade (–8, 8, 24…). Based on Thompson and Solomon (2005).

flux of air into the tropical stratosphere is often taken as a measure of the Brewer-Dobson circulation, but this does not distinguish the latitudinal distribution of the rising tropical air, which can affect the ozone distribution differently. Theory (e.g., Plumb and Eluszkiewicz, 1999; Semeniuk and Shepherd, 2001; Zhou et al., 2006) indicates that for annually averaged upwelling at the Equator to exist, wave Eliassen-Palm flux convergences must extend into the inner tropics (to about 12–15° latitude), and the distribution of the descending motions at middle and high latitudes depends on the distribution of Eliassen and Palm flux convergences there. However, the importance of tropical wave drag in driving the Brewer-Dobson circulation has recently been questioned by Ueyama and Wallace (2010), on the basis of their observational analysis. Thus interpreting trends in the modeled and observed Brewer-Dobson circulation will require further research.

As discussed later in Section 4.3.2, climate model simulations consistently predict an acceleration of the Brewer-Dobson circulation in response to increasing greenhouse gases (e.g., Rind et al., 1998; Butchart and Scaife, 2001), amounting to an average increase of about 2%/decade in the annual mean net upward mass flux at 70 hPa through the 21st century (Butchart et al., 2006; McLandress and Shepherd, 2009; Butchart et al., 2010; Chapter 4 of SPARC CCMVal, 2010). Since the Brewer-Dobson circulation partially determines the distribution of stratospheric ozone, the simulated trends in the

Brewer-Dobson circulation link human emissions of CO_2 with the distribution of stratospheric ozone. The simulated trends have implications for stratospheric ozone and water vapor trends, and thus for the radiative forcing of the troposphere and surface climate (as discussed in Section 4.3.2).

The detection of trends in the Brewer-Dobson circulation in observations is complicated by two factors:

1. The trends in the Brewer-Dobson circulation are small through 2010, and only in the next few decades are predicted to depart from the natural variability (Section 4.3.2).

2. The Brewer-Dobson circulation is not a measurable quantity and hence trends in the Brewer-Dobson circulation cannot be directly observed, but rather are inferred from changes in the horizontal structure of lower-stratospheric temperature, constituent trends, and trends in the estimated age of air.

The three primary lines of observational evidence for increases in the strength of the lower-stratospheric meridional circulation include (1) cooling in the lower stratosphere that exceeds the cooling predicted by ozone depletion in the tropics but is less than the cooling predicted as a direct radiative response to ozone depletion (Thompson and Solomon, 2009); (2) out-of-phase temperature trends between polar and tropical latitudes during the Northern Hemisphere and Southern Hemisphere cold seasons, with largest cooling in the tropics (Thompson and Solomon, 2009; Fu et al., 2010); and (3) localized decreases in ozone in the lower tropical stratosphere in trends derived from the SAGE instruments (Chapter 2 and Figure 2-27). In general, the evidence for changes in the Brewer-Dobson circulation based on the structure of lower-stratospheric ozone and temperature trends is most robust in the tropics and less clear at middle and high latitudes.

There are two primary caveats associated with the above lines of evidence:

1. Stratospheric age-of-air estimates based on balloon-borne in situ measurement of sulfur hexafluoride (SF_6) and CO_2 do not indicate statistically significant trends in the Brewer-Dobson circulation (Engel et al., 2009), albeit age-of-air estimates do not uniquely reflect the Brewer-Dobson circulation, and the uncertainty bars on such estimates are very large (i.e., the modeled trends in the Brewer-Dobson circulation lie within the uncertainty estimates of the stratospheric age-of-air measurements in numerous climate change simulations).

2. Trends in tropical lower-stratospheric ozone from the SAGE data are subject to considerable uncertainty (Chapter 2).

4.3 SIMULATIONS OF STRATOSPHERIC CLIMATE CHANGE

4.3.1 Simulation of Stratospheric Temperature Trends from Chemistry-Climate Models and Climate Models

Multiyear observations of stratospheric temperature clearly indicate both large variability on multiple timescales and long-term changes (Section 4.2.1). The thermal structure of the stratosphere is influenced by natural as well as anthropogenic factors. An important task is to understand the impacts of natural forcing on the stratosphere to enable the identification and quantification of implications of human activities. Several studies have been performed to describe the evolution of stratospheric temperature, in particular the observed cooling (e.g., Ramaswamy et al., 2006; Dall'Amico et al., 2010a; Gillett et al., 2010; Randel et al., 2009; see Figures 4-5 and 4-9 for example time series of stratospheric temperature).

Attribution of stratospheric temperature variations and long-term changes can be undertaken through comparison of observed changes with simulations by a hierarchy of numerical models considering radiative, dynamical, and chemical processes in the atmosphere. Such numerical models can be binned into two general classes: (1) climate models, i.e., atmospheric general circulation models that are coupled to an ocean model, but mostly do not resolve the whole stratosphere; and (2) chemistry-climate models, i.e., atmospheric general circulation models that are interactively coupled to a detailed chemistry module, almost fully consider the stratosphere, but so far are generally not coupled to an ocean model. Both types of models can be used to assess both natural and anthropogenic forcings affecting the behavior of the atmosphere.

The prime natural forcings of stratospheric temperature fluctuations on interannual and decadal timescales are the solar activity cycle (with a timescale of 11 years), the El Niño-Southern Oscillation (with a timescale of ~3–5 years), and explosive volcanic eruptions (with sporadic timescales). The quasi-biennial oscillation in tropical stratospheric zonal winds is internally generated but can be considered as a forcing for extratropical stratospheric variability. Most climate models and chemistry-climate models consider the ~11-year activity cycle of the sun (i.e., solar variability is explicitly enforced by variation in radiative heating and photolysis rates) and the radiative and chemical effects of sporadic large volcanic

eruptions (i.e., changes in heating rates and heterogeneous chemistry due to an enhanced aerosol loading). Climate models predict ocean temperatures and to varying degrees are able to capture coupled air-sea variability associated with the El Niño-Southern Oscillation (e.g., AchutaRao and Sperber, 2006). In most chemistry-climate models, ocean surface temperatures are prescribed, using either historical measurements or values derived from climate model simulations. In the latter case, the realism of the El Niño-Southern Oscillation and its related variability is constrained by the realism of the prescribed (climate model-calculated) sea surface temperatures.

Atmospheric models reaching up into the mesosphere and with sufficient vertical resolution in the whole model domain (i.e., less than 1 km) are able to generate stratospheric quasi-biennial-like oscillations (e.g., Giorgetta et al., 2006; Punge and Giorgetta, 2008). Additionally, an adequate description of stratospheric quasi-biennial-like oscillations in stratosphere resolving climate models requires small-scale gravity wave forcing (e.g., Takahashi, 1999; Scaife et al., 2000a) which is consistent with recent observational estimates (e.g., Ern and Preusse, 2009). Chemistry-climate models that do not generate a stratospheric quasi-biennial oscillation internally mostly have the observed behavior prescribed, i.e., by assimilating observed wind fields in the tropical lower stratosphere (see Morgenstern et al., 2010a).

In climate models and chemistry-climate models, the impact of human activities is generally considered as follows: long-lived greenhouse gases (i.e., CO_2, CH_4, and N_2O), anthropogenic aerosol loading, and ODSs (CFCs, HCFCs, and halons) are prescribed as either emissions or atmospheric concentrations. In chemistry-climate models, changes in the amount and distribution of water vapor and ozone are calculated in a self-consistent manner considering interactions of chemical, radiative, and dynamical (transport and mixing) processes, whereas in climate models, ozone fields are mostly prescribed without considering feedbacks; and effects of chemical processes on water vapor are neglected. Natural forcings such as changes in solar activity and explosive volcanic eruptions are also taken into account. Detailed summaries of suggested and used boundary conditions for recent chemistry-climate model simulations (see Chapter 3 of this report) have been given in Eyring et al. (2008), in Chapter 2 of the SPARC CCMVal report (2010), and in Morgenstern et al. (2010a)[1].

Figure 4-10 shows the time series of global-mean stratospheric temperature anomalies as derived from these chemistry-climate model simulations (colored lines) compared to satellite data (Microwave Sounding Unit/Stratospheric Sounding Unit) weighted over specific vertical levels (black lines). There is strong evidence for a large and significant cooling in most of the stratosphere during the last decades (Section 4.2.1; e.g., Randel et al., 2009; Randel, 2010; Thompson and Solomon, 2009). The observed stratospheric cooling has not evolved uniformly since the 1960s and the overall development is well reproduced by the majority of chemistry-climate models (see Figure 4-10).

Ramaswamy et al. (2006) noted that the observed cooling of the global lower stratosphere between 1979 and 2003 occurred in two distinct step-like transitions (see also Section 4.2.1). After a 2–3 year period of stratospheric warming due to enhanced aerosol loading of the stratosphere, these appeared subsequent to the two explosive volcanic eruptions, El Chichón (April 1982) and Mt. Pinatubo (June 1991), with each cooling transition being followed by a period of relatively steady temperatures. Ramaswamy et al. (2006) concluded that the anthropogenic factors forced the overall cooling and the natural factors modulated the temporal evolution of the cooling. Simulations performed with chemistry-climate models support these findings: the space-time structure of the observed cooling is largely attributable to the combined effect of stratospheric ozone depletion and increases in greenhouse gas concentrations, superimposed on effects due to solar irradiance variation and explosive volcanic eruptions (see Chapter 3 of SPARC CCMVal, 2010). Moreover, Thompson and Solomon (2009) provided observational analyses that indicate the step-like behavior of global mean stratospheric temperatures depends also on the temporal variability in global mean ozone following large volcanic eruptions. They argued that the warming and cooling pattern in global mean temperatures following major volcanic eruptions is consistent with the competing radiative and chemical effects of volcanic eruptions on stratospheric temperature and ozone. This conclusion was supported by a modeling exercise (Dall'Amico et al., 2010a) showing that if observed ozone values are prescribed in their model instead of the assumption of a "simple" linear ozone trend, the stepwise nature of the stratospheric cooling is better reproduced.

Thompson and Solomon (2009) also demonstrated that the contrasting latitudinal structures of recent stratospheric temperature (i.e., stronger cooling in the tropical lower stratosphere than in the extratropics) and ozone trends (i.e., enhanced ozone reduction in the tropical lower stratosphere) are consistent with the assumption of increases in the stratospheric overturning Brewer-Dobson circulation. The seasonality of tropical lower-stratospheric tem-

1 The CCMVal project uses chemistry-climate models to simulate the atmosphere from 1960 to about 2100. CCMVal-2 is the second CCMVal project (SPARC CCMVal, 2010). The scenarios used in CCMVal-2 are outlined in Chapter 2 of the SPARC CCMVal (2010) report. REF-B1 (1960-2006) is defined as a transient run from 1960 (with a 10-year spin-up period) to the present (see Table 3-2 of this Assessment).

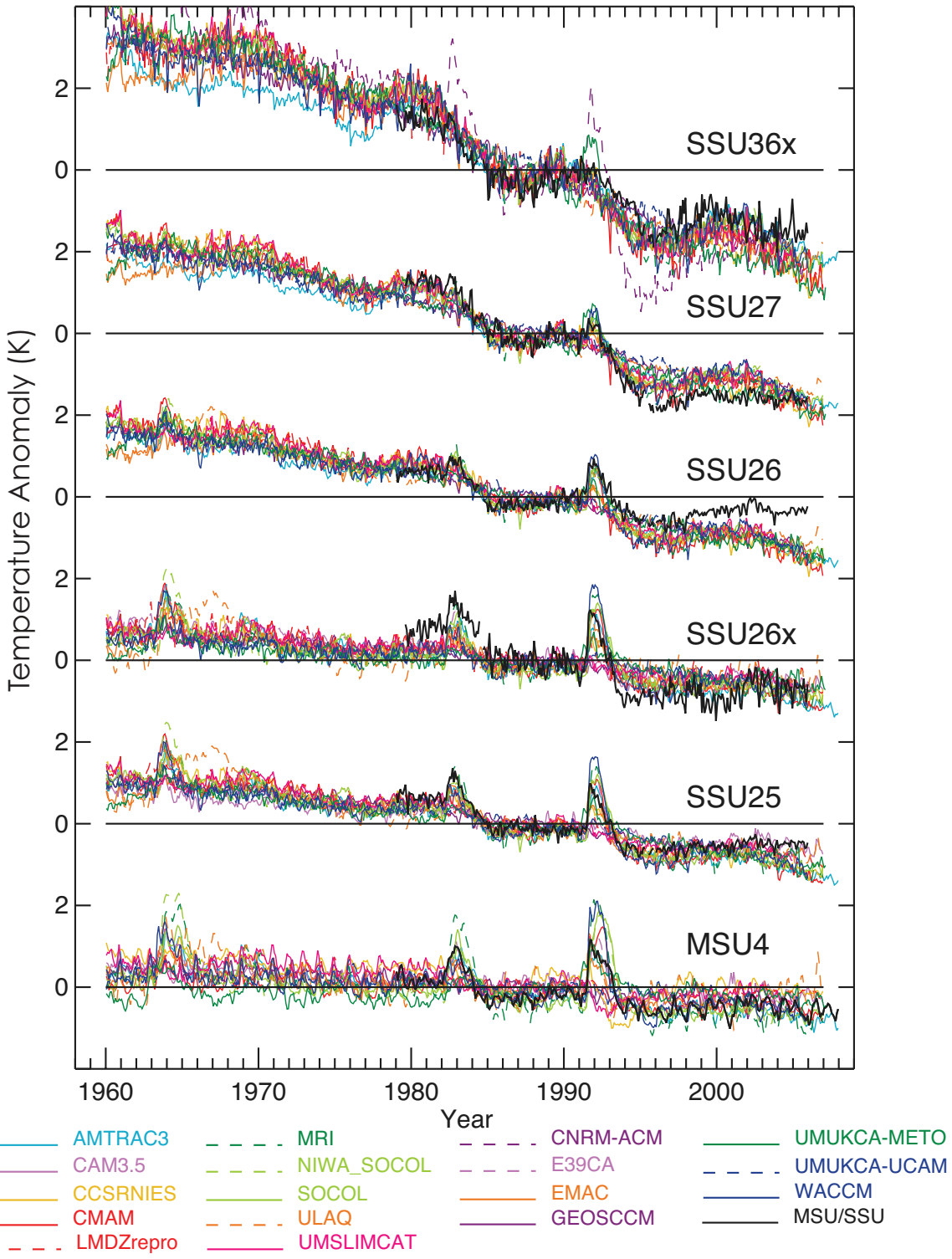

Figure 4-10. Global mean time series of satellite observed (Randel et al., 2009) and chemistry-climate model temperature anomalies (K) weighted for MSU/SSU weighting functions. The anomalies are calculated with respect to the period 1980–1994, as in the provided MSU/SSU anomalies. Exact weighting functions for the MSU/SSU satellite instruments can be found in Figure 1 of Randel et al. (2009). Channel 27 corresponds to ~34–52 km altitude, channel 36x to ~38–52 km, channel 26 to ~26–46 km, channel 25 to ~20–38 km, channel 26x to ~21–39 km, and channel MSU4 to ~13–22 km. See Table 3-1 in Chapter 3 of this Assessment for a description of the chemistry-climate models shown in the figure.

perature trends using the MSU4 (~13–22 km altitude) data (1979–2007) was examined by Fu et al. (2010). Evidence was given that the seasonality is a response to changes in the Brewer-Dobson circulation, as discussed further in Sections 4.2.2 and 4.3.2. Based on the same data set but focusing on the Southern Hemisphere, Lin et al. (2009) showed that the observed temperature patterns are characterized by cooling and warming regions of similar magnitudes, with strongest local trends occurring in austral spring. Canziani et al. (2008) found that the spring warming observed in the Southern Hemisphere stratosphere could be linked to an enhanced stationary planetary wavenumber 1 and increased total ozone associated with this wave at midlatitudes.

The results presented in Figure 4-10 show a better overall agreement between observations and chemistry-climate model results than in previous comparison studies (Eyring et al., 2006; WMO, 2007, Chapter 5). Global mean temperature anomalies, particularly the longer-term trend, derived from observations are reproduced well by most chemistry-climate model simulation results (Chapter 3 of SPARC CCMVal, 2010). On the one hand, this may be due to improved chemistry-climate models; on the other hand, this may be due to improvements in the retrievals of the observed temperature data. Nevertheless, there are still some differences in detail between observations and chemistry-climate model results in specific regions of the atmosphere, e.g., in the Arctic and Antarctic atmosphere (Austin et al., 2009). Since regional trends could be affected by various processes, possible reasons for such discrepancies can be manifold and need more specific investigations.

Figure 4-10 illustrates that many chemistry-climate models capture the leveling of the stratospheric temperature since the late 1990s. The impact of the prescribed sea-surface temperatures is apparent as MSU4 temperatures (centered ~13–22 km) and chemistry-climate model temperatures are particularly well correlated compared to other levels. A disagreement between the models and observations is clearly seen in Stratospheric Sounding Unit channel 26 (SSU26; centered near ~26–46 km) over the last decade. SSU26 has a maximum weight at about 5 hPa and a considerable contribution from the lower stratosphere. Although the agreement is better in Stratospheric Sounding Unit channel 27 (SSU27; centered near ~34–52 km), which peaks at 2 hPa with less contribution from the lower stratosphere, the timing and duration of the flattening is quite different between models and observations. So far the reasons for these findings are not understood.

The corresponding vertical profiles of global temperature trends derived from MSU/Stratospheric Sounding Unit data and chemistry-climate models are shown in Figure 4-11. The observed stratospheric trend between 1980 and 2005 is connected with emissions of CO_2 and ODSs (Shepherd and Jonsson 2008; Gillett et al., 2010) and is controlled radiatively by changes in CO_2, O_3, and H_2O concentrations (Shine et al., 2003). Jonsson et al. (2009) found that CO_2-induced cooling reduced upper-stratospheric ozone depletion by a factor of approximately 20% over the period from 1975–1995 (when the amount of stratospheric ODSs was increasing most rapidly) when compared with what would have been expected based on the ODS increases alone. This may not be true in the future as climate-ozone interaction becomes more important (see Section 4.5).

Nearly all chemistry-climate models successfully model the broad features of the observed temperature trend, with warming in the troposphere and cooling in

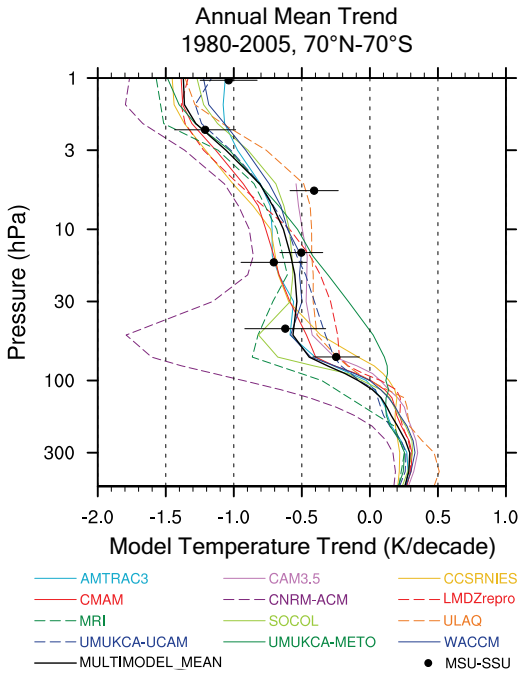

Figure 4-11. Near global (70°S–70°N) and annual mean trends for 1980-2005 (K/decade) for temperature of CCMVal REF-B1 model simulations. The figure includes satellite observed MSU/SSU trends and 95% confidence intervals. MSU/SSU data points include channels: MSU-4 (at 70 hPa), SSU25 (15 hPa), SSU26 (5 hPa), SSU27 (2 hPa), SSU15X (45 hPa), SSU26X (15 hPa), and SSU36X (1 hPa), where the specified pressure levels represent the approximate weighted mean heights derived from the MSU/SSU vertical weighting functions for each channel (see Randel et al., 2009). The solid black lines indicate the multi-model mean results. See Table 3-1 in Chapter 3 of this Assessment for a description of the chemistry-climate models shown in the figure. From Figure 3.2a from SPARC CCMVal (2010).

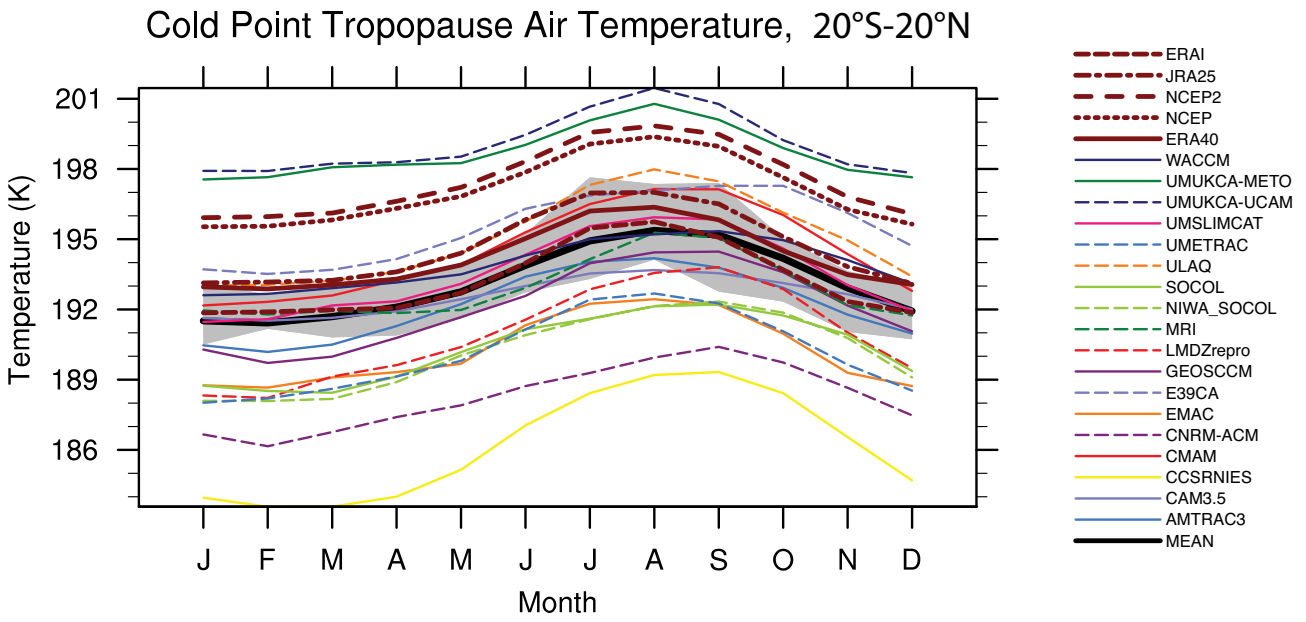

Figure 4-12. Annual cycle of tropical (20°S–20°N) cold point tropopause temperature (K) from chemistry-climate models and observations. Model output and observations are from the period 1980–1999. Gray shaded region is 3σ variability from ERA40 analyses. Reanalysis systems in brown with different line styles: European Centre for Medium-Range Weather Forecasts (ECMWF) 40-year reanalysis (ERA40; solid), ECMWF Interim Re-Analysis (ERAI; short dash), Japanese Re-Analysis (JRA25; dot dash), National Centers for Environmental Prediction (NCEP; dotted), and NCEP2 (long dashed). The multi-model mean (MEAN) is the thick black line. See Table 3-1 in Chapter 3 of this Assessment for a description of the chemistry-climate models shown in the figure. From Gettelman et al. (2010).

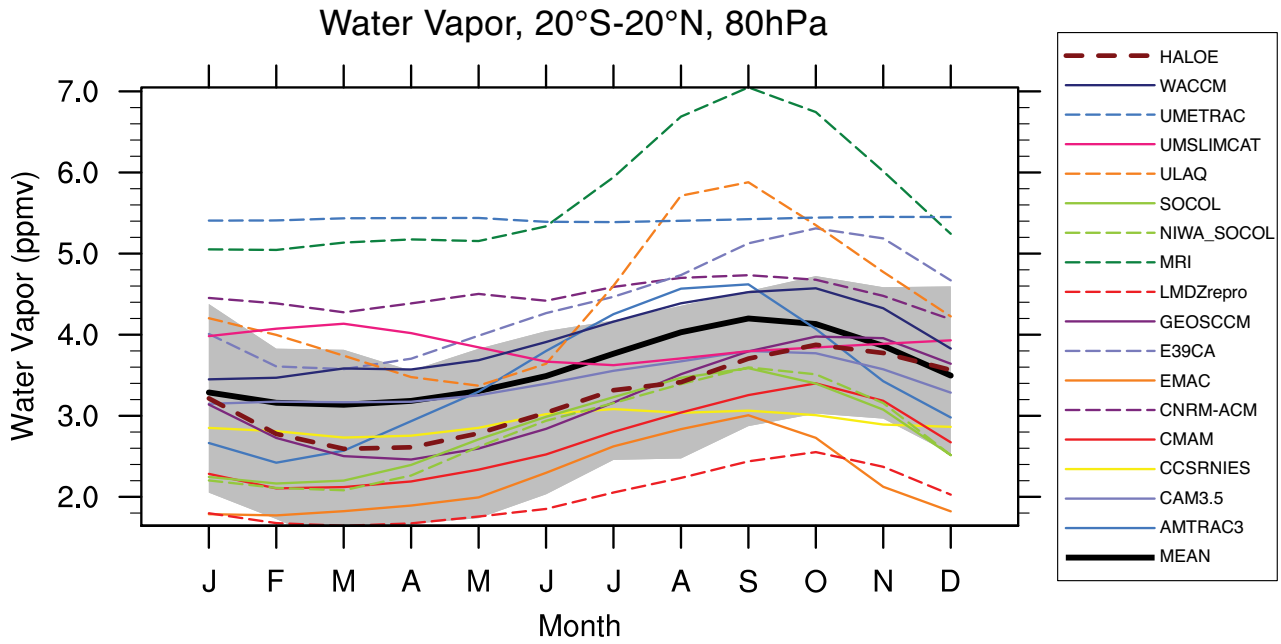

Figure 4-13. Annual cycle of tropical (20°S–20°N) water vapor mixing ratio at 80 hPa from chemistry-climate models and observations. Model output from the period 1992–2004. Gray shaded region is 3σ variability from HALOE observations over 1992–2004 (thick brown dashed line). The multi-model mean (MEAN) is the thick black line. See Table 3-1 in Chapter 3 of this Assessment for a description of the chemistry-climate models shown in the figure. From Gettelman et al. (2010).

the stratosphere over this period. It should be noted that the tropospheric warming is by construction constrained towards observations because the historically observed sea-surface temperatures are prescribed in most of the chemistry-climate models. In the stratosphere, most models capture the overall behavior of the vertical variations, with cooling maxima in the upper and lower stratosphere (Chapter 3 of SPARC CCMVal, 2010). This indicates that the natural and anthropogenic forcings considered in the chemistry-climate models seem to be sufficient to explain the global-mean temperature changes in the stratosphere over the last 50 years. Nevertheless, specific model results indicate that there are still several uncertainties.

For example, Gettelman et al. (2010) analyzed the annual cycle of the tropical cold point tropopause temperature, i.e., the region of lowest temperatures, comparing the results of chemistry-climate models (i.e., using the REF-B1 CCMVal-2 model fields; see footnote 1 in this section) with corresponding data derived from several reanalysis systems (Figure 4-12). Although almost all chemistry-climate models are able to reproduce the annual cycle, there are significant offsets between some models and observations. Interestingly, the multi-model mean is very close to ERA-40, and the model results presented in Figure 4-12 are generally in better agreement with observations than results from the chemistry-climate models used in the first set of CCMVal (CCMVal-1) experiments (Gettelman et al., 2009). The uncertainties in the chemistry-climate models' tropical cold point tropopause temperature affect the water vapor content of air entering the stratosphere (Figure 4-13), which is critical for the chemistry and the climate of the stratosphere (see also Section 4.1.3).

Other examples of model uncertainties were presented by Austin et al. (2008), who analyzed multidecadal simulations of chemistry-climate models concerning the presence of the 11-year solar activity cycle in ozone and temperature data, and compared it with respective satellite measurements. They showed that the currently available model systems have improved significantly compared to studies that were based on the previous generation of chemistry-climate models (e.g., Soukharev and Hood, 2006); model results and observations mostly agree, within stated uncertainties, with regard to the vertical structure of the ozone solar response, particularly in the tropics where a double vertical peak structure is now reproduced by chemistry-climate models with a minimum near 20 hPa, which is slightly below the minimum identified in observations (~10 hPa). The tropical temperature solar response calculated by the chemistry-climate models (Figure 4-14) also shows a "double peak," whereas temperature data derived from satellite based measurements (Stratospheric Sounding Unit and MSU) do not indicate such a vertical response pattern. However, it is likely that the Stratospheric Sounding Unit has insufficient vertical resolution to identify such a double peak structure (Gray et al., 2009).

Another uncertainty with regard to the impact of solar variability arises from recent measurements (April 2004–March 2008) of solar spectral irradiance acquired by the Solar Radiation and Climate Experiment satellite (Harder et al., 2009). While these observations show variations in total irradiance largely in line with previous solar activity cycles, they cast doubt on currently accepted models of the spectral composition of the irradiance variability. In particular they suggest much larger (by approximately a factor of six) differences at ultraviolet wavelengths, and negative changes (i.e., greater emissions at solar minimum relative to solar maximum) in the visible and near infrared. These measurements are currently available only over a four-year period during the final declining stages of the most recent solar cycle and therefore remain to be validated; however, if correct, they imply a much larger solar signal in stratospheric ozone (Haigh et al., 2010). The magnitudes of experimental uncertainties in both the irradiance and contemporaneous ozone data do not yet allow this to be tested.

Trends in stratospheric temperature could also be affected by changes in transport of radiatively active trace

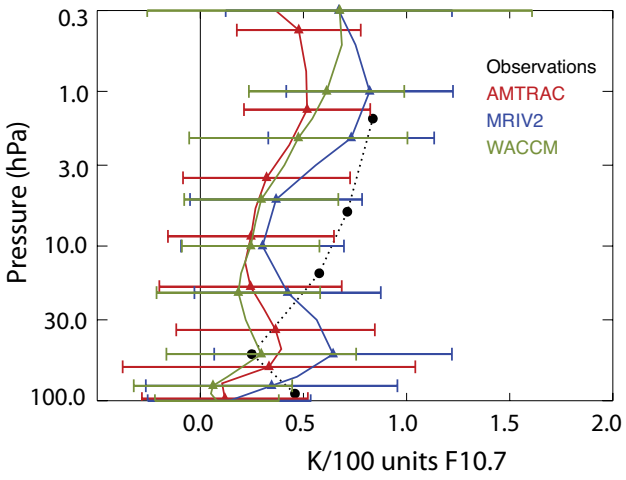

Figure 4-14. Temperature solar response averaged over the latitude range 25°S to 25°N. Units on x-axis in Kelvin per 100 units (in 10^{-22} W m^{-2} Hz^{-1}) of the solar radio flux at 10.7 cm (F10.7). The figure shows the results from ensemble simulations for models that consider the 11-year solar activity cycle. The analyzed periods are: 1960–2004 (AMTRAC), 1980–2004 (MRI), and 1950–2003 (WACCM). The solar cycle derived from SSU and MSU data is indicated by the dotted black line. Data derived from observations (1979–1997) were reprocessed from Scaife at al. (2000b). (From Figure 12 of Austin et al., 2008.)

gases via changes in stratospheric circulation that might be induced by climate change (e.g., Cook and Roscoe, 2009). As noted in Section 4.3.2, the stratospheric Brewer-Dobson circulation is likely to be modified in the presence of enhanced greenhouse gas concentrations. Certainly any change in the strength of the Brewer-Dobson circulation would alter the thermal structure of the stratosphere. Moreover, it must be considered that an intensified Brewer-Dobson circulation would affect stratosphere-troposphere mass transport and lead to a quicker turnover time of stratospheric air, i.e., lower age of stratospheric air.

The simulated mean temperature changes (i.e., multi-model mean values) from 1979 to 2000 derived from a subset of the CMIP3[2] coupled ocean-atmosphere climate model simulations are dominated by zonally symmetric radiative cooling due to ozone depletion. Based on this result Lin et al. (2009) concluded that the climate models fail to simulate the warming in the southern polar stratosphere (see Figure 4-6), indicating a lack of the Brewer-Dobson circulation strengthening in these models. This interpretation contradicts the statements given above referring to chemistry-climate model results. A reason could be that most of the climate models used do not adequately resolve the stratosphere and therefore inadequately reproduce the Brewer-Dobson circulation and its changes. On the other hand it is still questionable if the recent (1995–2008) warming of the polar lower stratosphere is a robust and statistically significant feature. Gravity wave parameterizations within the climate models may also contribute to these differences.

The stratospheric temperature trends simulated by the large ensemble of climate models available from the CMIP3 experiments have been evaluated in the IPCC Fourth Assessment Report, although the main emphasis there was on attribution of climate variations in the troposphere (Hegerl et al., 2007 in IPCC, 2007). Those climate models do not generally include stratospheric chemical processes but some include specified changes in stratospheric ozone concentrations. For example, Schwarzkopf and Ramaswamy (2008) analyzed simulations of a CMIP3 climate model (GFDL-CM2.1) for the period from 1861 to 2003. They showed that the global-mean cooling in the stratosphere (mainly due to enhanced CO_2 concentrations) became significant as early as the first quarter of the 20th century. Thereafter the magnitude of stratospheric cooling by mid-20th century at ~20–50 hPa exceeded the magnitude of the warming near the surface. By the late 1970s, significant stratospheric ozone depletion had begun, enhancing the cooling.

The observed global mean temperature trends in the troposphere and lower stratosphere for recent decades are simulated well by most chemistry-climate models (e.g., Figure 4-10), but are not generally as well simulated by some CMIP3 climate models (Figure 4-15; from Cordero and Forster, 2006). The observed global mean cooling trend in the lower stratosphere is grossly underestimated by climate models that do not include specified decreases in stratospheric ozone over the last three decades. Even climate models that include specified ozone decreases slightly underestimate the observed cooling trend (for details see Cordero and Forster, 2006). In addition, climate models that include specified increases in stratospheric volcanic aerosols appear to overestimate the warming of the lower stratosphere after major volcanic eruptions (Figure 4-15), possibly because they neglect the ozone changes associated with the eruption and do not include the influence of the stratospheric quasi-biennial oscillation (Dall'Amico et al., 2010a). Moreover, Waugh et al. (2009) showed that the calculated cooling simulated in response to ozone depletion is larger in a model with interactive chemistry (i.e., a chemistry-climate model) than that determined by the same underlying atmospheric general circulation model that prescribes the identical zonal mean ozone forcing.

Climate models have also been used to show that tropopause height variations are a sensitive indicator of temperature changes in the upper troposphere and lower stratosphere. They have enabled attribution of observed trends in mean tropopause height over the last three decades of the last century to the combined influence of increasing concentrations of greenhouse gases and aerosols and decreasing amounts of stratospheric ozone (Santer et al., 2003). More recently, Son et al. (2009a) investigated results derived from six chemistry-climate models and found that historical changes (since 1960) in tropopause height are linked to ozone depletion.

4.3.2 Simulation of Brewer-Dobson Circulation Trends in Chemistry-Climate Models

The Brewer-Dobson circulation is the stratospheric wave-driven circulation that transports mass and constituents upward in the tropics and poleward and downward at higher latitudes (see Section 4.2.2 for a more detailed description). In the 2006 Assessment (WMO, 2007), chemistry-climate models were found to consistently predict an acceleration of the Brewer-Dobson circulation in response to increasing greenhouse gas concentrations, amounting to an average increase of about 2%/decade in the annual mean net upward mass flux at 70 hPa through the 21st century. Butchart et al. (2006) also found that over half of the annual mean trend was explained by changes

[2] CMIP3 refers to simulations of 20th and 21st century climate organized by the Coupled Model Intercomparison Project Phase 3 for use in IPCC experiments (Meehl et al., 2007).

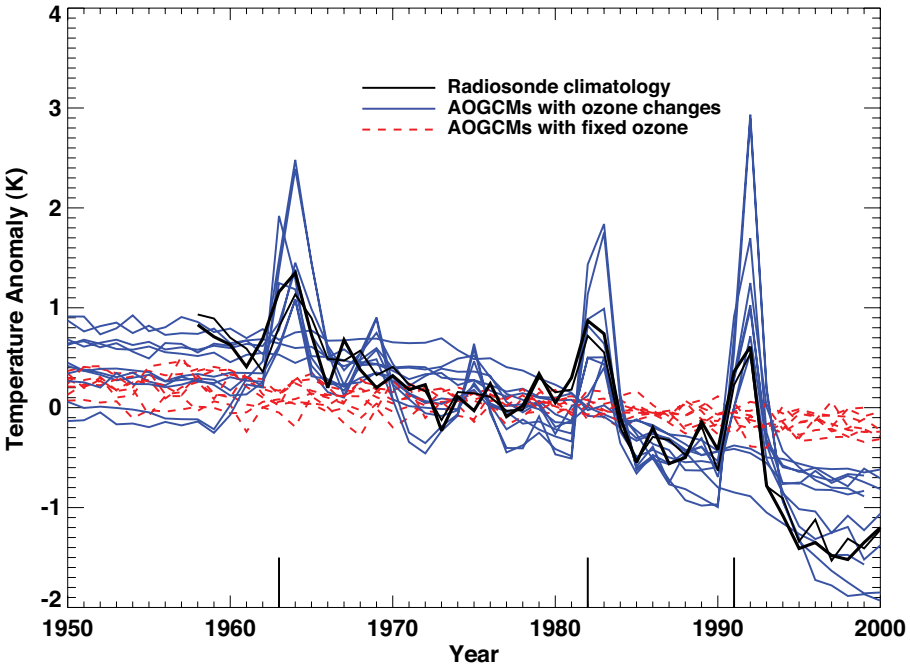

Figure 4-15. Time series of globally averaged annual temperature anomalies (K) at 50 hPa from radiosonde observations (black lines) and simulations of atmosphere-ocean general circulation models (AOGCMs; colored lines). Climate model simulations that included specified stratospheric ozone depletion, as well as increases in greenhouse gases and anthropogenic aerosols, are shown with blue lines, while model simulations that did not include stratospheric ozone depletion are shown with red dashed lines. Some, but not all, the models also include specified stratospheric volcanic aerosol amounts. Short vertical lines on the abscissa denote years of major volcanic eruptions. Figure modified from Cordero and Forster (2006).

in resolved wave drag, with the remainder assumed to be due to parameterized wave drag. They were unable to conclude whether changes in stratospheric ozone had any effect on the predicted trend in upward mass flux.

Subsequent to the previous Assessment (WMO, 2007) our understanding of the mechanisms driving the Brewer-Dobson circulation in simulations and its predicted future increase has advanced considerably. Chemistry-climate model intercomparison studies (Butchart et al., 2010; Chapter 4 of SPARC CCMVal, 2010) have shown that the ~2%/decade increase is a robust value for the lower stratosphere (Figure 4-16) in model simulations driven by comparable scenarios. Using a better set of model simulations (i.e., only transient simulations with common forcings using more mature models) and a more accurate calculation of the mass fluxes, Butchart et al. (2010) found that ~70% of the upward mass flux trend was due to parameterized orographic gravity wave drag, a value that was computed from only the subset of models that provided the gravity wave drag data. The importance of these waves in driving the acceleration of the Brewer-Dobson circulation has also been elucidated by a number of studies (Li et al., 2008; McLandress and Shepherd, 2009; Butchart et al., 2010). These studies have demonstrated that the predicted future increase in lower-stratospheric parameterized orographic gravity wave drag is a robust model response to climate change, resulting from the eastward acceleration of the subtropical jets which increases the gravity wave momentum flux reaching the lower stratosphere. While the parameterized momentum fluxes are not well constrained by observations, they do respond in a physically consistent manner to changes in the large-scale circulation. It should also be noted that the similarity of the model results might be due in part to the similarity of the orographic gravity wave parameterizations.

Another advance has been our understanding of the role of resolved wave drag. However, due to a lack of the necessary diagnostic data available for model intercomparison studies, only individual model studies have been undertaken. In comparing these studies, some caution is required since different definitions are used to characterize tropical upwelling. Using the net upward mass flux at 70hPa, McLandress and Shepherd (2009) examined the contributions from different zonal wavenumbers. They found that 60% of the net upward mass flux trend due to resolved wave drag resulted from planetary waves, with the remainder coming from synoptic waves. On the other hand, Garcia and Randel (2008) and Calvo and Garcia (2009) employed a fixed latitude range that did not encompass the subtropics to define tropical upwelling. In the former study the trend in tropical upwelling resulted from changes in resolved wave drag in the subtropical

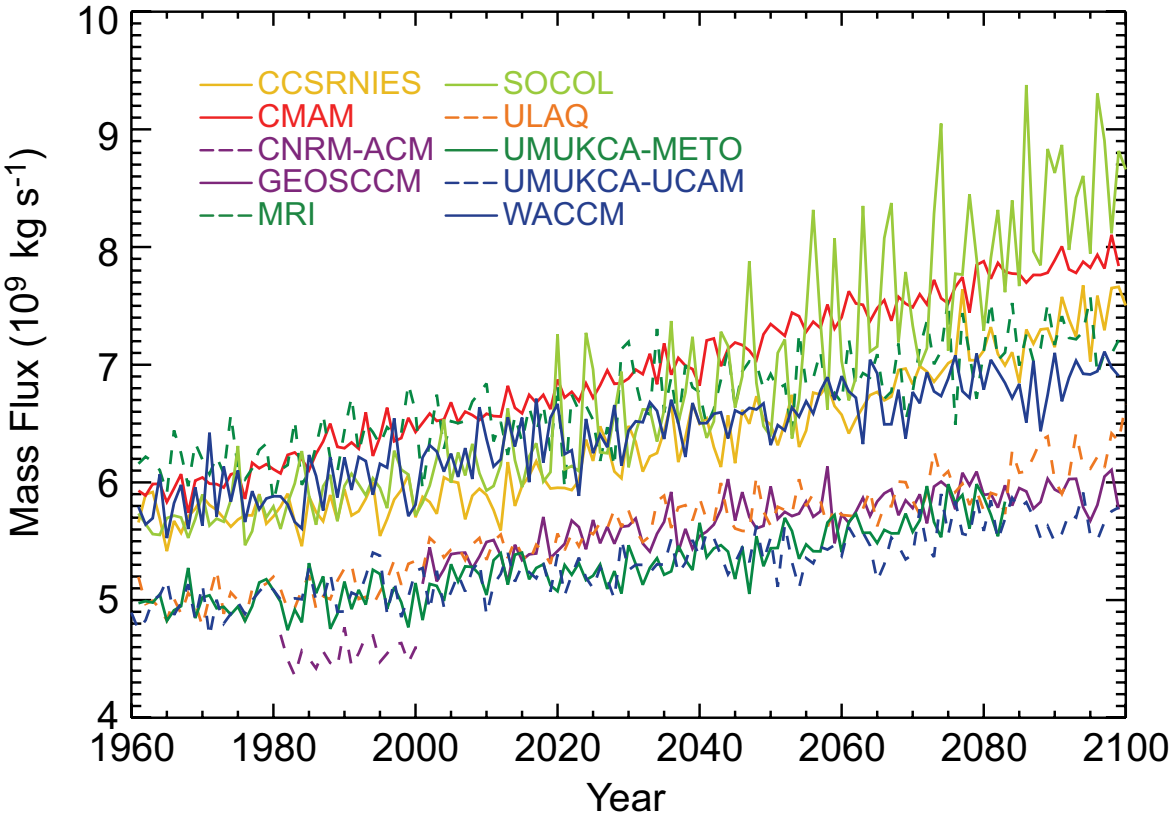

Figure 4-16. Annual mean upward mass flux (kg s^{-1}) at 70 hPa, calculated from residual mean vertical velocity between the turnaround latitudes of the Brewer-Dobson circulation, for the simulations prepared for the CCMVal SPARC report. See Table 3-1 in Chapter 3 of this Assessment for a description of the chemistry-climate models shown in the figure. Figure from Chapter 4 of SPARC CCMVal (2010).

lower stratosphere, which in turn resulted from enhanced wave propagation due to changes in the zonal mean zonal winds. Calvo and Garcia (2009) concluded that enhanced dissipation of quasi-stationary planetary waves forced by increased tropical convection were responsible for the upwelling trends, at least in a fixed latitude band. A similar conclusion about the role of convectively forced stationary waves was made by Deckert and Dameris (2008), although they did not quantify the impact of those waves on upwelling trends.

Consistent with the predicted increase in net upward mass flux, the mean age of stratospheric air is predicted to decrease (Austin and Li, 2006; Garcia and Randel, 2008; Oman et al., 2009; Butchart et al., 2010). Oman et al. (2009) examined the impact of a number of different factors affecting mean age, and concluded that their impact depended upon the time period examined. Over the past 40 years they found that ozone depletion was responsible for the simulated decrease in mean age, while later in this century after ozone has returned to 1980 levels, decreasing age was attributed to increasing greenhouse gas concentrations.

Another advance has been our understanding of the role of ozone depletion and recovery on the simulated net upward mass flux trends. Li et al. (2008) found that in the past nearly half of the trend in their simulations occurred in December-February. They attributed this to increased net downward mass flux in the Southern Hemisphere resulting from the delay in breakdown of the Antarctic polar vortex, which allowed Rossby waves to propagate higher into the summer stratosphere, thus driving the increased downwelling. The impact of ozone depletion (and recovery) on the upward mass flux trends was confirmed in McLandress et al. (2010) using a set of chemistry-climate model simulations in which greenhouse gas concentrations were held fixed in time and only ODSs were allowed to vary.

The role of parameterized orographic gravity wave drag in model simulations is better understood than the previous Assessment (WMO, 2007). However, much more needs to be done to validate such parameterizations, particularly since they play a key role in the simulated accelerations of the Brewer-Dobson circulation.

Various prescriptions exist for parameterizing the influences of unresolved gravity waves, but they are based on specifications of certain parameters that are not well constrained by observations at the present time. As long as chemistry-climate models are strongly dependent on the parametrization of gravity waves, the simulated changes in the Brewer-Dobson circulation will remain similarly dependent on the model treatment of such unresolved physical processes.

The mechanisms responsible for the increased resolved wave drag are also unclear. As discussed in McLandress and Shepherd (2009), differences in the way tropical upwelling is computed have made it difficult to come to a clear consensus on which types of resolved waves are responsible for the increase in the Brewer-Dobson circulation. Quantifying whether the increased resolved wave driving of the Brewer-Dobson circulation results from changes in wave sources in the troposphere or wave propagation in the stratosphere is an outstanding issue.

4.4 EFFECTS OF VARIATIONS IN STRATOSPHERIC CLIMATE ON THE TROPOSPHERE AND SURFACE

In this section we assess the linkages between stratospheric variability and climate change in the troposphere and at the Earth's surface. The section includes an assessment of radiative, dynamical and chemical coupling between the stratosphere and troposphere, but focuses primarily on the dynamical effects of the Antarctic ozone hole on surface climate. The evidence for a robust linkage between the Antarctic ozone hole and the surface flow in the Southern Hemisphere was assessed in Chapter 5 of WMO, 2007 (Baldwin and Dameris et al., 2007). Here we extend that assessment to include recent advances in our understanding of the linkages between the Antarctic ozone hole and surface climate change throughout the Southern Hemisphere. Key advances include a deeper understanding of the likely effects of Antarctic ozone depletion on surface weather, the circulation of the Southern Ocean, the distribution of Antarctic sea ice, and the Southern Hemisphere carbon cycle.

The primary novel effects of stratospheric climate variability on surface climate assessed in this section are summarized in Table 4-1. The text in Section 4.4 is organized into five components as follows:

Section 4.4.1, stratospheric composition and global-mean surface temperatures

Section 4.4.2, the Antarctic ozone hole and changes in Southern Hemisphere surface climate

Section 4.4.3, stratospheric climate change and the tropical tropospheric circulation

Section 4.4.4, stratospheric variability and tropospheric chemistry

Section 4.4.5, solar-induced variability at stratospheric levels and tropospheric climate

4.4.1 Effects of Stratospheric Composition Changes on Global-Mean Surface Temperature and Tropospheric Temperature

Previous World Meteorological Organization (WMO) Ozone Assessments (e.g., WMO, 2007) and the recent IPCC Assessment (IPCC, 2007) have evaluated radiative forcings associated with changes in stratospheric climate. Radiative forcings give an indication of surface temperature change, whereby positive forcings enhance the global mean surface temperature and negative forcings tend to cool the surface. Stratospheric ozone was most recently assessed to give a net radiative forcing of -0.05 ± 0.1 W/m^2 between 1750 and 2005 (Forster et al., 2007a). Water vapor concentration changes associated with methane oxidation between 1750 and 2005 were assessed to contribute a forcing of $+0.07 \pm 0.05$ W/m^2. The amount of stratospheric aerosol following volcanic eruptions can exert a strongly negative forcing on a short timescale, estimated to be roughly -3 W/m^2 following the eruption of Mt. Pinatubo. Note that volcanic eruptions can also have indirect forcings by affecting concentrations of ozone (see Chapter 3) and stratospheric water vapor (e.g., Joshi and Jones, 2009). The direct forcing of solar changes since 1750 is estimated to be small, although uncertainties exist in long-term trends in solar irradiance, in variations in its spectral composition, and also in its indirect effects on stratospheric ozone.

Figure 4-17 shows the ozone forcing since the 1970s evaluated from chemistry-climate models and observations using a single radiation model from Chapter 10 of SPARC CCMVal (2010). The 1970s-to-2004 radiative forcing is estimated to be -0.03 ± 0.2 W/m^2 (90% confidence range) from stratospheric ozone changes in 17 chemistry-climate model runs and $+0.03$ W/m^2 employing Randel and Wu (2007) observations. Negative net radiative forcings arise from models with ozone decline in the lowermost stratosphere, particularly at or near the tropopause. This stratospheric ozone forcing is not entirely of anthropogenic origin, but includes components due to the indirect effect of volcanic eruptions and solar irradiance change. The large spread is possibly due to an incorrect ozone response to volcanic eruptions in certain chemistry-climate models (Chapter 10 of SPARC CCMVal, 2010). Including the uncertainty in radiative transfer modeling would be unlikely to increase the uncertainty range (Chapter 3 of SPARC CCMVal, 2010). As differences between

Table 4-1. Highlights of Section 4.4: How stratospheric climate variations affect the troposphere and surface.

Affected Tropospheric Climate Parameters	Currently Observed Effects	Currently Understood Causes	Level of Scientific Understanding
1. Global radiative balance affecting global mean surface temperature (Section 4.4.1)	• Slight negative long-term radiative forcing from stratospheric ozone variations • Slight positive long-term radiative forcing from stratospheric water vapor from methane oxidation • Large decadal fluctuations in radiative forcing from stratospheric water vapor	Stratospheric ozone trends, stratospheric water vapor trends, stratospheric aerosol trends, and other greenhouse gas trends affect stratospheric temperatures. These affect both the shortwave and long-wave components of the radiative budget.	Very Strong
2. Tropical tropospheric temperature (Section 4.4.1)	Tropical upper-tropospheric cooling trend	Reduced tropical stratospheric ozone cools stratospheric temperatures. This reduces longwave radiative flux into the tropical troposphere.	Medium
3. Antarctic tropospheric temperature (Section 4.4.1)	Late spring and summer Antarctic tropospheric cooling	ODS-induced stratospheric ozone loss cools Antarctic stratosphere. This reduces longwave radiative flux into the Antarctic troposphere.	Medium-Strong
4. Southern Annular Mode (SAM) (Section 4.4.2.1)	Trend to positive index of SAM in Southern Hemisphere summer. Evident as falls in geopotential height over the pole and an eastward acceleration of the surface winds over the Southern Ocean.	ODS-induced stratospheric ozone loss cools the Antarctic stratosphere. This induces a stratospheric dynamical response that couples to the tropospheric SAM.	Strong
5. Southern Hemisphere extratropical winds, storm tracks, and precipitation (Section 4.4.2.2)	• Poleward shift of Southern Hemisphere extratropical jet in summer • Reduced low pressure systems at low latitude and increased at high latitudes • Poleward shift of Southern Hemisphere precipitation	Effects 5–9 are all related to the summertime tropospheric SAM trend (climate parameter 4.), which is caused by ODS-induced Antarctic stratospheric cooling.	Medium
6. Antarctic surface temperatures (Section 4.4.2.3)	• Summertime warming of Antarctic Peninsula and cooling trend of East Antarctic High Plateau		Medium-Strong
7. Antarctic sea ice (Section 4.4.2.3)	• Increase in summertime Antarctic sea ice extent		Medium
8. Southern Ocean temperatures and circulation (Section 4.4.2.4)	• Warming of Southern Ocean subsurface and poleward shift of Southern Ocean density structure		Low-Medium
9. Southern Ocean carbon cycle (Section 4.4.2.4)	• Reduction in Southern Ocean carbon uptake		Low-Medium
10. Width of tropical belt (Section 4.4.3)	Widening of tropical belt, with accompanying poleward shift of the jet streams, the downward branches of the Hadley Cell, and the region of high tropical tropopause	Attributed both to ODS-induced Antarctic ozone depletion and greenhouse warming.	Low

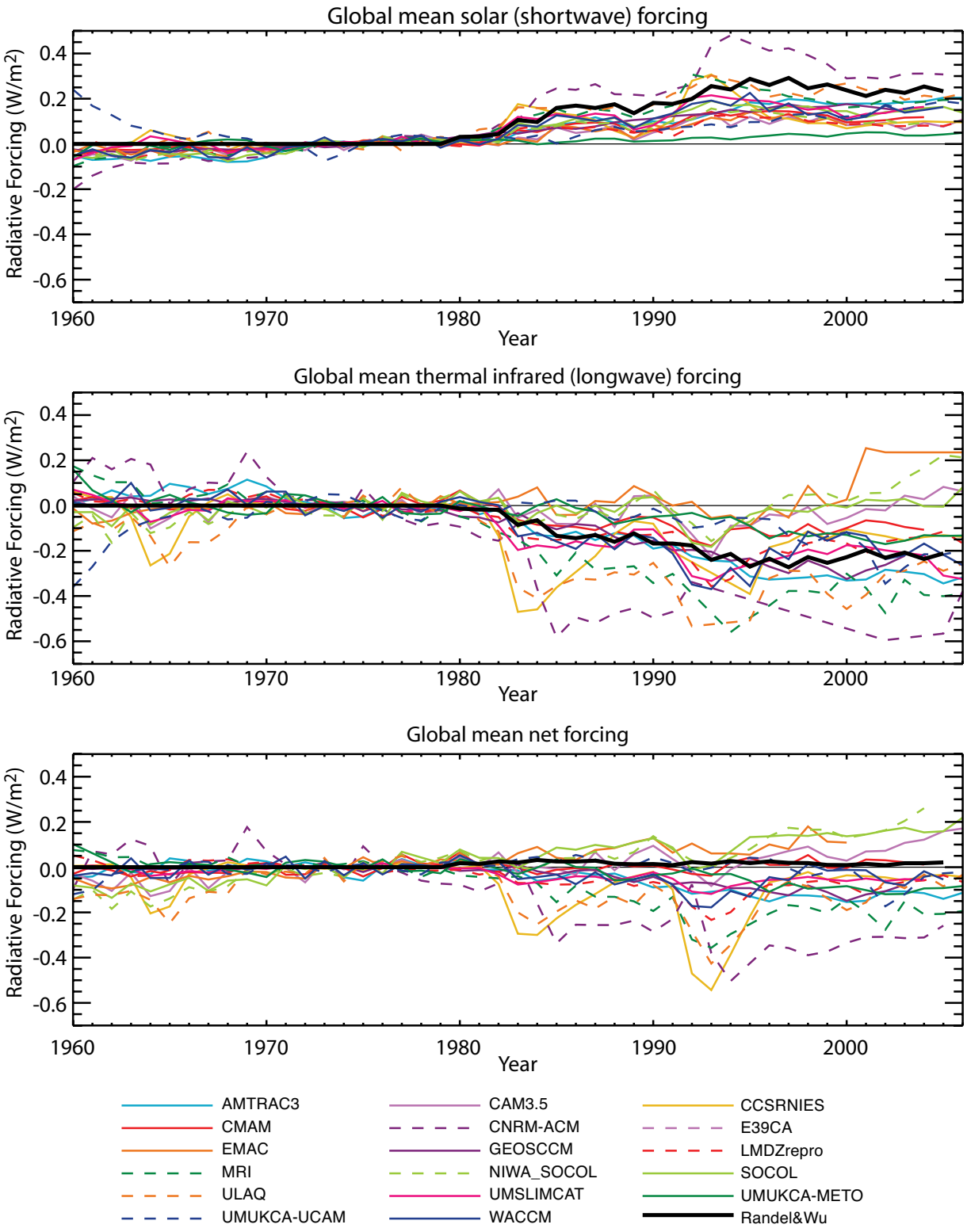

Figure 4-17. Stratospheric ozone global-mean radiative forcing (W/m^2) for shortwave (top), longwave (middle) and net (shortwave plus longwave) compared to the 1970s average, evaluated from the CCMVal REF-B1 scenario ozone fields (colored lines) and from the Randel and Wu (2007) observation-based data set (thick black line). See Table 3-1 in Chapter 3 of this Assessment for a description of the chemistry-climate models shown in the figure. Based on Chapter 10 of SPARC CCMVal (2010).

the SPARC CCMVal calculations and the IPCC assessment of the stratospheric ozone forcing are small, the IPCC assessment of this forcing is retained.

Decadal radiative effects of stratospheric composition changes are significant when compared to that from carbon dioxide, whose forcing increased by roughly 0.2 W/m^2 per decade since 1980 (Forster et al., 2007b). Solomon et al. (2010) estimated that the drop in stratospheric water vapor levels near the tropopause following 2000 (see Section 4.1.3) contributed a forcing of −0.1 W/m^2. They show that decadal variation of stratospheric water vapor concentrations likely contributed to an enhanced rate of surface warming in the 1990s (see also Forster and Shine, 2002) and a reduced rate of surface warming in the 2000s (see Figure 4-18).

Volcanic aerosols directly affect surface climate by reflecting solar radiation to space. Major volcanic eruptions cool global average surface temperatures for a few years following an eruption (Hansen et al., 1992; Robock, 2000), and also influence the patterns of Northern Hemisphere surface climate through effects on the Northern Annular Mode (e.g., Shindell et al., 2004; Stenchikov et al., 2006). Several studies have underscored that a major volcanic eruption not only perturbs the atmosphere but also cools the oceans, thereby affecting ocean heat uptake, sea level, and climate for many decades (Church et al., 2005; Delworth et al., 2005; Gleckler et al., 2006; Domingues et al., 2008; Gregory et al., 2006; Stenchikov et al., 2009). Thus the timescale over which volcanic effects need to be considered in climate studies is much longer than the time over which the aerosols are present in the stratosphere, and is controlled by multiple factors, including not only the stratospheric timescales but also the slow transport time within the deep ocean.

Recent studies have shown that the changes in radiative forcing from changes in stratospheric composition manifest themselves by directly changing temperatures in the free troposphere. This is in addition to any surface mediated temperature change. Parts of the observed tropospheric temperature trend in both the tropics and Southern Hemisphere polar regions have been linked to stratospheric ozone depletion and the associated stratospheric cooling trends (Forster et al., 2007b; Keeley et al., 2007; Grise et al., 2009).

In the tropics, observed cooling trends over 1985–2005 above 12 km in the upper troposphere do not appear to be linked to the local radiative impacts of ozone depletion in the upper troposphere but rather to the reduced downwelling longwave radiation associated with ozone depletion in the lower stratosphere (Forster et al., 2007b). The observed tropical upper-tropospheric temperature trends above 12 km are not well reproduced in climate model simulations, especially those with simple ozone prescriptions, suggesting the importance of properly prescribing tropical lower-stratospheric ozone in future

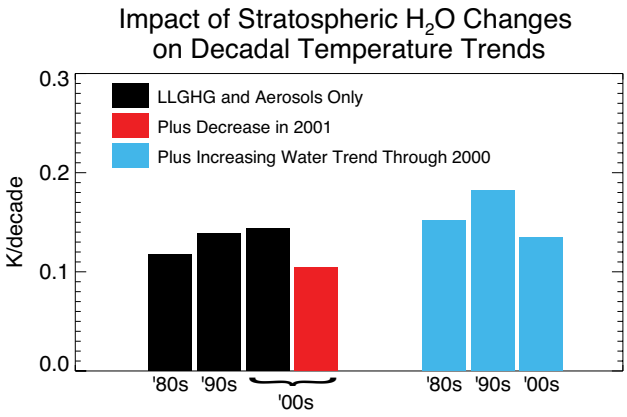

Figure 4-18. Decadal warming rates (K/decade) arising from (i) the long-lived greenhouse gases (LLGHG) and aerosols alone (black), as well as (ii) that obtained including the stratospheric water decline after 2000 (red) and (iii) including both the stratospheric water vapor decline after 2000 and the increase in the 1980s and 1990s (cyan). Based on Solomon et al. (2010).

climate modeling studies of the tropical upper troposphere (Forster et al., 2007b; Allen and Sherwood, 2008).

Several recent studies have suggested that the observed summertime cooling trends in the Antarctic free troposphere are at least partially attributable to decreases in downwelling longwave radiation emitted from the Antarctic lower stratosphere (Keeley et al., 2007; Grise et al., 2009). The decreases in downwelling longwave radiation appear to be driven primarily by the stratospheric temperature changes associated with ozone depletion (Grise et al., 2009), particularly the ozone depletion above the lowermost stratosphere (Keeley et al., 2007). A caveat to the above studies is that they prescribe zonally symmetric stratospheric ozone concentrations for their radiative calculations. Zonal asymmetries in prescribed ozone concentrations at Southern Hemisphere high latitudes have been shown to cause additional cooling in the stratosphere and upper troposphere (e.g., Waugh et al., 2009; Gillett et al., 2009), but most of this additional cooling appears to be driven by dynamical rather than radiative processes (Crook et al., 2008). Dall'Amico et al. (2010b) also show the importance of representing global ozone variability including the stratospheric quasi-biennial oscillation for simulating ozone-climate effects.

4.4.2 Surface Climate Impacts of the Antarctic Ozone Hole

As discussed in Section 4.2 and in Chapter 5 of the previous Ozone Assessment (Baldwin and Dameris

et al., 2007), the robust stratospheric cooling in the Antarctic spring associated with the ozone hole is coincident with an anomalous eastward[3] acceleration of the stratospheric polar vortex, and hence a delay in the springtime breakdown of the Southern Hemisphere stratospheric vortex. The trends in the Southern Hemisphere extratropical flow are not limited to stratospheric levels, but extend to Earth's surface during the spring/summer months of December and January, when the trends in the atmospheric flow are dominated by a poleward shift of the tropospheric zonal winds of the Southern Hemisphere (Thompson and Solomon, 2002; WMO, 2007). In WMO (2007), this tropospheric response was attributed to the Antarctic ozone hole, primarily based on the observational study of Thompson and Solomon (2002) and the modeling study of Gillett and Thompson (2003). In this section, we assess work since WMO (2007) on this stratosphere-troposphere connection and its implication for the surface climate of high southern latitudes.

In the stratosphere and troposphere, the spatial structure of the observed extratropical trends projects strongly upon the dominant and most persistent pattern of natural variability in the extratropical circulation: the Southern Annular Mode (Thompson and Wallace, 2000; Thompson and Solomon, 2002; Gillett and Thompson, 2003)[4]. In fact, the observational and modeling evidence outlined in Chapter 5 of the previous Ozone Assessment (Baldwin and Dameris et al., 2007) strongly suggests that the dynamical influence of the ozone hole on surface climate is manifested almost entirely in the structure of the Southern Annular Mode. However, we emphasize that the projection is clearest in the zonal mean and that the Southern Annular Mode does not account for all aspects of Southern Hemisphere climate trends: the trend in the annular mode is largest during summer (as noted below), it does not account for many zonally varying aspects of recent Southern Hemisphere climate change, and it may not fully account for zonally asymmetric forcing by ozone depletion (e.g., Crook et al., 2008).

That the response to the ozone hole is related to a persistent and dominant mode of internal variability like the Southern Annular Mode is expected based on general theoretical grounds (e.g., Leith, 1975; Gerber et al., 2008; Ring and Plumb, 2008) and also the fact that the annular mode dynamically connects the stratospheric and tropospheric circulations (Thompson and Wallace, 2000). The detailed dynamics of this stratosphere-to-troposphere link are still being explored; they have been linked to direct driving of the circulation by diabatic heating and changes to the eddy-induced stresses, to eddy mean-flow interactions in which the mean flow changes feed back onto the transient eddy driving field, to barotropic-mode dynamics, and to radiative driving (e.g., see Song and Robinson, 2004; Esler et al., 2006; Thompson et al., 2006; Simpson et al., 2009; Grise et al., 2009). But at this point, the precise dynamical mechanism(s) by which the tropospheric circulation responds to ozone depletion have not been fully elucidated.

Since WMO (2007), the robustness and seasonality of the tropospheric circulation response to Antarctic ozone depletion has been established in numerous climate simulations (e.g., Arblaster and Meehl, 2006; Miller et al., 2006; Cai and Cowan, 2007; Karpechko et al., 2008; Perlwitz et al., 2008; Fogt et al., 2009; Son et al., 2008, 2009b, 2010; Chapter 10 of SPARC CCMVal, 2010). Figure 4-19

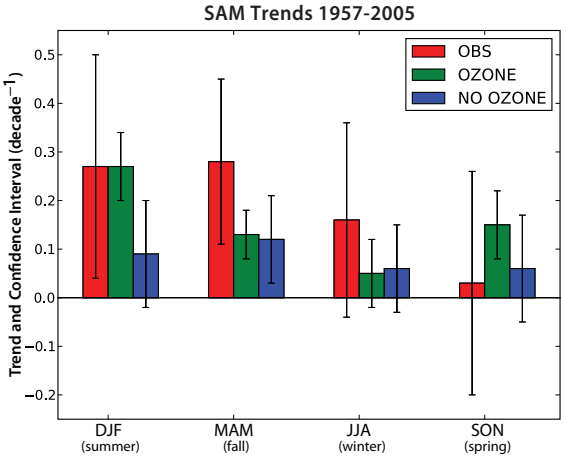

Figure 4-19. Seasonal trends over 1957–2005 in the SAM index (in units of decade^{-1}) from observations and the CMIP3 climate models with ("OZONE") and without ("NO OZONE") time-varying ozone forcing. The 95% confidence intervals reflect the number of time series involved in the trend analysis (see Fogt et al. 2009 for details). Data taken from Table 3 of Fogt et al. (2009).

3 When used in the context of the wind, "eastward" (toward the east) is synonymous with "westerly" (from the west). We use the "eastward" terminology throughout this chapter since the term "westerly" has an ambiguous definition depending on what it is used to describe.

4 The Southern Annular Mode (SAM) is the dominant pattern of variability in the Southern Hemisphere extratropical circulation (e.g., see Thompson and Wallace 2000 and discussions in Chapter 5 of WMO, 2007). Typically, it is defined to be the leading empirical orthogonal function (EOF) of the Southern Hemisphere geopotential or zonal wind. For an EOF calculation using monthly mean time series and using all months of the year, the SAM based on (1) zonally varying 850 hPa geopotential, (2) zonal mean 1000-50 hPa geopotential, and (3) zonal mean 1000-50 hPa zonal wind respectively explains (1) 27%, (2) 47%, and (3) 45% of the variance (Table 2 of Thompson and Wallace, 2000). In the troposphere, SAM variability is characterized by meridional excursions of the tropospheric jet. During the Southern Hemisphere spring, the SAM also corresponds to variations in the strength of the polar vortex in the stratosphere. SAM dynamics is understood to reflect interactions between waves and the zonal mean flow (e.g., Limpasuvan and Hartmann 2000).

(based on Table 3 of Fogt et al., 2009) provides an updated view of observed and simulated tropospheric circulation trends expressed in terms of the Southern Annular Mode. The positive trends in the Southern Annular Mode are most robust in observations and models during the austral summer and fall seasons (labeled DJF and MAM, respectively). During the austral summer season, a statistically significant positive Southern Annular Mode response is simulated only in those integrations that include the observed Antarctic ozone depletion (labeled "OZONE" in the figure). During the austral fall season, the simulated trends are half the observed value and occur whether or not ozone forcing is present. In the austral winter (labeled JJA), the observed and simulated trends are not significant. In the austral spring (labeled SON), there is a poorly understood discrepancy between the models and observations: the "OZONE" models produce a positive Southern Annular Mode trend when none is observed (Fogt et al., 2009).

The following caveat must be considered when interpreting the results in Figure 4-19: different models are included in the "OZONE" and "NO OZONE" sets in the figure, so it is difficult to cleanly attribute the Southern Annular Mode trend to ozone-related forcing in these simulations. We can begin to assess the separate effects of ozone and greenhouse gas forcing from a limited number of studies. For example, when ozone and greenhouse gas forcings are prescribed separately in the National Center for Atmospheric Research Community Climate System Model, it is clear that ozone forcing drives the primary Southern Annular Mode response in summer (Arblaster and Meehl, 2006). In addition, Sigmond et al. (2010) use timeslice integrations of the Canadian Middle Atmosphere Model to examine the effect of coupling to a dynamical ocean and sea ice model on the summertime Southern Annular Mode response to the ozone hole in the absence of greenhouse gas forcing. They find that the summertime Southern Annular Mode response is similar whether the ocean and sea ice state is prescribed or predicted. This implies that the ocean and sea ice response to the ozone hole have not caused further changes to the surface wind response to the ozone hole.

In the following subsections we assess our improved understanding of the surface climate impacts of the ozone-forced trends in the tropospheric circulation. We discuss how the trends in Figure 4-19 have affected the high-latitude climate of the Southern Hemisphere, including surface circulation and precipitation (Section 4.4.2.1), surface temperatures and sea ice (Section 4.4.2.2), Southern Ocean temperatures and circulation (Section 4.4.2.3), and the Southern Ocean's contribution to the global carbon cycle (Section 4.4.2.4). Research in this area has advanced rapidly since the previous Assessment. In the absence of Arblaster and Meehl (2006)-type studies in which ozone and greenhouse gas forcing are separately applied within coupled ocean-atmosphere climate models, we are not able to quantitatively assess the net impact of ozone forcing on the annual mean forcing of the Southern Annular Mode trends for the broader set of coupled climate models. There is an urgent need for such simulations to more precisely connect ODS-related ozone depletion to Southern Hemisphere climate change.

Climate impacts of Northern Hemisphere ozone depletion are not covered in this Assessment, since no definitive connection has been made between Northern Hemisphere ozone depletion and surface climate (e.g., Figure 4-9; Thompson and Solomon, 2005), despite the presence of pronounced stratosphere-troposphere coupling in association with dynamic variability in the stratospheric vortex (e.g., Baldwin and Dunkerton, 2001). The lack of an ozone-surface climate response in the Northern Hemisphere is consistent with the weak ozone losses observed there (Chapter 2; Solomon et al., 2007) and thus the weak radiative forcing and temperature trends in the Arctic stratosphere that are masked by relatively high natural variability in some seasons (Grise et al., 2009; Section 4.2).

4.4.2.1 Effects on Winds, Storm Tracks, and Precipitation

The austral summer trends in the Southern Annular Mode and strengthening of the eastward winds over the Southern Ocean are associated with a poleward shift of the extratropical jets in the Southern Hemisphere troposphere in summer (Gillett and Thompson, 2003; Archer and Caldeira, 2008). As would be expected from such a shift, observational studies reveal reductions in the number of low pressure systems and extratropical storms in Southern Hemisphere middle latitudes (e.g., Simmonds and Keay, 2000; Rao et al., 2003; Vera, 2003; Bengtsson et al., 2006; Pezza et al., 2007, 2008) and increases at high latitudes (e.g., Lynch et al., 2006). These changes in the storm tracks are apparent in both winter and summer. There are some suggestions of increases in the intensity of storms in the storm track (Simmonds and Keay, 2000) but a more recent analysis suggests that this result might be an artifact of changes in the available input data for the reanalyses considered (Bengtsson et al., 2006).

Onshore winds and extratropical weather systems are the causes of much of the precipitation over land in Southern Hemisphere middle latitudes. Hence, the changes in the Southern Annular Mode and the Southern Hemisphere storm track are expected to have led to changes in precipitation. Many recent studies have considered observed changes in regional precipitation over the past few decades and links to changes in Southern Hemisphere circulation. They have tried to separate the influences of the Southern Annular Mode from those due to decadal variations in El Niño-Southern Oscillation, the two major

factors affecting circulation variations in the Southern Hemisphere middle latitudes. No studies have directly attributed observed regional precipitation changes in summer to stratospheric ozone depletion yet, probably due to the large variability of regional precipitation and the sparse network of observing stations. However, a recent analysis of the CMIP3 ensemble of climate model simulations (CMIP3 is defined in Footnote 2 in Section 4.3.1) suggests a signal due to stratospheric ozone depletion in the multi-model average that includes increases in summer precipitation in the Southern Hemisphere high latitudes and decreases in middle latitudes due to stratospheric ozone depletion (Son et al., 2009b). This signal is likely to have contributed to observed changes in precipitation but might not be apparent relative to natural variability.

During the summer season, the positive polarity of the Southern Annular Mode is linked to increased precipitation in southeastern Australia (Gillett et al., 2006; Hendon et al., 2007; Meneghini et al., 2007) and South Africa (Gillett et al., 2006) and reduced precipitation in southwest New Zealand (Renwick and Thompson, 2006; Griffiths, 2006; Ummenhofer et al., 2009) and southwest South America (Gillett et al., 2006).

The increase in wind speeds over the Southern Ocean can generate more sea spray and lead to increases in natural cloud condensation nuclei for the formation of reflective low clouds in Southern Hemisphere summer (Korhonen et al., 2010). In a modeling study using observed wind trends input into an global aerosol model, Korhonen et al. (2010) find that the Southern Hemisphere wind trends since the 1980s give rise to a more than 20% increase in cloud condensation nuclei concentrations in the 50°S –65°S latitude band and a negative cloud radiative forcing of −0.7 W/m^2. The latter, when added to the negative radiative forcing from stratospheric ozone loss, gives an ozone-related regional negative radiative forcing comparable to the positive radiative forcing from greenhouse gas increases over the same period.

4.4.2.2 Effects on Surface Temperatures and Sea Ice

The ozone hole-related summertime trends in the Southern Annular Mode are also linked to changes in Antarctic surface temperatures and sea ice. The Antarctic Peninsula region has experienced exceptional recent warming in austral summer (in excess of 1°C/decade at some stations) since the late 1970s, greatly exceeding the global average and making it one of the fastest changing regions on Earth (e.g., Marshall et al., 2006; Zazulie et al., 2010). In contrast, a summer seasonal cooling trend has been noted at stations on the high plateau of east Antarctica (e.g., Thompson and Solomon, 2002; Turner et al., 2005), and these are linked to the previously noted circulation changes. The stronger eastward flow associated with the recent summertime trend in the Southern Annular Mode has reduced the effectiveness of blocking by the topography of the peninsula, allowing more maritime airmasses to penetrate across the peninsula and causing summer season warming on the east side of the peninsula that is three times stronger than that observed on the west side (Marshall et al., 2006). Thus both the spatial and seasonal patterns of the observed summertime surface climate changes in the past several decades support the identification of the Southern Annular Mode and ozone loss as a key factor in summertime climate change over much of Antarctica. The breakup of the Larsen-B ice shelf in 2002 was likely due at least in part to the remarkable warming in the Antarctic Peninsula region (Marshall et al., 2006).

The effect of changes in circulation on Antarctic sea ice has been probed using numerical analyses constrained by observed (reanalyzed) winds and temperatures (Goosse et al., 2009). This approach suggests that strengthening of the eastward winds has likely affected the spatial pattern of sea ice distributions, mainly through changes in sea ice advection (Goosse et al., 2009). The spatial pattern of satellite-observed recent changes in sea ice, with increased ice extent in the Ross Sea region and decreases near the peninsula, is well reproduced when atmospheric circulation and temperature changes are considered (as shown in Figure 4-20, taken from Goosse et al., 2009). Atmospheric circulation changes in response to ozone loss have been probed by several models, including e.g., Gillett and Thompson (2003) and Turner et al. (2009). Natural variability in the Southern Annular Mode, the El Niño-Southern Oscillation and/or the Pacific Decadal Oscillation may also contribute to recent trends in sea ice (Udagawa et al., 2009), as could other factors such as changes in precipitation or ocean heat transport (Zhang, 2007).

The very sparse spatial coverage of long-term Antarctic temperature records makes it difficult to derive trends averaged over the continent as a whole. Recently, reconstruction methods employing statistical approaches to data filling have been employed to derive trends averaged across Antarctica, drawing from composites using a range of station data, ice cores, and available automated weather stations (Chapman and Walsh, 2007; Monaghan et al., 2008; Steig et al., 2009). Strong warming has been derived for the west Antarctic region in some of these analyses (e.g., Steig et al., 2009), although this is heavily dependent on data from a single record (Byrd station). The most recent reconstruction suggests that Antarctica taken as a whole shows warming when the time period since 1957 is considered (Steig et al., 2009), although weaker warming is seen in some other reconstructions from 1960 (see Figure 4-21). Steig et al. (2009) and Gillett et al. (2008) suggest an important role for greenhouse gases in driving Antarctic temperatures especially prior

to onset of the ozone hole. This finding does not contradict the recent summer season cooling observed over east Antarctica since 1980 in association with the ozone hole; indeed those observations are included in the analysis (see Figure 4-21).

4.4.2.3 Effects on Southern Ocean Temperatures and Circulation

The summertime trend in the Southern Annular Mode implies an associated poleward shift and intensification of the surface zonal wind stress field and its curl (Oke and England, 2004; Cai and Cowan, 2007; Fyfe et al., 2007). In this subsection, we discuss the implications of the poleward intensification of the surface wind stress for the Southern Ocean temperature and circulation. Greenhouse gas forcing and ozone forcing both appear to affect the tropospheric surface winds, with the ozone-forced signal peaking in austral summer (e.g., Kushner et al., 2001; Thompson and Solomon, 2002; Gillett and Thompson, 2003; Miller et al., 2006; Arblaster and Meehl, 2006; Haigh and Roscoe, 2009). The following discussion is thus relevant to projections of Southern Ocean change under increasing greenhouse gases and ozone recovery (Section 4.5). However, we will focus on effects that can be plausibly linked to tropospheric impacts of stratospheric ozone depletion. Southern Ocean impacts also have implications for global climate and the Southern Ocean carbon cycle (Section 4.4.2.4).

Some of the influence of surface wind stress on the Southern Ocean can be understood by using surface wind stress and its curl to diagnose Ekman transport and pumping (e.g., Fyfe and Saenko, 2006; Cai and Cowan, 2007). In the classical description, the surface eastward winds drive (1) the eastward Antarctic Circumpolar Current and (2) a meridional overturning circulation that consists of upwelling to the south of the Antarctic Circumpolar Current, northward flow at the surface at the latitude of the current, and downwelling to the north of the current. When ozone forcing results in a poleward intensification of the surface wind stress field, the Antarctic Circumpolar Current and wind-driven overturning circulation are expected to similarly undergo a poleward intensification. From the preindustrial period to the end of the 20th century, Fyfe and Saenko (2006) diagnose, on the basis of wind stress output from the CMIP3 models, a poleward shift of about 0.9 degrees latitude and a 5% strengthening of the Antarctic Circumpolar Current for the ensemble mean of the CMIP3 models. Cai and Cowan (2007) find that the ensemble mean of the CMIP3 "OZONE" simulations (which include ozone depletion) produce a zonal wind stress trend (expressed as a Southern Annular Mode trend) that is consistent with trends inferred from National Centers for Environmental Prediction/National Center for Atmospheric Research reanalyzed winds, and diagnose an accompanying change to the wind-driven ocean circulation in the subtropics and extratropics for these simulations. Consistent with Miller et al. (2006) and Son et al. (2009b), Cai and Cowan (2007) find that the "NO OZONE" simulations do not, on average, produce a realistic wind stress/Southern Annular Mode trend.

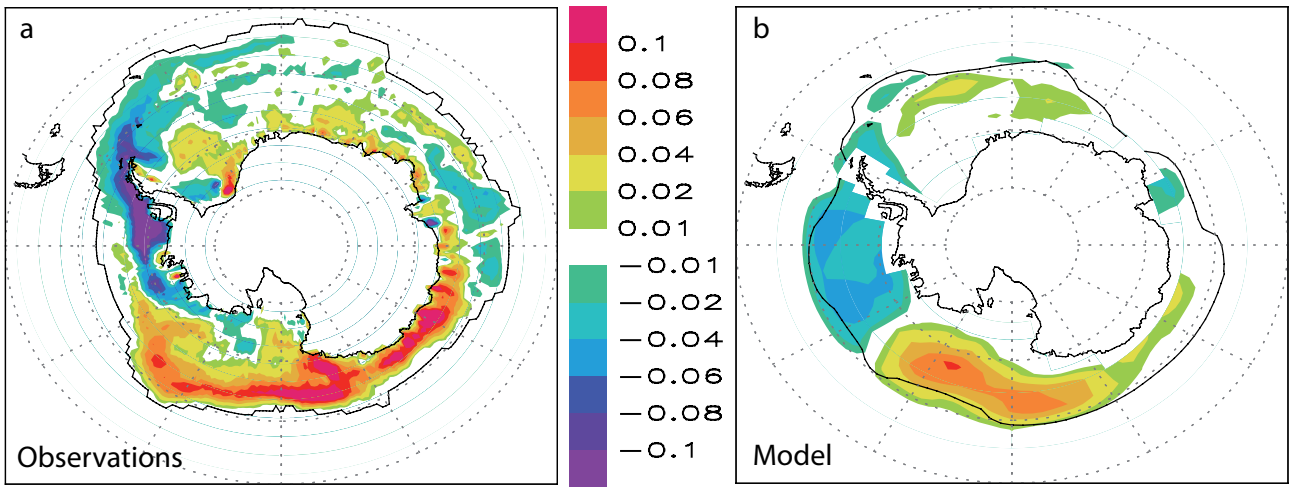

Figure 4-20. The trend of annual-mean sea ice concentration over the period 1980–2000 for (a) the observations (Rayner et al., 2003) and (b) for the model results averaged over the six simulations with data assimilation (units are the fractional change per decade). The black line represents the location of the climatological average September ice edge, as defined by an annual ice concentration equal to 15%, for the observations (a) and the model (b). Based on Goosse et al. (2009).

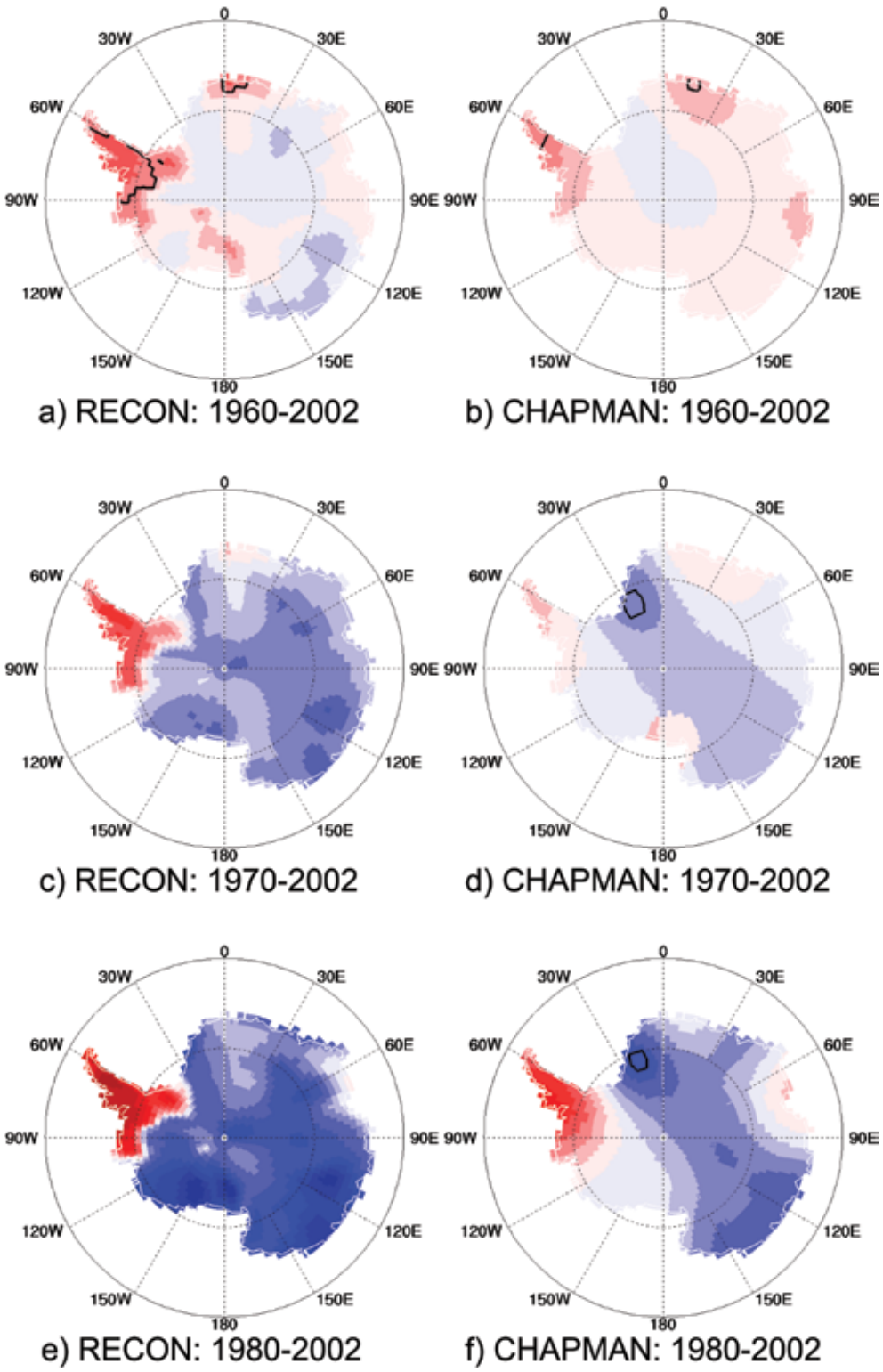

Figure 4-21. Spatial plots of the temporal trends (K/decade) of annual near-surface temperature for three different periods: (a and b) 1960–2002, (c and d) 1970–2002, and (e and f) 1980–2002. Figures a, c, and e are from the RECON temperature reconstruction, and Figures b, d, and f are from the CHAPMAN temperature reconstruction (figure from Monaghan et al., 2008; reconstructions described in that paper).

Key oceanographic observations[5] and ocean model analysis support the viewpoint that the ocean circulation responds to the wind stress changes in a manner consistent with wind-driven ocean circulation theory. In particular, a significant temperature trend to depths up to 1200 m has been observed in the Antarctic Circumpolar Current (Gille, 2002, 2008; Aoki et al., 2003; Sprintall, 2008; Böning et al., 2008). Figure 4-22a shows observed oceanic temperature trends as a function of depth and dynamic height, which serves as a meridional coordinate, from Gille (2008). There is strong subsurface warming in the Antarctic Circumpolar Current, which is located in the 0.4–1.2 m dynamic height range. The subsurface warming is in large part consistent with a poleward shift of the ocean temperature structure by 1° latitude every 40 years (Figure 4-22b): 87% of the trend below 200m in the Antarctic Circumpolar Current region is explained by this construction. Important aspects of trends in the Antarctic Circumpolar Current region are reproduced in ocean models and in the CMIP3 coupled models, which allow a significant portion of the subsurface warming to be attributed to changes in the wind stress field (Oke and England, 2004; Fyfe, 2006; Fyfe et al., 2007; Gille, 2008). For example, Oke and England (2004), using an ocean model driven by prescribed atmospheric forcings, and Fyfe et al. (2007), using an ocean model coupled to a simplified atmospheric model, obtain intensified subsurface warming when realistic surface wind stress trends are imposed.

Since we can attribute much of the poleward shift in the surface wind stress to ozone forcing (Gillett and Thompson, 2003; Cai and Cowan, 2007; Son et al., 2009b; Fogt et al., 2009), we can infer that ozone forcing in the 1970–2000 period contributes to the observed subsurface warming in the Southern Ocean. That is, the stratospheric ozone-induced change in the Southern Ocean opposes the effects of global warming of the Earth's surface; greenhouse gas forcing warms the ocean surface and increases high latitude precipitation, which stratifies the ocean surface and thereby reduces oceanic mixing of heat (and, by extension, the uptake of anthropogenic carbon dioxide). In the Geophysical Fluid Dynamics Laboratory coupled models CM2.0 and CM2.1, Russell et al. (2006) find that the enhanced Ekman transport signal associated with positive Southern Annular Mode-related wind trends counteracts this and contributes to an increased heat uptake. The implications of the circulation changes for the Southern Ocean carbon cycle are discussed in Section 4.4.2.4. Under ozone recovery (Section 4.5), the ozone-forced Southern Annular Mode trend in December, January, and February is expected to weaken or change sign (see Section 4.5); this effect would tend to reduce ocean heat uptake, but the net effect will depend on the combined effects of CO_2 increases and ozone recovery on the Southern Annular Mode.

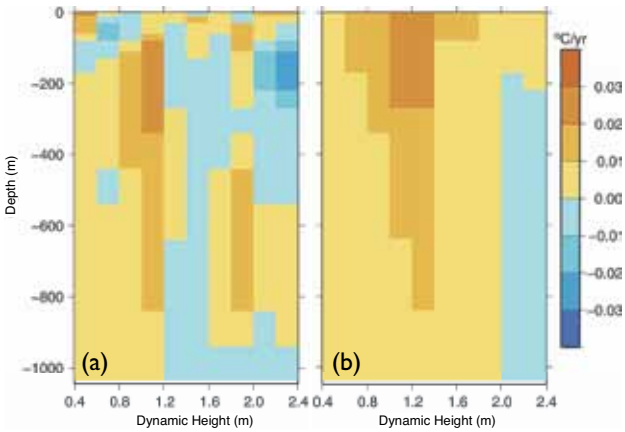

Figure 4-22. (a) Rate of change of ocean temperature (°C/yr) as a function of dynamic height (m), which serves as a meridional coordinate, from ship-based and autonomous float data. The Antarctic Circumpolar Current is in the range 0.4–1.2 m. (b) Effective rate of change of ocean temperature (°C/yr) that would result if ocean temperature structure were shifted poleward at a rate of 1° latitude per 40 years. Based on Gille (2008).

Recent oceanographic literature provides some caveats about the straightforward connection between wind stress and Southern Ocean circulation. The complication relates to the effects of oceanic mesoscale (10 to 50 km scale) eddies, which are responsible for much of the transport of heat and constituents in the Southern Ocean. The CMIP3 generation ocean models cannot explicitly resolve mesoscale eddies and instead parameterize their effects with dynamically motivated mixing schemes (Gent and McWilliams, 1990). A developing body of work (e.g., Radko and Marshall, 2003; Hallberg and Gnanadesikan, 2006; Meredith and Hogg, 2006; Böning et al., 2008; Screen et al., 2009) shows that when they are explicitly resolved, mesoscale eddy effects could modify some of the conclusions presented above. In particular, for relatively fine ocean model resolution, the mesoscale eddy field can respond strongly to changes in wind stress and can counteract some of the changes to the Ekman circulation among other effects (e.g., Hallberg and Gnanadesikan, 2006; Meredith and Hogg, 2006; Screen et al., 2009). In a sensitivity test, Fyfe et al. (2007) impose this kind of effect in a coarse resolution ocean model, but their approach has not been independently validated. Furthermore, not

5 It is outside the scope of this report to assess the calibration and sampling of long-term ocean observations; we will place more confidence in conclusions that have been repeatedly verified in the literature.

all aspects of observed changes in the density structure in the Antarctic Circumpolar Current are represented by the wind-driven ocean circulation theory. In particular, intensification of the wind-driven Antarctic Circumpolar Current is associated with an increased slope (baroclinicity) of density surfaces. This increased slope is seen in CMIP3 class ocean models (e.g., Russell et al., 2006) but has not been detected in observations, which might be the result of mesoscale eddy effects (Böning et al., 2008). Solid conclusions will require a better understanding of uncertainties in trend analysis of multidecadal ocean observations. Nevertheless, since this recent work has implications for Southern Ocean circulation, density structure, temperatures, and carbon cycle, and connects to global climate issues, it appears that high resolution ocean models will be required to fully evaluate the role of Antarctic ozone depletion in Southern Ocean climate change (see also Ito et al., 2010).

To summarize, the dynamical coupling between the stratosphere and troposphere in conjunction with forcing by the ozone hole suggests that the wind-driven Southern Ocean circulation should intensify as a result of polar stratospheric ozone depletion. This effect may contribute to observed subsurface warming in the Southern Hemisphere and has the potential to attenuate some of the surface global warming associated with greenhouse gas increases. Some predictions of the changes to the Antarctic Circumpolar Current and the Southern Hemisphere overturning could be dependent on ocean model resolution; thus, high-resolution ocean models will likely be required to assess with confidence how the Antarctic ozone hole and ozone recovery are likely to affect the Southern Ocean.

4.4.2.4 Stratospheric Links to Southern Ocean Carbon

The summertime trend in the Southern Annular Mode also provides a potential link between stratospheric ozone depletion and the flux of carbon at the Earth's surface: the ozone hole is linked to changes in the surface winds, and those changes in the surface winds are expected to affect the flux of carbon at the ocean surface. Our current understanding of these linkages is assessed below.

The primary anthropogenic driver of climate change is the emission of more than 9 gigatonnes of carbon (GtC) annually in the form of CO_2, mainly due to fossil fuel burning with smaller contributions from land use change (Forster et al., 2007a). Thus the processes that remove atmospheric carbon dioxide are critical to understanding current climate change.

The Southern Ocean plays a key role in the uptake of global carbon dioxide. As carbon dioxide increases, the net sink of CO_2 in the Southern Ocean would be expected to increase in the absence of other changes. However, recent studies suggest that the Southern Ocean carbon sink has not strengthened over about the past two decades, and this behavior has been linked to changes in winds. Strong eastward winds drive a northward Ekman circulation in the Southern Ocean, which pushes surface waters away from the Antarctic continent and drives a strong ocean circulation that brings up water and dissolved carbon from the deep ocean.

As evidenced in Figure 4-23, the regions displaying broad reductions in carbon uptake correspond to those that underlie the largest tropospheric wind changes associated with the Southern Annular Mode, as obtained in a model driven by ozone depletion. Numerous studies have recently probed how changes in wind stress linked to the Southern Annular Mode have influenced carbon uptake in the Southern Ocean using a range of different approaches, some relying on global climate models, some on models forced by National Centers for Environmental Prediction/National Center for Atmospheric Research reanalyzed winds, some making use of inversion methods based on CO_2 observations, and some using station-based observations of atmospheric CO_2 (Wetzel et al., 2005; Butler et al., 2007; Le Quéré et al., 2007; Lenton and Matear, 2007; Lovenduski et al., 2008; Lenton et al., 2009; Khatiwala et al., 2009).

The observation-based inversion studies are subject to uncertainties in sampling and in the winds prescribed from reanalysis (Baker et al., 2006; Law et al., 2008; Le Quéré et al., 2007). Nevertheless these different types of analyses, including both models and inversion methods, support recent reductions in Southern Ocean carbon uptake. Taken together, this body of work suggests that the changes in wind stress over about the past three decades have reduced the net Southern Ocean carbon uptake by about 0.6–5 Gt (about 0.02–0.16 GtC/yr) compared to the trend that should be expected due to increasing atmospheric CO_2. One context for these numbers is provided by comparison to full compliance with the Kyoto Protocol, which corresponds to a reduction of global carbon emissions of about 0.5 GtC/yr by 2012 (see Velders et al., 2007, and Chapter 5 of this Assessment). The dominant mechanism for a reduction in carbon uptake is generally thought to be stronger upwelling and subsequent outgassing of natural carbon from the deep ocean induced by the wind stress changes (Le Quéré et al., 2007; Lovenduski et al., 2008; Hall and Visbeck, 2002). Note that both natural and anthropogenic carbon fluxes must be considered in assessing changes in the net carbon flux. Lenton et al. (2009) emphasized the dominant role of ozone depletion in driving the change in net carbon uptake in model simulations that explicitly tested the role of ozone versus other greenhouse gas forcings. Khatiwala et al. (2009) noted that only a small change (about 5%) in the ocean carbon sink is required to explain the observations.

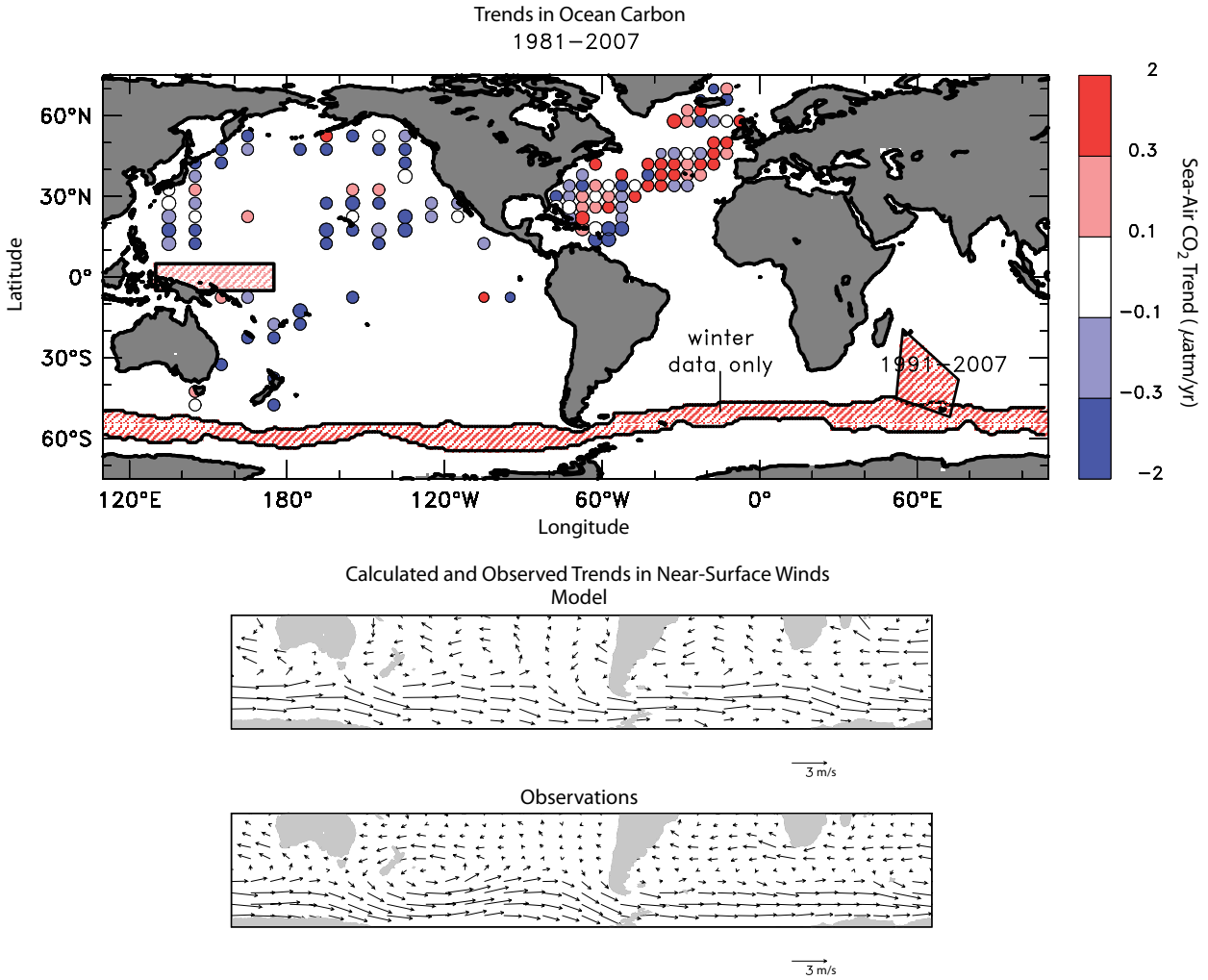

Figure 4-23. Top panel shows trends in the observed partial pressure of CO_2 for ocean minus air, for 1981–2007 (μatm/yr). The observed trends shown by the circles are calculated by fitting a linear trend to repeated measurements of surface-ocean and air CO_2. Positive (red) values indicate regions where the partial pressure of CO_2 in the ocean is increasing faster than atmospheric CO_2, indicating a weakening of the net ocean uptake (from Le Quéré et al., 2009). Large, medium, and small circles are plotted for trends with errors of <0.25, 0.25–0.50, and >0.50 μatm yr^{-1}, respectively. Trends are also shown for three broader areas where only a single estimate can be made (areas shown by hatching). As indicated on the figure, the trends in southern circumpolar waters were estimated from austral winter data only, whereas the trends in the South Indian Ocean were estimated for 1991–2007 only. No seasonal cycle was removed from the data in the western equatorial Pacific region. The amplitudes of the trends in the hatched regions are: equatorial Pacific warm pool (near Indonesia), +0.3 ± 2 μatm/yr; Southern Ocean, +0.5 ± 0.6 μatm/yr; South Indian Ocean, +0.4 ± 0.1 μatm/yr . See Le Quéré et al. (2009) for details. The middle panel shows December–February calculated trends in near-surface winds at southern middle and high latitudes, from global model simulations forced by observed ozone depletion from 1979 to 1997, while the bottom panel shows observed December–May wind trends in the same region (based on Gillett and Thompson, 2003). Units on the bottom two panels are meters/second.

The downward transport of anthropogenic carbon by stronger overturning and the increasing thermal stratification of the Southern Ocean are also important to carbon and heat uptake, but analyses of the data suggest that these effects have been overwhelmed by the effect of strengthening eastward flow on natural carbon fluxes (Le Quéré et al., 2007). Ito et al. (2010) suggest that higher spatial resolution may be needed to ensure accurate evaluation of

the oceanic processes that could contribute to the carbon uptake and its changes.

Future changes in the Southern Ocean carbon sink are subject to an uncertain combination of processes. As recovery of the ozone hole occurs, the circumpolar eastward wind changes related to ozone depletion should reverse (Section 4.5). However, the weakening of the circumpolar eastward flow due to ozone recovery is expected to be roughly compensated for by a strengthening of the circumpolar eastward flow due to increases in carbon dioxide and other greenhouse gases by late 21st century in summer (see Section 4.5). The effect of the eastward flow on the ocean carbon uptake this century will depend on the rate of increase of anthropogenic carbon in the surface ocean and the relative strength of the downward transport of anthropogenic carbon compared to the upward transport of natural carbon, which are both linked to changes in the ocean circulation (see, e.g., Zickfeld et al., 2008). Further, the extent to which the ocean circulation will adjust to altered stratification and winds over long timescales is uncertain.

4.4.3 Stratospheric Variations and the Width of the Tropical Belt

Changes in the tropical and extratropical tropopause layer, and their relation to changes in stratosphere/troposphere exchange of trace constituents, particularly water vapor, were addressed in the 2006 Ozone Assessment (Chapters 2 and 5: Law and Sturges et al., 2007, and Baldwin and Dameris et al., 2007). Since that assessment, research has linked tropopause changes with changes in several other stratospheric and upper-tropospheric features. For example:

- the region of low column ozone values typical of the tropics has expanded in the Northern Hemisphere (Hudson et al., 2006);
- the jet streams have moved poleward in both hemispheres (Fu et al., 2006; Archer and Caldeira, 2008);
- the downward branches of the Hadley cell (where deep clouds are relatively rare compared with the upward branch) have moved poleward, as seen in outgoing longwave radiation, a surrogate for cloud top temperature (Hu and Fu, 2007). Mean meridional mass flux changes independently support this finding of Hadley cell expansion (Hu and Fu, 2007); and
- the region of high tropical tropopause expanded poleward in both hemispheres (Seidel and Randel, 2007).

The qualitative consistency of these observed changes in independent data sets suggests a widening of the tropical belt of between 2 and 5 degrees latitude between 1979 and 2005 (Figure 4-24), as summarized by Seidel et al. (2008) and Reichler (2009). Combined with an increase in the height of the tropical tropopause (Zhou et al., 2001; Santer et al., 2003; Seidel and Randel, 2006), the widening contributes to an increase in the volume of the tropical troposphere of ~5%.

Widening of the tropical belt (i.e., the region of globe with tropical characteristics), including poleward migration of the jet streams and associated migration of storm tracks, could be associated with changes in global precipitation patterns. Lu et al. (2007) found a significant correlation between expansion of the tropical belt, as determined by the location of the downward branches of the Hadley circulation, and the location of the subtropical dry zones in climate models. Poleward movement of precipitation patterns in climatically sensitive subtropical regions might be among the most significant surface climate impacts of tropical expansion, and may already have begun in North America (Seager et al., 2007). Zhou et al. (2001) also note that circulation changes related to tropical belt-widening impacting troposphere-to-stratosphere transport

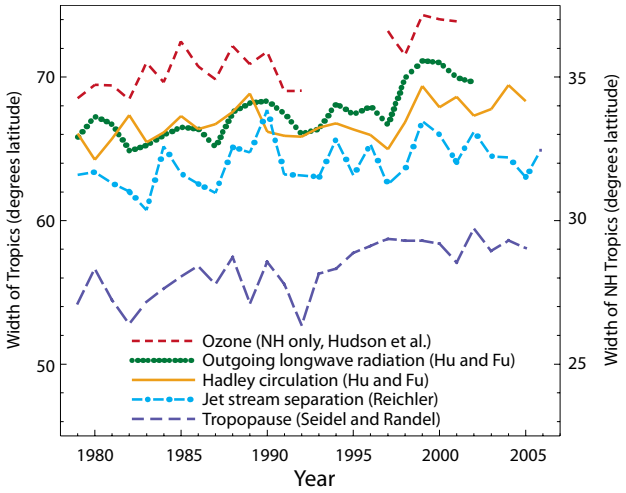

Figure 4-24. Changes in several estimates of the width of the tropical belt since 1979 (in degrees latitude). These include the width of the Hadley circulation, based on both outgoing longwave radiation and horizontal winds streamfunction (Hu and Fu, 2007); the separation of the Northern and Southern Hemisphere subtropical jet-stream cores (Reichler, 2009); the width of the region of frequent high tropopause levels (Seidel and Randel, 2007); and the width of the region with tropical column ozone levels (Northern Hemisphere only, right axis, Hudson et al., 2006). (Based on Seidel et al., 2008.)

may produce changes in the average stratospheric entry value of water vapor.

The cause(s) of these observed changes, their relation to changes in the lower troposphere and at the surface, and the likelihood that they will continue or be reversed in the future, are areas of active research. Insights into these issues have been obtained from two types of global climate models. One is coupled atmosphere-ocean global climate models, particularly the CMIP3 models, which consider ocean feedback but do not represent stratospheric processes in great detail. A second type is coupled chemistry-climate models, with more complete representation of the stratosphere but without an interactive ocean model. However, results to date from both CMIP3 and coupled chemistry-climate model simulations are uncertain because neither type of model includes all relevant processes and because the horizontal resolution of these global model systems is generally several degrees of latitude, which may make it difficult to resolve smaller but significant changes of the horizontal extent of the tropics.

Simulations of past climate change by CMIP3 models that include increases in greenhouse gas concentrations and stratospheric ozone depletion reveal changes in the width of the tropics as measured by changes in the region of high (tropical) tropopause heights (Lu et al., 2009), and modeled tropopause height changes have been linked to poleward migration of the jet streams (Lorenz and DeWeaver, 2007; Son et al., 2009b). More fundamentally, model simulations have linked imposed perturbations in heating of the stratosphere to tropospheric dynamical changes, including latitudinal shifts in jet streams (Simpson et al., 2009). But the widening simulated by CMIP3 models, for both the 20th and 21st centuries, is smaller than the observed widening over the last several decades (Johanson and Fu, 2009), suggesting both that the widening is not the result of natural variability alone (because it is not found in control simulations without anthropogenic forcing) and that the responsible mechanisms may not be well represented by those models.

The importance of stratospheric processes, particularly those related to ozone loss and recovery, is highlighted by comparison of CMIP3 and chemistry-climate model simulations (and projections) of tropopause height changes (Son et al., 2009a). Son et al. (2010) find that the increase in width of the Southern Hemisphere tropics in the CCMVal-2 models is linearly related to the simulated amount of ozone depletion. Lu et al. (2009) also show that widening of the tropics only occurs when they include the radiative impact of ozone depletion in their simulation. Different mechanisms may be responsible for different aspects of the observed changes in the width of the tropical zone, with halocarbons influencing ozone changes and tropopause height change at the subtropical edges of the tropical belt, and with sea surface temperatures and CO_2 influencing tropopause changes within the tropical region (Deckert and Dameris, 2008; Lamarque and Solomon, 2010).

4.4.4 Effects of Stratospheric Variations on Tropospheric Chemistry

Changes in the stratosphere can also affect chemical processes in the troposphere in two principal ways. First, the return of air from the stratosphere at midlatitudes to high latitudes is the sink of many stratospheric chemical species. This stratosphere-troposphere transport is an important term in the overall budget of tropospheric ozone. Second, the overhead column of stratospheric ozone affects the penetration of UV radiation to the troposphere. Changes in column ozone are particularly important for modulating UVB radiation (wavelength less than 320 nanometers) which causes photolysis of O_3 to yield excited $O(^1D)$ atoms. $O(^1D)$ reacts with H_2O in the main formation reaction of tropospheric hydroxyl radicals (OH), the most important tropospheric oxidant. Any changes in the tropospheric circulation, which are driven from the stratosphere, can also change the distribution of tropospheric ozone.

The stratosphere can affect tropospheric chemistry through other mechanisms. For example, stratospheric radiative or circulation changes that contribute to different surface temperatures may impact emissions. However, these contributions will be very small compared to the large tropospheric climate changes induced by increasing atmospheric greenhouse gases. Therefore, this report concentrates on the impact of stratosphere-troposphere transport and column ozone changes. Isaksen et al. (2009) have recently reviewed tropospheric chemistry-climate interactions.

Tropospheric ozone levels are determined by the complex interaction between photochemistry and transport. The primary sources of tropospheric ozone are transport from the stratosphere and in situ photochemical production, and the main sinks are photochemistry and surface deposition. The net global tropospheric ozone burden is a small residual of these terms. Although it is recognized that input of ozone-rich air from the stratosphere (via stratosphere-troposphere transport) is an important term in this overall burden, there are significant variations in its quantification, which is usually done through diagnosing the stratosphere-troposphere transport term in global 3-D models (e.g., Stevenson et al., 2006). Wild (2007) and Wu et al. (2007) updated estimates of terms in the tropospheric ozone budget and investigated the causes of model-model differences from sensitivity runs of their own models. Wild (2007) concluded that some previous differences in modeled budgets could be reconciled by using updated

chemical mechanisms, but uncertainties in stratosphere-troposphere transport remained. Wu et al. (2007) found that the model-model differences were determined largely by differences in emissions and stratosphere-troposphere transport. The current best estimate of this term from observations is 550 ± 140 teragrams (Tg) per year (Olsen et al., 2001), which is in good agreement with model estimates of 550 ± 170 Tg/yr (Stevenson et al., 2006). The mean lifetime of ozone in the troposphere is around 25 days. Variations in the modeled tropospheric ozone burden, e.g., 340 ± 40 Tg (corresponding to a mean mixing ratio of approximately 45 ± 5 parts per billion by volume, ppbv) from Stevenson et al. (2006), are much smaller than variations in stratosphere-troposphere transport, although similar to variations in other ozone budget terms. Therefore, large variations in modeled flux from the stratosphere are not reflected in such large variations in the mean tropospheric ozone burden; the large photochemical and deposition terms damp out these variations.

Observations showed substantial declines in ozone throughout the troposphere in 1992–1993 following the eruption of Mt. Pinatubo (see Fusco and Logan, 2003) and a good correlation between trends in lower-tropospheric and lower-stratospheric ozone from 1992–2004 (Ordóňez et al., 2007). These declines were generally largest in the upper troposphere and linked to ozone loss in the lower stratosphere (which is discussed in Chapter 2). Terao et al. (2008) showed that stratospheric ozone contributes significantly (30–40% at midlatitudes to high latitudes) to the spring O_3 maximum at 500 hPa. The effects of past decreases in stratospheric ozone are not usually included in models used to estimate the tropospheric ozone budget. Fusco and Logan (2003) looked at the impact of decreases in lower-stratospheric ozone in their study of tropospheric ozone changes from 1970–1995. They found that decreases in lower stratosphere ozone might have reduced the stratospheric source by 30% over this time period. More recently, Hsu and Prather (2009) diagnosed the contribution of stratosphere-troposphere transport to the tropospheric ozone budget and included the effect of stratospheric ozone depletion from 1979 to 2004. They found a reduction of up to 10% in the stratosphere-troposphere transport ozone flux, but this caused only a small decrease in mean tropospheric ozone of 1 ppb (about 2%).

A number of older studies investigated how decreases in column ozone in the 1980s and 1990s affected tropospheric OH trends (e.g., Madronich and Granier, 1992; Bekki et al., 1994; Fuglestvedt et al., 1994; Granier et al., 1996). More recently, Duncan and Logan (2008) used a three-dimensional (3-D) model to investigate the impact of various forcings, including changing overhead column ozone, on tropospheric OH and carbon monoxide (CO) from 1988–1997. During this relatively short period, overhead column ozone decreased due to the solar cycle phase and eruption of Mt. Pinatubo, as well as the long-term trends in ozone-depleting substances. The decreased ozone column led to important year round increases in OH, where a −3% change in the column caused a +4% change in OH. In spring/summer at higher latitudes, column ozone changes of −10% caused an increase in OH of about +8%. This contribution from stratospheric ozone variations makes an important contribution to the overall variability in tropospheric OH of ±10% over the past few decades inferred from methyl chloroform (Bousquet et al., 2005; Prinn et al., 2005). This contribution to increased OH made a small impact on the model CO trends, about 0.1–0.2 Tg/yr averaged over the period considered compared to a CO burden of about 500 Tg. However, this change was compensated for by an increase from oxidation of increasing CH_4, while changes in fossil fuel emissions had a much larger impact regionally.

Isaksen et al. (2005) studied the impact of decreased column ozone on tropospheric chemistry under different pollution conditions. They imposed a uniform global decrease in column ozone, affecting only their model's photolysis calculation, and studied the impact on surface ozone. They found that in polluted regions, i.e., regions of net tropospheric ozone production, the increased photochemical activity from faster photolysis led to more ozone production which in turn led to an additional 1 ppb surface ozone for the 10% column reduction over continental Europe in January. In contrast, in cleaner remote regions the enhanced photochemical activity increased the net sink of ozone. The largest effect was a decrease of 3 ppb at low latitudes to midlatitudes, but a change of 10% in the ozone column represents a large perturbation for these latitudes. Overall, these changes in surface ozone are therefore small.

4.4.5 Influence of the Stratosphere on the Impact of Solar Variability on Surface Climate

Changes in the stratosphere in response to solar variability have the potential to influence tropospheric climate by many of the radiative and dynamical processes outlined in Sections 4.4.1–4.4.4 above. Some specific linkages between solar variability, the stratosphere, and surface climate are assessed below. More detailed discussions of many of the issues related to the impact of solar variability on climate are presented by Gray et al. (2010).

The signals in stratospheric ozone and temperature produced by 11-year solar cycle variations in incoming radiation have been discussed in Section 2.4.3.2 of Chapter 2 and Section 4.3.1 of this chapter, respectively. While some details of the responses are not fully understood, a picture is emerging in the tropics in which the temperature

of the tropical upper stratosphere is warmer by 1.1–1.8 K and the lower stratosphere warmer by 0.5–0.8 K when the sun is more active, relative to when it is quiet (Randel et al., 2009; Gray et al., 2010). There is a related signal in zonal winds in a strengthening of the subtropical lower mesospheric jet in the winter hemisphere during high solar activity (Frame and Gray, 2010). A solar signal has also been detected in the stratospheric polar night jet in both hemispheres, and thus in the annular modes, (e.g., Kodera, 2002; Boberg and Lundstedt, 2002; Thejll et al., 2003; Kuroda and Kodera, 2004, 2005; Kuroda et al., 2007; Lee and Hameed, 2007; Barriopedro et al., 2008; Lee et al., 2008). Most of these studies, however, have used simple linear regression or confined their discussions to correlation coefficients. Hence they detect only the linear component of the response, and have not considered the impact of other potential forcing factors such as volcanic eruptions. Analyses using data sets that include the most recent solar maximum period, during which there was no major coincident volcanic activity, have now shown that a separation is indeed possible (Frame and Gray, 2010).

In a multiple regression analysis, Keckhut et al. (2005) find a temperature response in the tropics in rocketsonde and lidar data similar to that in the reanalysis studies. The response includes a seasonally varying out-of-phase signal in midlatitudes that Hampson et al. (2005) relate to the occurrence of stratospheric warmings. Haigh and Roscoe (2006) carried out a multiple regression analysis of time series of the Northern and Southern Annular Mode indices throughout the depth of the atmosphere. No significant response to the 11-year solar cycle was found if the solar and stratospheric quasi-biennial oscillation terms were included separately, but when they were combined into a single term (in which the phase of solar activity modulates the stratospheric quasi-biennial oscillation) to represent their interaction, a strongly significant result was found. This finding is consistent with the original results of Labitzke (1987), in which polar stratospheric height data were sorted by phase of the stratospheric quasi-biennial oscillation and level of solar activity.

Variations in incoming total solar irradiance of order 0.1% occur over the 11-year solar activity cycle (Fröhlich and Lean, 2004) resulting in a top-of-atmosphere radiative forcing of approximately 0.2 W m^{-2}. On multidecadal timescales underlying variations in total solar irradiance are less certain, but assessments suggest that there has been an overall increase in the range 1–4 W m^{-2} since the year 1700, giving a top-of-atmosphere radiative forcing of 0.17–0.67 W m^{-2} since that date (Gray et al., 2010). The amount of radiation reaching the tropopause, which provides a better indicator of climate radiative forcing, is dependent on the spectral composition of the radiation and the response of stratospheric ozone. This effect has been assessed to be a small addition to the radiative forcing value (Larkin et al., 2000), but recent measurements from the Solar Radiation and Climate Experiment satellite (Harder et al., 2009) indicate that there may be compensating changes at UV and visible wavelengths which imply that solar radiative forcing at the tropopause would be out of phase with that at the top of the atmosphere due to absorption of the UV in the stratosphere (Haigh et al., 2010).

As well as direct radiative effects, variations in solar activity may produce a solar signal in the troposphere "top-down" from an initial response in the stratosphere. Early model studies of UV variations in the stratosphere (Haigh, 1996, 1999; Shindell et al., 1999; Balachandran et al., 1999; Larkin et al., 2000) obtained a response in the troposphere even though the near-surface in these model runs was constrained by imposed, seasonally varying, sea-surface temperatures. The main response to enhanced UV and stratospheric ozone in these models is (1) an expansion of the Hadley cell and (2) a poleward movement of the tropical convective maxima, the tropospheric jets, and the midlatitude storm tracks. The pattern of these anomalies was similar to the signal found in tropospheric zonal winds in reanalysis data (Haigh, 2003; Frame and Gray, 2010) and also in upper air temperatures and geopotential heights (Brönnimann et al., 2006) using a data set based on radiosonde and aircraft observations dating back to 1922. The amplitude of the modeled pattern depended on the magnitude of the ozone change but was generally about half the amplitude of that observed. The new Solar Radiation and Climate Experiment data, however, imply that the ozone response, and thus presumably the tropospheric response to the stratospheric warming, might be significantly larger.

This signal has the same spatial structure as, and thus presumably involves similar eddy-mean flow feedbacks to, the dominant pattern of atmospheric variability, i.e., the atmospheric annular modes. Feedback of the tropospheric zonal wind changes on the tropospheric eddy momentum fluxes appears to be important in establishing and maintaining the response to stratospheric forcing, as discussed in Section 4.4.2 (see also Polvani and Kushner, 2002; Kushner and Polvani, 2004, 2006; Song and Robinson, 2004). Coupling between the Hadley circulation and midlatitude eddies may also play a key part; in a mechanistic study focusing on the processes involved in a response to solar forcing, Haigh et al. (2005) obtained a zonal mean tropospheric response, qualitatively similar to the observed 11-year solar response, by imposing anomalous diabatic heating in the low latitude lower stratosphere. Consistent with this result, the enhanced Hadley circulation response in the coupled chemistry-climate model simulations of Shindell et al. (2006) was linked to the additional condensational heating in the upper tropical troposphere and lower stratosphere relative to simulations with fixed ozone. Imposing a generic stratospheric heat-

ing in a simplified climate model, Simpson et al. (2009) have shown that it is the response of the eddy momentum fluxes to changes in structure of the tropopause region that drives the tropospheric response, so that details of the stratospheric response to solar variability may be important in determining the tropospheric signal.

Matthes et al. (2006), using a general circulation model with prescribed sea-surface temperatures, found the response to UV variability in tropical vertical velocity was not uniformly distributed in longitude but was largest over the Indian and West Pacific Oceans—indicating an influence on the Walker circulation similar to that found in observations by Kodera (2004) and Kodera et al. (2007). The weakened ascent during solar maximum in the tropical troposphere of their model may result from the increased static stability in the tropopause region suppressing convection (Kodera and Shibata, 2006; Matthes et al., 2006).

Other studies have also identified solar influences on the strength and extent of the Walker circulation. van Loon et al. (2007) and Meehl et al. (2008) show a strengthening, at peak years of the 11-year solar cycle, which they identify as distinct from any El Niño-Southern Oscillation signal (van Loon and Meehl, 2008) although their approach has been questioned by Roy and Haigh (2010) and Zhou and Tung (2010). The associated sea-surface temperature response at the peak years of the 11-year solar cycle is a cooler than normal equatorial eastern Pacific and poleward-shifted intertropical and South Pacific convergence zones with a warming following with a lag of a couple of years (Meehl et al., 2008; White and Liu, 2008).

The mechanisms invoked to explain this sea-surface temperature response involve changes in the visible radiation absorbed by the tropical oceans, along with coupled air-sea interactions, and thus may be termed "bottom-up" rather than the "top-down" processes involving the stratosphere that are the focus of this report. Recent modeling studies (Rind et al., 2008; Meehl et al., 2009) have suggested that both pathways may combine to produce an amplified response to a small solar forcing. However, the responses probably depend on complex nonlinear interactions between different processes that have yet to be elaborated. Furthermore, all the mechanisms depend crucially on the spectral composition of the solar irradiance variability of which current understanding is currently being challenged by data from the Solar Radiation and Climate Experiment Spectra Irradiance Monitor (SIM) instrument (see the discussion in Section 4.3.1).

4.5 WHAT TO EXPECT IN THE FUTURE

The stratosphere is expected to change over the rest of this century in response to a range of forcing factors. Concentrations of the main anthropogenic greenhouse gases (CO_2, N_2O and CH_4, hydrofluorocarbons (HFCs), and SF_6) are expected to continue to rise for at least several decades, but concentrations of halogenated ODSs have leveled off and are expected to decrease. Future stratospheric aerosol loading (especially from volcanoes) is unpredictable. Chapter 5 of this Assessment provides a number of possible scenarios of emissions and concentrations of anthropogenic greenhouse gases. These atmospheric concentration changes will affect both ozone concentrations and stratospheric climate in the future. The evolution of the future ozone layer is discussed extensively in Chapter 3. Here we briefly assess the predicted changes through 2100 in the stratospheric climate changes assessed in this chapter.

4.5.1 Stratospheric Temperatures

The evolution of stratospheric temperature is expected to depend on three main factors: the recovery of the ozone layer, increasing concentrations of most greenhouse gases, and the resulting changes to the mean overturning circulation in the stratosphere (the Brewer-Dobson circulation). At least one experiment predicts that changes in Arctic sea ice will drive changes in polar stratospheric wave forcing and thus temperatures (Scinocca et al., 2009). The recovery of the Antarctic ozone hole is expected to lead to higher temperatures in the Antarctic stratosphere during spring, and a reduction in the strength of the stratospheric polar vortex as the effects of ozone loss diminish. Outside the Antarctic stratosphere, future changes in stratospheric ozone are expected to lead to a reversal of the ozone-induced cooling observed in both the lowermost and upper stratosphere (Chapter 10 of SPARC CCMVal, 2010). However, in general the warming associated with ozone recovery will be outweighed by a larger cooling effect due to continued greenhouse gas increases (Chapter 5 of WMO, 2007; Chapter 10 of SPARC CCMVal, 2010; McLandress et al., 2010; Jonsson et al., 2009).

The projected evolution of stratospheric temperatures in the 21st century depends on both the choice of scenario and climate model used to project that scenario. All scenarios have CO_2 continuing to increase, with ODSs and stratospheric chlorine loading decreasing. An example of trends at 1 hPa is shown in Figure 4-25 for the NASA Goddard Space Flight Center (GSFC) Goddard Earth Observing System chemistry-climate model (GEOS) under the CCMVal REF-B2 scenario[6]. CO_2-induced cooling (including its effect on ozone) dominates the response, although ozone recovery reduces the rate of cooling over the next few decades. Under this scenario all the CCMVal models exhibit global cooling in the middle and upper

6 See SPARC CCMVal 2010, Chapter 2, for scenario details.

stratosphere by several degrees, with much smaller temperature changes of undetermined sign in the lower stratosphere (typically less than 0.5 K) (Chapter 3 of SPARC CCMVal, 2010).

Temperatures in the lower tropical stratosphere and tropopause region could be significantly affected if atmospheric concentrations of HFCs rise. At the one ppb level HFCs give an additional warming of 0.2–0.5 K to the lower tropical stratosphere region. This range depends on the spectral absorption characteristics of the HFC (Forster and Joshi, 2005). Note the HFCs with small atmospheric lifetimes are unlikely to reach high enough concentrations to have an appreciable effect (see Chapter 5 of this Assessment).

4.5.2 Brewer-Dobson Circulation

Atmospheric model simulations forced with increased greenhouse gas concentrations exhibit an acceleration of the Brewer-Dobson circulation (e.g., Rind et al., 1998; Butchart and Scaife, 2001; Butchart et al., 2010). This is an extremely robust response in the current generation of chemistry-climate models, as discussed in Section 4.3. The implications of a future increase in the Brewer-Dobson circulation are substantial. Such an increase would change the spatial distribution of stratospheric ozone, with increased total ozone at high latitudes and decreased total ozone in the tropics (see Figure 3-3 in Chapter 3 of this Assessment). It would also increase the stratosphere-to-troposphere ozone flux (Hegglin and Shepherd, 2009), and it would decrease the net age of stratospheric air (e.g., Austin and Li, 2006; Garcia and Randel, 2008; Oman et al., 2009; Butchart et al., 2010).

However, as noted in Section 4.2, the observational evidence for an increase in the Brewer-Dobson circulation is unclear. The observed decreases in tropical stratospheric temperatures are consistent with increased upwelling in the lower tropical stratosphere (e.g., Thompson and Solomon, 2005, 2009; Randel et al., 2009) as are the observed decreases in lower tropical stratospheric ozone (Randel and Wu, 2007; Chapter 2). But the reliability of the ozone and temperature data for assessing relatively small trends in this region of the atmosphere is still under investigation (e.g., Randel and Wu, 2006; Chapter 2). Estimates of long-term variations in age of air based on midlatitude balloon measurements of SF_6 and CO_2 over 1975–2005 have substantial uncertainties, but suggest no significant trends (Engel et al., 2009). Some effort has been made to use reanalyses to diagnose trends in the Brewer-Dobson circulation but without success due to inhomogeneities in the observational record and reanalyzed products (Iwasaki et al., 2009).

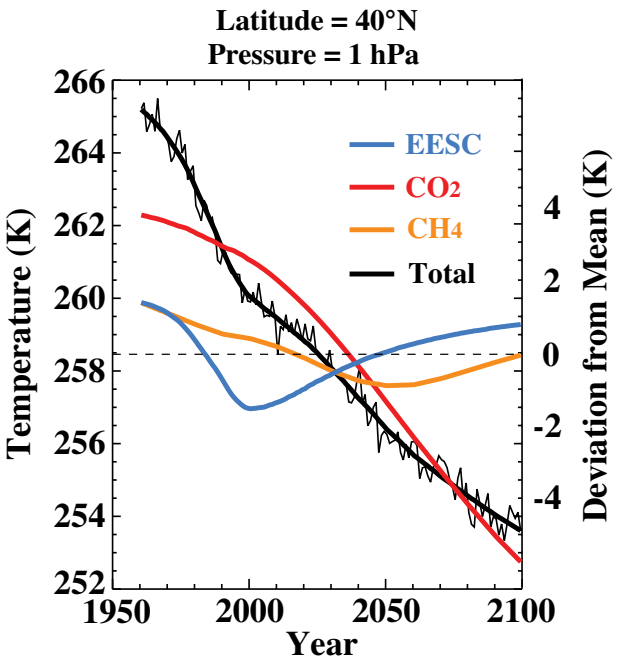

Figure 4-25. Time series of simulated temperatures (K) at 40°N and 1 hPa (thin black line), with the statistical fit as the heavy black line. Data are for the NASA GSFC GEOS chemistry-climate model under the CCMVal REF-B2 scenario. Scale on left shows temperatures for this time series. Scale on right shows deviations from the mean temperature due to changes in equivalent effective stratospheric chlorine (blue line), CO_2 (red line), and CH_4 (orange line). Based on Stolarski et al. (2010).

4.5.3 Stratospheric Water Vapor

Modeling studies of future greenhouse gas increases project that the tropical tropopause will warm and rise in altitude (Gettelman et al., 2009). One effect of a warmer tropical tropopause is an increase in stratospheric water vapor globally. Assumed increases in anthropogenic contributions to tropospheric methane, along with the possibility that natural sources of methane may increase in a warming climate, would also contribute to increases in stratospheric water vapor. Projected decreases in the net age of stratospheric air (Section 4.5.2) could lead to a slight decrease in stratospheric water vapor.

As presented in Gettelman et al. (2010), there is significant spread in chemistry-climate models' representation of both tropical cold point temperatures (Figure 4-12) and 80-hPa water vapor (used to represent stratospheric entry values), as shown in Figure 4-13. The trend in the historical record of tropical radiosonde cold point temperatures also does not agree with the multi-model

mean; the amplitude of the observed trend is more than an order of magnitude larger than the modeled trend (Gettelman et al., 2009). Given the discrepancies between modeled and measured tropical temperatures and lower-stratospheric water, we cannot provide any reliable prediction as to what the future evolution of stratospheric water vapor will be in a climate with increasing greenhouse gas concentrations.

4.5.4 Tropopause Height and Width of the Tropical Belt

Chemistry-climate models project that the tropopause height will continue to increase in the future, but with a trend weaker than that in the recent past (Son et al., 2009a; Gettelman et al., 2009). The reduced trend appears to be directly associated with stratospheric ozone recovery in the Southern Hemisphere in summer. With recovery of the ozone layer, chemistry-climate models also suggest that the observed trend toward widening of the tropics may weaken in the Southern Hemisphere in summer (Son et al., 2009a; Son et al., 2009b). However, our confidence in the magnitude of projected changes in the width of the tropics is limited by (1) discrepancies in such predictions derived from CMIP3 models and chemistry-climate models (Johanson and Fu, 2009; Son et al., 2009a) and (2) an incomplete understanding of the dynamics of the changes (Reichler, 2009).

4.5.5 Radiative Effects and Surface Temperature

By the middle of this century, global average concentrations of ozone-depleting substances may return to levels prior to 1960, but increasing concentrations of greenhouse gases are expected to alter stratospheric temperatures and circulation. Consequently, the ozone distribution will not simply return to its state prior to 1960. The altered ozone concentrations will continue to exert an anomalous radiative forcing on surface climate. Portmann and Solomon (2007) computed an ozone forcing at 2100 from CO_2, N_2O, and CH_4 changes under a range of IPCC Special Report on Emissions (i.e., SRES) scenarios. Although the induced ozone column changes were relatively large (up to a 5% change in the column, globally averaged) the overall radiative forcing since pre-1970 ranged between -0.1 W m^{-2} and $+0.1$ W m^{-2}. This small forcing is a result of most of the associated ozone change occurring in the upper stratosphere, where it only contributed a small radiative forcing (see Section 4.2.2 and Chapter 3).

4.5.6 Tropospheric Annular Modes and Stratosphere-Troposphere Coupling

As discussed in Section 4.4.2, only climate models that include observed changes in stratospheric ozone are able to reproduce the observed positive trend in the tropospheric Southern Annular Mode during austral summer over the past few decades. We infer that polar stratospheric ozone losses have been the dominant driver of the observed trend in the Southern Hemisphere surface circumpolar flow, as has been confirmed in those models that separately include ozone forcing with other radiative forcings held fixed (Gillett and Thompson, 2003; Shindell and Schmidt, 2004; Arblaster and Meehl, 2006).

In the absence of other forcings, stratospheric ozone recovery is expected to drive an equatorward shift in the Southern Hemisphere extratropical jet in the 21st century in austral summer that projects onto the negative polarity of the annular modes (e.g., Son et al., 2008). In contrast, future increases in atmospheric carbon dioxide concentrations are expected to lead to positive trends in the annular modes in both hemispheres (e.g., Fyfe et al., 1999; Kushner et al., 2001; Cai et al., 2003; Shindell and Schmidt, 2004; Brandefelt and Källén, 2004; Yin, 2005; Miller et al., 2006; Arblaster and Meehl, 2006; Lu et al., 2008), although the amplitudes of the greenhouse gas induced trends vary from simulation to simulation (Yin, 2005; Miller et al., 2006). The effects of ozone recovery and increasing carbon dioxide on the Southern Annular Mode are expected to approximately cancel through the middle of the 20th century during austral summer, as evidenced in both CCMVal-2 simulations and CMIP3 simulations (e.g., Figure 4-26; SPARC CCMVal, 2010[7]). CMIP3 models without ozone recovery (Figure 4-26d) exhibit a weak positive Southern Annular Mode trend, which is presumably dominated by the greenhouse gas forcing.

There are several important caveats in the interpretation of annular mode trends. First, simulations of 20th century climate tend to place the Southern Hemisphere jet farther equatorward than is observed (Fyfe and Saenko, 2006; Son et al., 2010; Kidston and Gerber, 2010). The reasons for these biases are not well understood. But they seem to be important, as differences in the projected magnitude of the trend in the Southern Hemisphere are well correlated with biases in the latitude of the jet in the simulation of 20th century climate; models with a larger equatorward bias simulate a larger poleward shift in jet location, and vice versa (Son et al., 2010; Kidston and Gerber,

[7] Note that the CCMVal-2 results shown in Figure 4-26 differ somewhat from those based on the previous generation CCMVal-1 models (Son et al., 2008; Perlwitz et al., 2008). Those runs indicate an equatorward shift of the jet at the surface in December, January, and February.

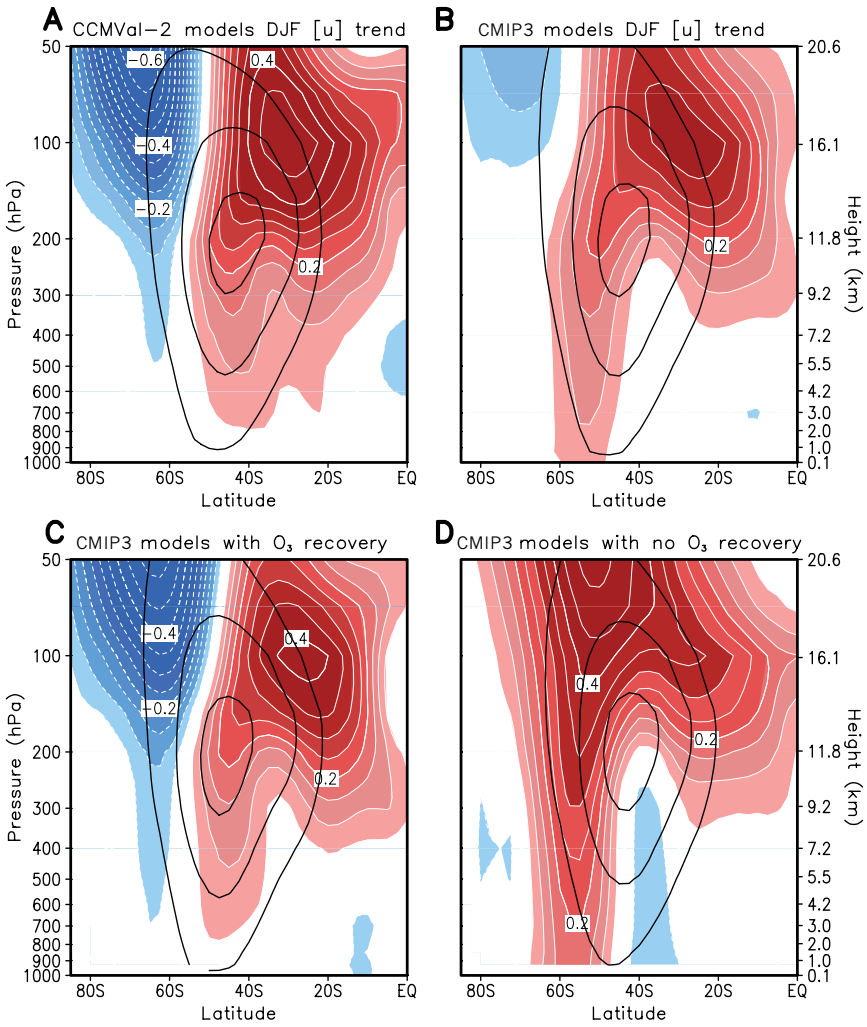

Figure 4-26. Trends in December-to-February (DJF) zonal-mean zonal wind. The multi-model mean trends between 2001 and 2050 are shown for the CCMVal-2 models (A), the CMIP3 models (B), the CMIP3 models with prescribed ozone recovery (C), and the CMIP3 models with no ozone recovery (D). Shading and contour intervals are 0.05 m s^{-1} $decade^{-1}$. Deceleration and acceleration are indicated with blue and red colors, respectively, and trends weaker than 0.05 m s^{-1} $decade^{-1}$ are omitted. Superimposed black solid lines are DJF zonal-mean zonal wind averaged from 2001 to 2010, with a contour interval of 10 m s^{-1}, starting at 10 m s^{-1}. From Son et al. (2008, 2010).

2010). This suggests that climate models may tend to overestimate the 21st century poleward shift in jet location (Kidston and Gerber, 2010).

An additional caveat involves the definition of the annular modes in the presence of a changing climate. Normally, the annular mode patterns are based on geopotential anomalies relative to a fixed climatology, such as for 1960–2010. In long model integrations including climate change, the future annular mode index is calculated by projecting anomalies (relative to 1960–2010) onto the annular mode patterns. However, the projected widespread warming of the troposphere will lift geopotential heights at all latitudes in the free troposphere, with the largest increases in the tropics. Because the annular mode patterns emphasize changes over the polar caps, much of the projected changes to geopotential will not be reflected in the annular mode index. Thus, the annular mode patterns are not a good proxy for long-term projected changes to hemispheric geopotential (e.g., Fyfe, 2003; Gerber et al., 2010). The zonal-mean response to anthropogenic forcing also appears to have a distinctive baroclinic signature that is very different from the annular modes (Woollings, 2008). Shindell and Schmidt (2004) note a similar decoupling of the signatures of global warming and the Southern Annular Mode.

It is possible to modify the definition of the annular modes to compensate for the effects of tropospheric warming, but the resulting annular mode trends are not comparable to annular mode trends calculated using standard methodologies. For example, Morgenstern et al. (2010b) used a modified definition of the Northern Annular Mode (NAM) that partially accounts for the effects of tropospheric warming. With this modified definition, in the CCMVal-2 models, increasing CO_2 is generally associated with trends towards the negative polarity of the NAM in winter. An alternate methodology is to remove the slowly varying trend in geopotential heights from the climatology, resulting in annular mode indices that have no long-term trends (the geopotential height trends are contained in the slowly varying climatology). Using this method, Gerber et al. (2010) found that the structure and month-to-month variability of the annular modes remain

relatively robust over time in CMIP3 and CCMVal-2 model integrations of the 21st century (again, the trends in the mean of the annular mode indices are contained in the slowly varying climatology).

4.5.7 Tropospheric Chemistry

The future increases in stratospheric ozone will also impact tropospheric chemistry. The effects can be expected to be the reverse of the impacts of stratospheric ozone depletion over the past few decades discussed in Section 4.4.4. If stratospheric cooling leads to a thicker ozone layer than in the past ("super recovery") then future impacts may be larger. Decreasing UV radiation reaching the lower atmosphere is expected to decrease tropospheric OH. Duncan and Logan (2008) analysed past CO trends. Based on their analysis, OH decreases due to ozone recovery would augment rather than cancel the positive impact of likely increasing CH_4 on CO trends. In any case, based on calculations during the period of ozone loss (Section 4.4.4), the impact is likely to be small but it remains to be quantified.

The flux of stratospheric ozone into the troposphere may also change in a future climate. Even with the same rate of mass transport, ozone increases in the lower stratosphere would lead to larger ozone transport into the troposphere. However, the stratosphere-troposphere transport mass flux may also change. Stevenson et al. (2006) studied the climate of 2030 using 9 different models. They found ozone stratosphere-troposphere transport will increase by 0–19%. Zeng et al. (2008) investigated the impact of climate change on the tropospheric ozone budget using a 3-D chemistry-climate model with a relatively low lid and simple representation of stratospheric chemistry. For a 2100 atmosphere, they found that a doubling of CO_2 caused an 80% increase in ozone transport from the stratosphere, which led to increases in tropospheric ozone down to the surface. Similar studies using low-lid tropospheric chemistry models by Collins et al. (2003) and Sudo et al. (2003) showed large stratosphere-troposphere transport increases by 2100 of 40% and 130%, respectively.

Recently, Hegglin and Shepherd (2009) investigated the impact of climate change on ozone in the lower atmosphere in a model with full stratospheric chemistry. Under a moderate greenhouse gas emissions scenario they found the stratosphere-troposphere transport of ozone increased by 23% between 1965 and 2095 due to changes in the Brewer-Dobson circulation, i.e., a smaller value than the low-lid tropospheric models cited above, but for a different greenhouse gas scenario. Hegglin and Shepherd (2009) also investigated the impact of the changes in vertical and latitudinal distribution of ozone on surface UV. Between 1965 and 2095 they found surface clear-sky UV fluxes decreased by 9% at northern high latitudes, increased by 4% in the tropics and increased by up to 20% at high southern latitudes. These changes in the clear-sky UV flux, due to circulation-induced changes in lower-stratospheric ozone, are different from those expected based on ozone recovery from halocarbon-induced depletion, and illustrate the importance of dynamics in controlling total ozone in the future as halocarbons decrease. Future UV levels will also be affected by changes in cloud cover (see Chapter 3, Section 3.4).

Future changes in the stratosphere-troposphere transport of ozone from ten chemistry-climate models have been assessed in Chapter 10 of SPARC CCMVal (2010). The report provided a comparison of the chemistry-climate model stratosphere-troposphere transport ozone flux with observations and other model studies for past and future time periods related to ozone depletion (1965–2000), ozone recovery (2000–2035), and climate change (1965–2095). The chemistry-climate model multi-model mean of the change in the stratosphere-troposphere transport ozone flux attributable to climate change (1965–2095) was slightly larger in the Northern Hemisphere (17%) than in the Southern Hemisphere (14%). The chemistry-climate model multi-model mean was generally consistent in terms of relative changes with the Canadian model results shown in Hegglin and Shepherd (2009), but showed a reduction in Northern Hemisphere stratosphere-troposphere transport ozone flux from 1965–2000 due to ozone depletion, as well as a weaker long-term increase in Northern Hemisphere stratosphere-troposphere transport ozone flux over 1965–2095 due to climate change. Over the period 2000–2030, the CCMVal-2 models showed increases in the global stratosphere-troposphere transport ozone flux of 10.3 (±2.0)% (see CCMVal, 2010, Chapter 10, Figure 10-22), which is toward the upper end of the range from tropospheric models reported by Stevenson et al. (2006).

4.5.8 Solar and Volcanic Influences

The existing observational record is short, and hence we do not fully understand the limits of natural variability in the stratosphere. Based on our current understanding, the influence of explosive volcanic eruptions on stratospheric ozone depletion is linked to heterogeneous chemistry on the surface of particles, and is very sensitive to the amount of chlorine loading (Section 3.2.5). Hence potential future volcanic eruptions are expected to be associated with increasingly less ozone depletion as chlorine declines, and are even expected to result in ozone increases by midcentury (Tie and Brasseur, 1995). On the other hand, the direct effects of major volcanic eruptions on climate (including surface cooling, stratospheric warming, winter season weather patterns, and changes in ocean heat content and sea level rise) are expected to continue to

occur in a manner that scales with the stratospheric aerosol abundance.

Future stratospheric temperatures and ozone levels will depend on variations in the solar radiation incident at the Earth. The sun is currently in an anomalously quiescent state (Fröhlich, 2009), which makes prediction of its future behavior and total solar irradiance highly uncertain. Furthermore, recent space-based measurements (Harder et al., 2009) have cast doubt on currently accepted models of the ozone response to solar variability. That said, while the impact of future variations in solar irradiance is highly uncertain, it is unlikely that solar variability will have more than a minor effect on ozone levels relative to the effects of the reduction in chlorine loading.

REFERENCES

AchutaRao, K., and K.R. Sperber, ENSO simulation in coupled ocean-atmosphere models: Are the current models better?, *Clim. Dyn.*, *27*, 1-15, doi: 10.1007/s00382-006-0119-7, 2006.

Allen, R.J., and S.C. Sherwood, Warming maximum in the tropical upper troposphere deduced from thermal winds, *Nature Geosci.*, *1*, 399-403, doi: 10.1038/ngeo208, 2008.

Aoki, S., M. Yoritaka, and A. Masuyama, Multidecadal warming of subsurface temperature in the Indian sector of the Southern Ocean, *J. Geophys Res.*, *108*, 8081, doi: 10.1029/2000JC000307, 2003.

Arblaster, J.M., and G.A. Meehl, Contributions of external forcings to Southern Annular Mode trends, *J. Clim.*, *19* (12), 2896-2905, doi: 10.1175/JCLI3774.1, 2006.

Archer, C.L., and K. Caldeira, Historical trends in the jet streams, *Geophys. Res. Lett.*, *35*, L08803, doi: 10.1029/2008GL033614, 2008.

Austin, J., and F. Li, On the relationship between the strength of the Brewer–Dobson circulation and the age of stratospheric air, *Geophys. Res. Lett.*, *33*, L17807, doi: 10.1029/2006GL026867, 2006.

Austin, J., K. Tourpali, E. Rozanov, H. Akiyoshi, S. Bekki, G. Bodeker, C. Brühl, N. Butchart, M. Chipperfield, M. Deushi, V.I. Fomichev, M.A. Giorgetta, L. Gray, K. Kodera, F. Lott, E. Manzini, D. Marsh, K. Matthes, T. Nagashima, K. Shibata, R.S. Stolarski, H. Struthers, and W. Tian, Coupled chemistry-climate model simulations of the solar cycle in ozone and temperature, *J. Geophys. Res.*, *113*, D11306, doi: 10.1029/2007JD009391, 2008.

Austin, J., R.J. Wilson, H. Akiyoshi, S. Bekki, N. Butchart, C. Claud, V.I. Fomichev, P. Forster, R.R. Garcia, N.P. Gillett, P. Keckhut, U. Langematz, E. Manzini, T. Nagashima, W.J. Randel, E. Rozanov, K. Shibata, K.P. Shine, H. Struthers, D.W.J. Thompson, F. Wu, and S. Yoden, Coupled chemistry climate model simulations of stratospheric temperatures and their trends for the recent past, *J. Geophys. Res.*, *36*, L13809, doi: 10.1029/2009GL038462, 2009.

Baker, D.F., R.M. Law, K.R. Gurney, P. Rayner, P. Peylin, A.S. Denning, P. Bousquet, L. Bruhwiler, Y.-H. Chen, P. Ciais, I.Y. Fung, M. Heimann, J. John, T. Maki, S. Maksyutov, K. Masarie, M. Prather, B. Pak, S. Taguchi, and Z. Zhu, TransCom 3 inversion intercomparison: Impact of transport model errors on the interannual variability of regional CO_2 fluxes, 1988–2003, *Global Biogeochem. Cycles*, *20*, GB1002, doi: 10.1029/2004GB002439, 2006.

Balachandran N., D. Rind, P. Lonergan, and D. Shindell, Effects of solar cycle variability on the lower stratosphere and the troposphere, *J. Geophys. Res.*, *104*, (D22) 27321-27339, 1999.

Baldwin, M., and M. Dameris (Lead Authors), J. Austin, S. Bekki, B. Bregman, N. Butchart, E. Cordero, N. Gillett, H.-F. Graf, C. Granier, D. Kinnison, S. Lal, T. Peter, W. Randel, J. Scinocca, D. Shindell, H. Struthers, M. Takahashi, and D. Thompson, Climate-ozone connections, Chapter 5 in *Scientific Assessment of Ozone Depletion: 2006*, Global Ozone Research and Monitoring Project–Report No. 50, 572 pp., World Meteorological Organization, Geneva, Switzerland, 2007.

Baldwin, M.P., and T.J. Dunkerton, Stratospheric harbingers of anomalous weather regimes, *Science*, *244* (5542), 581-584, 2001.

Barriopedro, D., R. Garcia-Herrera, and R. Huth, Solar modulation of Northern Hemisphere winter blocking, *J. Geophys. Res.*, *113*, D14118, doi: 10.1029/2008JD009789, 2008.

Bekki, S., K.S. Law, and J.A. Pyle, Effect of ozone depletion on atmospheric CH_4 and CO concentrations, *Nature*, *371*, 595-597, doi: 10.1038/371595a0, 1994.

Bengtsson, L., K. Hodges, and E. Roeckner, Storm tracks and climate change, *J. Clim.*, *19* (15), 3518-3543, doi: 10.1175/JCLI3815.1, 2006.

Boberg, F., and H. Lundstedt, Solar wind variations related to fluctuations of the North Atlantic oscillation, *Geophys. Res. Lett.*, *29*, doi: 10.1029/2002GL014903, 2002.

Böning, C.W., A. Dispert, M. Visbeck, S.R. Rintoul, and F.U. Schwarzkopf, The response of the Antarctic Circumpolar Current to recent climate change, *Nature Geosci.*, *1*, 864-869, doi: 10.1038/ngeo362, 2008.

Bousquet, P., D.A. Hauglustaine, P. Peylin, C. Carouge, and P. Ciais, Two decades of OH variability as inferred by an inversion of atmospheric transport and chemistry of methyl chloroform, *Atmos. Chem. Phys.*, *5*, 2635-2656, doi: 10.5194/acp-5-2635-2005, 2005.

Brandefelt, J., and E. Källén, The response of the Southern Hemisphere atmospheric circulation to an en-

hanced greenhouse gas forcing, *J. Clim.*, *17* (22), 4425-4442, doi: 10.1175/3221.1, 2004.

Brewer, A.W., Evidence for a world circulation provided by the measurements of helium and water vapour distribution in the stratosphere, *Quart. J. Roy. Meteorol. Soc.*, *75* (326), 351-363, doi: 10.1002/qj.49707532603, 1949.

Brönnimann, S., T. Ewen, T. Griesser, and R. Jenne, Multidecadal signal of solar variability in the upper troposphere during the 20th century, *Space Sci. Rev*., *125* (1-4), 305-315, doi: 10.1007/s11214-006-9065-2, 2006.

Butchart, N., and A.A. Scaife, Removal of chlorofluorocarbons by increased mass exchange between the stratosphere and troposphere in a changing climate, *Nature*, *410*, 799-802, 2001.

Butchart, N., A.A. Scaife, M. Bourqui, J. de Grandpré, S.H.E. Hare, J. Kettleborough, U. Langematz, E. Manzini, F. Sassi, K. Shibata, D. Shindell, and M. Sigmond, Simulations of anthropogenic change in the strength of the Brewer-Dobson circulation, *Clim. Dyn.*, *27* (7-8), 727-741, 2006.

Butchart, N., I. Cionni, V. Eyring, T.G. Shepherd, D.W. Waugh, H. Akiyoshi, J. Austin, C. Brühl, M.P. Chipperfield, E. Cordero, M. Dameris, R. Deckert, S. Dhomse, S.M. Frith, R.R. Garcia, A. Gettelman, M.A. Giorgetta, D.E. Kinnison, F. Li, E. Mancini, C. McLandress, S. Pawson, G. Pitari, D.A. Plummer, E. Rozanov, F. Sassi, J.F. Scinocca, K. Shibata, B. Steil, and W. Tian, Chemistry-climate model simulations of 21st century stratospheric climate and circulation changes, *J. Clim*., *23* (20), doi: 10.1175/2010JCLI3404.1, 2010.

Butler, A.H., D.W.J. Thompson, and K.R. Gurney, Observed relationships between the Southern Annular Mode and atmospheric carbon dioxide, *Global Biogeochem. Cycles*, *21*, GB4014, doi: 10.1029/2006GB002796, 2007.

Cai, W., and T. Cowan, Trends in Southern Hemisphere circulation in IPCC AR4 models over 1950–99: Ozone depletion versus greenhouse forcing, *J. Clim*., *20* (4), 681-693, doi: 10.1175/JCLI4028.1, 2007.

Cai, W., P.H. Whetton, and D.J. Karoly, The response of the Antarctic oscillation to increasing and stabilized atmospheric CO_2, *J. Clim.*, *16* (10), 1525-1538, 2003.

Calvo, N., and R.R. Garcia, Wave forcing of the tropical upwelling in the lower stratosphere under increasing concentrations of greenhouse gases, *J. Atmos. Sci*., *66* (10), 3184-3196, doi: 10.1175/2009JAS3085.1, 2009.

Canziani, P.O., F.E. Malanca, and E.A. Agosta, Ozone and upper troposphere/lower stratosphere variability and change at southern midlatitudes 1980–2000: Decadal variations, *J. Geophys. Res.*, *113*, D20101, doi: 10.1029/2007JD009303, 2008.

CCSP (U.S. Climate Change Science Program), *Temperature Trends in the Lower Atmosphere: Steps for Understanding and Reconciling Differences*, edited by T.R. Karl, S.J. Hassol, C.D. Miller, and W.L. Murray, Synthesis and Assessment Product 1.1, A Report by the Climate Change Science Program and the Subcommittee on Global Change Research, 164 pp., Washington, D.C., 2006.

Chapman, W.L., and J.E. Walsh, A synthesis of Antarctic temperatures, *J. Clim.*, *20* (16), 4096-4117, doi: 10.1175/JCLI4236.l, 2007.

Chin, M., and D. Davis, A reanalysis of carbonyl sulfide as a source of stratospheric background sulfur aerosol, *J. Geophys. Res*., *100* (D5), 8993-9005, 1995.

Christy, J.R., R.W. Spencer, W.B. Norris, W.D. Braswell, and D.E. Parker, Error estimates of version 5.0 of MSU-AMSU bulk atmospheric temperatures, *J. Atmos. Oceanic Technol.*, *20* (5), 613-629, 2003.

Church, J. A., N.J. White, and J.M. Arblaster, Significant decadal-scale impact of volcanic eruptions on sea level and ocean heat content, *Nature*, *438*, 74-77, doi: 10.1038/nature04237, 2005.

Clough, S., and M. Iacono, Line-by-line calculation of atmospheric fluxes and cooling rates. 2. Application to carbon dioxide, ozone, methane, nitrous oxide and the halocarbons, *J. Geophys. Res.*, *100* (D8), 16519-16535, 1995.

Collins, W.J., R.G. Derwent, B. Garnier, C.E. Johnson, M.G. Sanderson, and D.S. Stevenson, Effect of stratosphere-troposphere exchange on the future tropospheric ozone trend, *J. Geophys. Res.*, *108* (D12), 8528, doi: 10.1029/2002JD002617, 2003.

Cook, P.A., and H.K. Roscoe, Variability and trends in stratospheric NO_2 in Antarctic summer, and implications for stratospheric NO_y, *Atmos. Chem. Phys.*, *9*, 3601-3612, doi: 10.5194/acp-9-3601-2009, 2009.

Cordero, E.C., and P.M.deF. Forster, Stratospheric variability and trends in models used for the IPCC AR4, *Atmos. Chem. Phys.*, *6*, 5369-5380, 2006.

Crook, J.A., N.P. Gillett, and S.P.E. Keeley, Sensitivity of Southern Hemisphere climate to zonal asymmetry in ozone, *Geophys. Res. Lett.*, *35*, L07806, doi: 10.1029/2007GL032698, 2008.

Crutzen, P.J., The possible importance of CSO for the sulfate layer of the stratosphere, *Geophys. Res. Lett.*, *3* (2), 73-76, 1976.

Dall'Amico, M., L.J. Gray, K.H. Rosenlof, A.A. Scaife, K.P. Shine, and P.A. Stott, Stratospheric temperature trends: Impact of ozone variability and the QBO, *Clim. Dyn.*, *34* (2-3), doi: 10.1007/s00382-009-0604-x, 2010a.

Dall'Amico, M., P.A. Stott, A.A. Scaife, L.J. Gray, K.H. Rosenlof, and, A.Y. Karpechko, Impact of stratospheric variability on tropospheric climate change,

Clim. Dyn., *34* (2-3), 399-417, doi: 10.1007/s00382-009-0580-1, 2010b.

Deckert, R., and M. Dameris, Higher tropical SSTs strengthen the tropical upwelling via deep convection, *Geophys. Res. Lett.*, *35*, L10813, doi: 10.1029/2008GL033719, 2008.

Delworth, T.L., V. Ramaswamy, and G.L. Stenchikov, The impact of aerosols on simulated ocean temperature and heat content in the 20th century, *Geophys. Res. Lett.*, *32*, L24709, doi: 10.1029/2005GL024457, 2005.

Deshler, T., A review of global stratospheric aerosol: Measurements, importance, life cycle, and local stratospheric aerosol, *Atmos. Res.*, *90* (2-4), 223-232, doi: 10.1016/j.atmosres.2008.03.016, 2008.

Dhomse, S., M. Weber, and J. Burrows, The relationship between tropospheric wave forcing and tropical lower stratospheric water vapor, *Atmos. Chem. Phys.*, *8*, 471-480, 2008.

Dlugokencky, E.J., L. Bruhwiler, J.W.C. White, L.K. Emmons, P.C. Novelli, S.A. Montzka, K.A. Masarie, P.M. Lang, A.M. Crotwell, J.B. Miller, and L.V. Gatti, Observational constraints on recent increases in the atmospheric CH_4 burden, *Geophys. Res. Lett.*, *36*, L18803, doi: 10.1029/2009GL039780, 2009.

Dobson, G.M.B., Origin and distribution of the polyatomic molecules in the atmosphere, *Proc. Roy. Soc. London*, *236*, 1205, 187-193, 1956.

Domingues, C.M., J.A. Church, N.J. White, P.J. Gleckler, S.E. Wijffels, P.M. Barker, and J.R. Dunn, Improved estimates of upper-ocean warming and multi-decadal sea-level rise, *Nature*, *453*, 1090-1093, doi: 10.1038/nature07080, 2008.

Duncan, B.N., and J.A. Logan, Model analysis of the factors regulating the trends and variability of carbon monoxide between 1988 and 1997, *Atmos. Chem. Phys.*, *8*, 7389-7403, 2008.

Engel, A., T. Möbius, H. Bönisch, U. Schmidt, R. Heinz, I. Levin, E. Atlas, S. Aoki, T. Nakazawa, S. Sugawara, F. Moore, D. Hurst, J. Elkins, S. Schauffler, A. Andrews, and K. Boering, Age of stratospheric air unchanged within uncertainties over the past 30 years, *Nature Geosci.*, *2*, 28-31, doi: 10.1038/ngeo388, 2009.

Ern, M., and P. Preusse, Wave fluxes of equatorial Kelvin waves and QBO zonal wind forcing derived from SABER and ECMWF temperature space-time spectra, *Atmos. Chem. Phys.*, *9*, 3957-3986, 2009.

Esler, J.G., L.M. Polvani, and R.K. Scott, The Antarctic stratospheric sudden warming of 2002: A self-tuned resonance?, *Geophys. Res. Lett.*, *33*, L12804, doi: 10.1029/2006GL026034, 2006.

Eyring, V., N. Butchart, D.W. Waugh, H. Akiyoshi, J. Austin, S. Bekki, G.E. Bodeker, B.A. Boville, C. Brühl, M.P. Chipperfield, E. Cordero, M. Dameris, M. Deushi, V.E. Fioletov, S.M. Frith, R.R. Garcia, A. Gettelman, M.A. Giorgetta, V. Grewe, L. Jourdain, D.E. Kinnison, E. Mancini, E. Manzini, M. Marchand, D.R. Marsh, T. Nagashima, P.A. Newman, J.E. Nielsen, S. Pawson, G. Pitari, D.A. Plummer, E. Rozanov, M. Schraner, T.G. Shepherd, K. Shibata, R.S. Stolarski, H. Struthers, W. Tian, and M. Yoshiki, Assessment of temperature, trace species, and ozone in chemistry-climate model simulations of the recent past, *J. Geophys. Res.*, *111*, D22308, doi: 10.1029/2006JD007327, 2006.

Eyring, V., A. Gettelman, N.R.P. Harris, S. Pawson, T.G. Shepherd, D.W. Waugh, H. Akiyoshi, N. Butchart, M.P. Chipperfield, M. Dameris, D.W. Fahey, P.M.deF. Forster, P.A. Newman, M. Rex, R.J. Salawitch, and B.D. Santer, Report on the Third SPARC CCMVal Workshop, SPARC Newsletter No. 30, 17-19, available: http://www.atmosp.physics.utoronto.ca/SPARC/Newsletter30Web/CCMVal.html, 2008.

Feck, T., J.-U. Grooβ, and M. Riese, Sensitivity of Arctic ozone loss to stratospheric H_2O, *Geophys. Res. Lett.*, *35*, L01803, doi: 10.1029/2007GL031334, 2008.

Fogt, R.L., A.J. Monaghan, J. Perlwitz, D.H. Bromwich, J.M. Jones, and G.J. Marshall, Historical SAM variability. Part II: Twentieth-century variability and trends from reconstructions, observations, and the IPCC AR4 models, *J. Clim.*, *22* (20), 5346-5355, 2009.

Forster, P.M.deF., and K.P. Shine, Assessing the climate impact of trends in stratospheric water vapor, *Geophys. Res. Lett.*, *29*, doi: 10.1029/2001GL013909, 2002.

Forster, P.M.deF., and M. Joshi, The role of halocarbons in the climate change of the troposphere and stratosphere, *Clim. Change*, *71* (1-2), 249-266, doi: 10.1007/s10584-005-5955-7, 2005.

Forster, P., V. Ramaswamy, P. Artaxo, T. Berntsen, R. Betts, D.W. Fahey, J. Haywood, J. Lean, D.C. Lowe, G. Myhre, J. Nganga, R. Prinn, G. Raga, M. Schulz, and R. Van Dorland, Changes in atmospheric constituents and in radiative forcing, Chapter 2 in *Climate Change 2007: The Physical Science Basis. Contribution of Working Group I to the Fourth Assessment Report of the Intergovernmental Panel on Climate Change*, edited by S. Solomon, D. Qin, M. Manning, Z. Chen, M. Marquis, K.B. Averyt, M.Tignor, and H.L. Miller, 996 pp., Cambridge University Press, Cambridge, U.K. and New York, NY, U.S.A., 2007a.

Forster, P.M., G. Bodeker, R. Schofield, S. Solomon, and D.W.J. Thompson, Effects of ozone cooling in the tropical lower stratosphere and upper troposphere, *Geophys. Res. Lett.*, *34*, L23813, doi: 10.1029/2007GL031994, 2007b.

Frame, T.H.A., and L.J. Gray, The 11-year solar cycle in

ERA-40 data: An update to 2008, *J. Clim*., *23* (8), doi: 10.1175/JCLI3150.1, 2213-2222, 2010.

Free, M., and D.J. Seidel, Comments on "Biases in stratospheric and tropospheric temperature trends derived from historical radiosonde data," *J. Clim.*, *20* (14), 3704-3709, doi: 10.1175/JCLI4210.1, 2007.

Free, M., and J. Lanzante, Effect of volcanic eruptions on the vertical temperature profile in radiosonde data and climate models, *J. Clim.*, *22* (11), 2925-2939, doi: 10.1175/2008JCLI2562.1, 2009.

Free, M., S.J. Seidel, J.K. Angell, J. Lanzante, I. Durre, and T.C. Peterson, Radiosonde Atmospheric Temperature Products for Assessing Climate (RATPAC): A new data set of large-area anomaly time series, *J. Geophys. Res.*, *110*, D22101, doi: 10.1029/2005JD006169, 2005.

Fröhlich, C., Evidence of a long-term trend in solar irradiance, *Astron. Astophys*., *501* (3), L27-L30, doi: 10.1051/0004-6361/200912318, 2009.

Fröhlich, C., and J. Lean, Solar radiative output and its variability: Evidence and mechanisms, *Astron Astrophys Rev 12* (4), 273-320, doi: 10.1007/s00159-004-0024-1, 2004.

Fu, Q., C.M. Johanson, S.G. Warren, and D.J. Seidel, Contribution of stratospheric cooling to satellite-inferred tropospheric temperature trends, *Nature*, *429*, 55-58, doi: 10.1038/nature02524, 2004.

Fu, Q., C.M. Johanson, J.M. Wallace, and T. Reichler, Enhanced mid-latitude tropospheric warming in satellite measurements, *Science*, *312* (5777), 1179-1179, doi: 10.1126/science.1125566, 2006.

Fu, Q., S. Solomon, and P. Lin, On the seasonal dependence of tropical lower-stratospheric temperature trends, *Atmos. Chem. Phys*., *10*, 2643-2653, doi: 10.5194/acp-10-2643-2010, 2010.

Fueglistaler, S., and P.H. Haynes, Control of interannual and longer-term variability of stratospheric water vapor, *J. Geophys. Res.*, *110*, D24108, doi: 10.1029/2005JD006019, 2005.

Fueglistaler, S., A.E. Dessler, T.J. Dunkerton, I. Folkins, Q. Fu, and P.W. Mote, Tropical tropopause layer, *Rev. Geophys.*, *47*, RG1004, doi: 10.1029/2008RG000267, 2009.

Fuglestvedt, J.S., J.E. Jonson, and I.S.A. Isaksen, Effects of reductions in stratospheric ozone on tropospheric chemistry through changes in photolysis rates, *Tellus*, *46B* (3), 172-192, 1994.

Funatsu, B., C. Claud, P. Keckhut, and A. Hauchecorne, Cross-validation of Advanced Microwave Sounding Unit and lidar for long-term upper-stratospheric temperature monitoring, *J. Geophys. Res*., *113*, D23108, doi: 10.1029/2008JD010743, 2008.

Fusco, A.C., and J.A. Logan, Analysis of 1970-1995 trends in tropospheric ozone at Northern Hemisphere midlatitudes with the GEOS-CHEM model, *J. Geophys. Res*., *108*, 4449, doi: 10.1029/2002JD002742, 2003.

Fyfe, J.C., Separating extratropical zonal wind variability and mean change, *J. Clim.*, *16 (5)*, 863-874, 2003.

Fyfe, J.C., Southern Ocean warming due to human influence, *Geophys. Res. Lett.*, *33*, L19701, doi: 10.1029/2006GL027247, 2006.

Fyfe, J.C., and O.A. Saenko, Simulated changes in the extratropical Southern Hemisphere winds and currents, *Geophys. Res. Lett.*, *33*, L06701, doi: 10.1029/2005GL025332, 2006.

Fyfe, J.C., G.J. Boer, and G.M. Flato, The Arctic and Antarctic oscillations and their projected changes under global warming, *Geophys. Res. Lett.*, *26* (11), 1601-1604, 1999.

Fyfe, J.C., O.A. Saenko, K. Zickfeld, M. Eby, and A.J. Weaver, The role of poleward-intensifying winds on Southern Ocean warming, *J. Clim*., *20* (21), 5391-5400, doi: 10.1175/2007JCLI1764.1, 2007.

Garcia, R.R., and W.J. Randel, Acceleration of the Brewer-Dobson circulation due to increases in greenhouse gases, *J. Atmos. Sci.*, *65* (8), 2731-2739, doi: 10.1175/2008JAS2712.1, 2008.

Geller, M.A., X. Zhou, and M. Zhang, Simulations of the interannual variability of stratospheric water vapor, *J. Atmos. Sci.*, *59* (6), 1076-1085, 2002.

Gent, P.R., and J.C. McWilliams, Isopycnal mixing in ocean circulation models, *J. Phys. Ocean.*, *20* (1), 150-155, 1990.

Gerber, E.P., S. Voronin, and L.M. Polvani, Testing the annular mode autocorrelation timescale in simple atmospheric general circulation models, *Mon. Wea. Rev.*, *136*, 1523-1536, doi: 10.1175/2007MWR2211.1, 2008.

Gerber, E.P., M.P. Baldwin, H. Akiyoshi, J. Austin, S. Bekki, P. Braesicke, N. Buchart, M. Chipperfield, M. Dameris, S. Dhomse, S.M. Firth, R.R. Garcia, H. Garney, A. Gettelman, S.C. Hardiman, O. Morgenstern, J.E. Nielsen, S. Pawson, T. Peter, D.A. Plummer, J.A. Pyle, E. Rozanov, J.F. Scinocca, T.G. Shepherd, and D. Smale, Stratosphere-troposphere coupling and annular mode variability in chemistry-climate models, *J. Geophys. Res.*, *115*, D00M06, doi: 10.1029/2009JD013770, 2010.

Gettelman, A., T. Birner, V. Eyring, H. Akiyoshi, S. Bekki, C. Brühl, M. Dameris, D.E. Kinnison, F. Lefevre, F. Lott, E. Mancini, G. Pitari, D.A. Plummer, E. Rozanov, K. Shibata, A. Stenke, H. Struthers, and W. Tian, The tropical tropopause layer 1960-2100, *Atmos. Chem. Phys.*, *9*, 1621-1637, 2009.

Gettelman, A., M.I. Hegglin, S.-W. Son, J. Kim, M. Fujiwara, T. Birner, S. Kremser, M. Rex, J.A. Añel, H. Akiyoshi, J. Austin, S. Bekki, P. Braesike, C.

Brühl, N. Butchart, M. Chipperfield, M. Dameris, S. Dhomse, H. Garny, S.C. Hardiman, P. Jöckel, D.E. Kinnison, J.F. Lamarque, E. Mancini, M. Marchand, M. Michou, O. Morgenstern, S. Pawson, G. Pitari, D. Plummer, J.A. Pyle, E. Rozanov, J. Scinocca, T.G. Shepherd, K. Shibata, D. Smale, H. Teyssèdre, and W. Tian, Multimodel assessment of the upper troposphere and lower stratosphere: Tropics and global trends, *J. Geophys. Res.*, *115*, D00M08, doi: 10.1029/2009JD013638, 2010.

Gille, S.T., Warming of the Southern Ocean since the 1950s, *Science*, *295* (5558), 1275-1277, doi: 10.1126/science.1065863, 2002.

Gille, S.T., Decadal-scale temperature trends in the Southern Hemisphere ocean, *J. Clim.*, *21* (18), 4749-4765, doi: 10.1175/2008JCLI2131.1, 2008.

Gillett, N.P., and D.W.J. Thompson, Simulation of recent Southern Hemisphere climate change, *Science*, *302* (5643), 273-275, 2003.

Gillett, N.P., T.D. Kell, and P.D. Jones, Regional climate impacts of the Southern Annular Mode, *Geophys. Res. Lett.*, *33*, L23704, doi: 10.1029/2006GL027721, 2006.

Gillett, N.P., D.A. Stone, P.A. Stott, T. Nozawa, A.Yu. Karpechko, G.C. Hegerl, M.F. Wehner, and P.D. Jones, Attribution of polar warming to human influence, *Nature Geosci.*, *1*, 750-754, doi: 10.1038/ngeo338, 2008.

Gillett, N.P., J.F. Scinocca, D.A. Plummer, and M.C. Reader, Sensitivity of climate to dynamically-consistent zonal asymmetries in ozone, *Geophys. Res. Lett.*, *36*, L10809, doi: 10.1029/2009GL037246, 2009.

Gillett, N.P., H. Akiyoshi , S. Bekki , V. Eyring , R. Garcia, C.A. McLinden, A. Yu. Karpechko, D.A. Plummer, E. Rozanov, J. Scinocca, and K. Shibata, Attribution of observed changes in stratospheric ozone and temperature, *Atmos. Chem. Phys. Discuss., 10*, 17341-17367, doi: 10.5194/acpd-10-17341-2010, 2010.

Giorgetta, M.A., E. Manzini, E. Roeckner, M. Esch, and L. Bengtsson, Climatology and forcing of the quasi-biennial oscillation in the MAECHAM5 model, *J. Clim.*, *19* (16), 3882-3901, doi: 10.1175/JCLI3830.1, 2006.

Gleckler, P.J., K. AchutaRao, J.M. Gregory, B.D. Santer, K.E. Taylor, and T.M.L. Wigley, Krakatoa lives: The effect of volcanic eruptions on ocean heat content and thermal expansion, *Geophys. Res. Lett.*, *33*, L17702, doi: 10.1029/2006GL026771, 2006.

Goosse, H., W. Lefebvre, A. de Montety, E. Crespin, and A.H. Orsi, Consistent past half-century trends in the atmosphere, the sea ice, and the ocean at high southern latitudes, *Clim. Dyn.*, *33* (7-8), doi: 10.1007/s00382-008-0500-9, 2009.

Granier, C., J.-F. Müller, S. Madronich, and G.P. Brasseur, Possible causes for the 1990-1993 decrease in the global tropospheric CO abundances: A three-dimensional sensitivity study, *Atmos. Env.*, *30* (10-11), 1673-1682, doi: 10.1016/1352-2310(95)00397-5, 1996.

Gray, L.J., S.T. Rumbold, and K. Shine, Stratospheric temperature and radiative forcing response to 11-year solar cycle changes in irradiance and ozone, *J. Atmos. Sci.*, *66* (8), 2402-2417, doi: 10.1175/2009JAS2866.1, 2009.

Gray, L.J., J. Beer, M. Geller, J.D. Haigh, M. Lockwood, K. Matthes, U. Cubasch, D. Fleitmann, R.G. Harrison, L. Hood, J. Luterbacher, G.A. Meehl, D. Shindell, B. van Geel, and W. White, Solar influence on climate, *Rev. Geophys.*, in press, 2010.

Gregory, J.M., J.A. Lowe, and S.F.B. Tett, Simulated global-mean sea level change over the last half-millennium, *J. Clim.*, *19* (18), 4576-4591, doi: 10.1175/JCLI3881.1, 2006.

Griffiths, G.M., Changes in New Zealand daily rainfall extremes 1930–2004, *Weather and Climate*, *26*, 3-46, 2006.

Grise, K.M., D.W.J. Thompson, and P.M. Forster, On the role of radiative processes in stratosphere-troposphere coupling, *J. Clim.*, *22* (15), 4154-4161, doi: 10.1175/2009JCLI2756.1, 2009.

Haigh, J.D., The role of stratospheric ozone in modulating the solar radiative forcing of climate, *Nature*, *370* (6490), 544-546, 1994.

Haigh, J.D., The impact of solar variability on climate, *Science*, *272* (5264), 981-984, doi: 10.1126/science272.5264.981, 1996.

Haigh, J.D., A GCM study of climate change in response to the 11-year solar cycle, *Quart. J. Roy. Meteorol. Soc.*, *125* (555), 871-892, 1999.

Haigh, J.D., The effects of solar variability on the Earth's climate, *Phil. Trans. Roy. Soc. A*, *361* (1802), 95-111, 2003.

Haigh, J.D., and J.A. Pyle, Ozone perturbation experiments in a two-dimensional circulation model, *Quart. J. Roy. Meteorol. Soc.*, *108*, 551-574, 1982.

Haigh, J.D., and H.K. Roscoe, Solar influences on polar modes of variability, *Meteorol. Z.*, *15* (3), 371-378, 2006.

Haigh, J.D., and H.K. Roscoe, The final warming date of the Antarctic polar vortex and influences on its interannual variability, *J. Clim.*, *22* (22), 5809-5819, 2009.

Haigh, J.D., M. Blackburn, and R. Day, The response of tropospheric circulation to perturbations in lower-stratospheric temperature, *J. Clim.*, *18*, 3672-3685, 2005.

Haigh, J.D., A.R. Winning, R. Toumi, and J.W. Harder, An influence of solar spectral variations on radiative forcing of climate, *Nature*, *467*, 696-699, doi:

10.1038/nature09426, 2010.

Haimberger, L., Homogenization of radiosonde temperature time series using innovation statistics, *J. Clim*., *20* (7), 1377-1403, doi: 10.1175/JCLI4050.1, 2007.

Haimberger, L., C. Tavolato, and S. Sperka, Toward elimination of the warm bias in historic radiosonde temperature records—Some new results from a comprehensive intercomparison of upper-air data, *J. Clim*., *21* (18), 4587-4606, doi: 10.1175/2008JCLI1929.1, 2008.

Hall, A., and M. Visbeck, Synchronous variability in the Southern Hemisphere atmosphere, sea ice, and ocean resulting from the Annular Mode, *J. Clim.*, *15* (21), 3043-3057, doi: 10.1175/1520-0442(2002)015<3043:SVITSH>2.0.CO;2, 2002.

Hallberg, R., and A. Gnanadesikan, The role of eddies in determining the structure and response of the wind-driven Southern Hemisphere overturning: Results from the Modeling Eddies in the Southern Ocean (MESO) project, *J. Phys. Ocean.*, *36* (12), 2232-2252, doi: 10.1175/JPO2980.1, 2006.

Hampson J., P. Keckhut, A. Hauchecorne, and M.L. Chanin, The effect of the 11-year solar-cycle on the temperature in the upper-stratosphere and mesosphere: Part II: Numerical simulation and role of planetary waves, *J. Atmos. Sol. Terr. Phys*., *67*, 948-958, 2005.

Hansen, J., A. Lacis, R. Ruedy, and M. Sato, Potential climate impact of Mount Pinatubo eruption, *Geophys. Res. Lett.*, *19* (2), 215-218, doi: 10.1029/91GL02788, 1992.

Harder, J.W., J.M. Fontenla, P. Pilewskie, E.C. Richard, and T.N. Woods, Trends in solar spectral irradiance variability in the visible and infrared, *Geophys. Res. Lett*., *36*, L07801, doi: 10.1029/2008GL036797, 2009.

Hegerl, G.C., F.W. Zwiers, P. Braconnot, N.P. Gillett, Y. Luo, J.A. Marengo Orsini, N. Nicholls, J.E. Penner, and P.A. Stott, Understanding and attributing climate change, Chapter 9 in *Climate Change 2007: The Physical Science Basis*. *Contribution of Working Group I to the Fourth Assessment Report of the Intergovernmental Panel on Climate Change*, edited by S. Solomon, D. Qin, M. Manning, Z. Chen, M. Marquis, K.B. Averyt, M. Tignor, and H.L. Miller, 996 pp., Cambridge University Press, Cambridge, U.K. and New York, NY, U.S.A., 2007.

Hegglin, M.I., and T.G. Shepherd, Large climate-induced changes in ultraviolet index and stratosphere-to-troposphere ozone flux, *Nature Geosci.*, *2*, 687-691, doi: 10.1038/ngeo604, 2009.

Hendon, H.H., D.W.J. Thompson, and M.C.Wheeler, Australian rainfall and surface temperature variations associated with the Southern Hemisphere Annular Mode, *J. Clim.*, *20* (11), 2452-2467, doi: 10.1175/JCLI4134.1, 2007.

Hofmann, D.J., Increase in the stratospheric background sulfuric acid aerosol mass in the past 10 years, *Science*, *248* (4958), 996-1000, doi: 10.1126/science.248.4958.996, 1990.

Hofmann, D.J., J. Barnes, M. O'Neill, M. Trudeau, and R. Neely, Increase in background stratospheric aerosol observed with lidar at Mauna Loa Observatory and Boulder, Colorado, *Geophys. Res. Lett.*, *36*, L15808, doi: 10.1029/2009GL039008, 2009.

Holton, J.R., and A. Gettelman, Horizontal transport and the dehydration of the stratosphere, *Geophys. Res. Lett.*, *28* (14), 2799-2802, 2001.

Hsu J., and M.J. Prather, Stratospheric variability and tropospheric ozone, *J. Geophys. Res.*, *114*, D06102, doi: 10.1029/2008JD010942, 2009.

Hu, Y., and Q. Fu, Observed poleward expansion of the Hadley circulation since 1979, *Atmos. Chem. Phys.*, *7*, 5229-5236, 2007.

Hudson, R.D., M.F. Andrade, M.B. Follette, and A.D. Frolov, The total ozone field separated into meteorological regimes—Part II: Northern Hemisphere mid-latitude total ozone trends, *Atmos. Chem. Phys.*, *6*, 5183-5191, 2006.

IPCC, *Climate Change 2007: The Physical Science Basis. Contribution of Working Group I to the Fourth Assessment Report of the Intergovernmental Panel on Climate Change*, edited by S. Solomon, D. Qin, M. Manning, Z. Chen, M. Marquis, K.B. Averyt, M. Tignor, and H.L. Miller, 996 pp., Cambridge University Press, Cambridge, U.K. and New York, NY, U.S.A., 2007.

IPCC/TEAP (Intergovernmental Panel on Climate Change/Technology and Economic Assessment Panel), *IPCC/TEAP Special Report on Safeguarding the Ozone Layer and the Global Climate System: Issues Related to Hydrofluorocarbons and Perfluorocarbons*, prepared by Working Groups I and III of the Intergovernmental Panel on Climate Change, and the Technical and Economic Assessment Panel, edited by B. Metz, L. Kuijpers, S. Solomon, S.O. Andersen, O. Davidson, J. Pons, D. de Jager, T. Kestin, M. Manning, and L. Meyer, 488 pp., Cambridge University Press, Cambridge, U.K. and New York, NY, U.S.A., 2005.

Isaksen, I.S.A., C. Zerefos, K. Kourtidis, C. Meleti, S.B. Dalsøren, J.K. Sundet, A. Grini, P. Zanis, and D. Balis, Tropospheric ozone changes at unpolluted and semipolluted regions induced by stratospheric ozone changes, *J. Geophys. Res.*, *110*, D02302, doi: 10.1029/2004JD004618, 2005.

Isaksen, I., C. Grainer, G. Myhre, T.K. Berntsen, S.B. Dal-

seren, M. Gauss, Z. Klimont, R. Benestad, P. Bousquet, W. Collins, T. Cox, V. Eyring, D. Fowler, S. Fuzzi, P. Jöckel, P. Laj, U. Lohmann, M. Malone, P. Monks, A.S.H. Prevot, F. Raes, A. Richter, B. Rognerud, M. Schulz, D. Shindell, D.S. Stevenson, T. Storelvmo, W.-C. Wang, M. van Weele, M. Wild, and D. Wuebbles, Atmospheric composition change: Climate-Chemistry interactions, *Atmos. Env.*, *43* (33), 5138-5192, doi: 10.1016/j.atmosenv.2009.08.003, 2009.

Ito, T., M. Woloszyn, and M. Mazloff, Anthropogenic carbon dioxide transport in the Southern Ocean driven by Ekman flow, *Nature*, *463*, 80-83, doi: 10.1038/natureo8687, 2010.

Iwasaki, T., H. Hamada, and K. Miyazaki, Comparisons of Brewer-Dobson circulations diagnosed from reanalyses, *J. Meteor. Soc. Jap*., *87* (6), 997-1006, 2009.

Jäger, H., Long-term record of lidar observations of the stratospheric aerosol layer at Garmisch-Partenkirchen, *J. Geophys. Res.*, *110*, D08106, doi: 10.1029/2004JD005506, 2005.

Jensen, E., and L. Pfister, Transport and freeze-drying in the tropical tropopause layer, *J. Geophys. Res.*, *109*, D02207, doi: 10.1029/2003JD004022, 2004.

Johanson, C.M., and M. Fu, Hadley cell widening: Model simulations versus observations, *J. Clim*., *22* (10), 2713-2725, doi: 10.1175/2008JCLI2620.1, 2009.

Jones, R.L., J.A. Pyle, J.E. Harries, A.M. Zavody, J.M. Russell III, and J.C. Gille, The water vapour budget of the stratosphere studied using LIMS and the SAMS satellite data, *Quart. J. Roy. Meteor. Soc.*, *112 (474)*, 1127-1143, doi: 10.1256/smsqj.47411, 1986.

Jonsson, A.I., V.I. Fomichev, and T.G. Shepherd, The effect of nonlinearity in CO_2 heating rates on the attribution of stratospheric ozone and temperature changes, *Atmos. Chem. Phys.*, *9*, 8447-8452, 2009.

Joshi, M.M., and G.S. Jones, The climatic effects of the direct injection of water vapour into the stratosphere by large volcanic eruptions, *Atmos. Chem. Phys.*, *9*, 6109-6118, 2009.

Karpechko, A.Yu., N.P. Gillett, G.J. Marshall, and A.A. Scaife, Stratospheric influence on circulation changes in the Southern Hemisphere troposphere in coupled climate models, *Geophys. Res. Lett.*, *35*, L20806, doi: 10.1029/2008GL035354, 2008.

Karpetchko, A., E. Kyrö, and B.M. Knudsen, Arctic and Antarctic polar vortices 1957-2002 as seen from the ERA-40 reanalyses, *J. Geophys. Res.*, *110*, D21109, doi: 10.1029/2005JD006113, 2005.

Keckhut, P., C. Cagnazzo, M.-L. Chanin, C. Claud, and A. Hauchecorne, The 11-year solar-cycle effects on the temperature in the upper-stratosphere and mesosphere: Part I–Assessment of observations, *J. Atmos. Sol. Terr. Phys* , *67*, 940-947, doi: 10.1016/j.jastp.2005.01.008, 2005.

Keeley, S.P.E., N.P. Gillett, D.W.J. Thompson, S. Solomon, and P.M. Forster, Is Antarctic climate most sensitive to ozone depletion in the mid or lower stratosphere?, *Geophys. Res. Lett.*, *34*, L22812, doi: 10.1029/2007GL031238, 2007.

Khatiwala, S., F. Primeau, and T. Hall, Reconstruction of the history of anthropogenic CO_2 concentrations in the ocean, *Nature*, *462*, 346-349, doi: 10.1038/nature08526, 2009.

Khaykin, S., J.-P. Pommereau, L. Korshunov, V. Yushkov, J. Nielsen, N. Larsen, T. Christensen, A. Garnier, A. Lukyanov, and E. Williams, Hydration of the lower stratosphere by ice crystal geysers over land convective systems, *Atmos. Chem. Phys.*, *9*, 2275-2287, 2009.

Kidston, J., and E.P. Gerber, Intermodel variability of the poleward shift of the austral jet stream in the CMIP3 integrations linked to biases in 20th century climatology, *Geophys. Res. Lett*., *37*, L09708, doi: 10.1029/2010GL042873, 2010.

Kirk-Davidoff, D.B., E.J. Hintsa, J.G. Anderson, and D.W. Keith, The effect of climate change on ozone depletion through changes in stratospheric water vapour, *Nature*, *402*, 399-401, doi: 10.1038/46521, 1999.

Kley, D., J.M. Russell III, and C. Phillips, *SPARC Assessment of Upper Tropospheric and Stratospheric Water Vapor*, WCRP-No. 113, WMO/TD-No. 1043, SPARC Report No.2, 2000.

Kodera, K., Solar cycle modulation of the North Atlantic Oscillation: Implication in the spatial structure of the NAO, *Geophys. Res. Lett.*, *29* (8), 1218, doi: 10.1029/2001GL014557, 2002.

Kodera, K., Solar influence on the Indian Ocean Monsoon through dynamical processes, *Geophys. Res. Lett.*, *31*, L24209, doi: 10.1029/2004GL020928, 2004.

Kodera, K., and K. Shibata, Solar influence on the tropical stratosphere and troposphere in the northern summer, *Geophys. Res. Lett.*, *33*, L19704, doi: 10.1029/2006GL026659, 2006.

Kodera, K., K. Coughlin, and O. Arakawa, Possible modulation of the connection between the Pacific and Indian Ocean variability by the solar cycle, *Geophys. Res. Lett.*, *34*, L03710, doi: 10.1029/2006GL027827, 2007.

Korhonen, H., K.S. Carslaw, P.M. Forster, S. Mikkonen, N.D. Gordon, and H. Kokkola, Aerosol climate feedback due to decadal increases in Southern Hemisphere wind speeds, *Geophys. Res. Lett.*, *37*, L02805, doi: 10.1029/2009GL041320, 2010.

Kuroda, Y., and K. Kodera, Role of the Polar-night Jet Oscillation on the formation of the Arctic Oscillation in the Northern Hemisphere winter, *J. Geophys. Res.*, *109*, D11112, doi: 10.1029/2003JD004123, 2004.

Kuroda, Y., and K. Kodera, Solar cycle modulation of the Southern Annular Mode, *Geophys. Res. Lett.*, *32*, L13802, doi: 10.1029/2005GL022516, 2005.

Kuroda, Y., M. Deushi, and K. Shibata, Role of solar activity in the troposphere-stratosphere coupling in the Southern Hemisphere winter, *Geophys. Res. Lett.*, *34*, L21704, doi: 10.1029/2007GL030983, 2007.

Kushner, P.J., and L.M. Polvani, Stratosphere-troposphere coupling in a relatively simple AGCM: The role of eddies, *J. Clim.*, *17* (3), 629-639, 2004.

Kushner, P.J., and L.M. Polvani, Stratosphere-troposphere coupling in a relatively simple AGCM: Impact of the seasonal cycle, *J. Clim.*, *19* (21), 5721-5727, 2006.

Kushner, P., I.M. Held, and T.L. Delworth, Southern Hemisphere atmospheric circulation response to global warming, *J. Clim.*, *14* (10), 2238-2249, 2001.

Labitzke, K., Sunspots, the QBO and the stratospheric temperature in the north polar region, *Geophys. Res. Lett.*, *14* (5), 535-537, 1987.

Lamarque, J.-F., and S. Solomon, Impact of changes in climate and halocarbons on recent lower stratosphere ozone and temperature trends, *J. Clim*., *23* (10), 2599-2611, doi: 10.1175/2010JCLI3179.1, 2010.

Lambert, A., W.G. Read, N.J. Livesey, M.L. Santee, G.L. Manney, L. Froidevaux, D.L. Wu, M.J. Schwartz, H.C. Pumphrey, C. Jimenez, G.E. Nedoluha, R.E. Cofield, D.T. Cuddy, W.H. Daffer, B.J. Drouin, R.A. Fuller, R.F. Jarnot, B.W. Knosp, H.M. Pickett, V.S. Perun, W.V. Snyder, P.C. Stek, R.P. Thurstans, P.A. Wagner, J.W. Waters, K.W. Jucks, G.C. Toon, R.A. Stachnik, P.F. Bernath, C.D. Boone, K.A. Walker, J. Urban, D. Murtagh, J.W. Elkins, and E. Atlas, Validation of the Aura Microwave Limb Sounder middle atmosphere water vapor and nitrous oxide measurements, *J. Geophys*. *Res.*, *112*, D24S36, doi: 10.1029/2007JD008724, 2007.

Lanzante, J.R., S.A. Klein, and D.J. Seidel, Temporal homogenization of monthly radiosonde temperature data. Part I: Methodology, *J. Clim*., *16* (2), 224-240, 2003.

Larkin, A., J.D. Haigh, and S. Djavidnia, The effect of solar UV irradiance variations on the Earth's atmosphere, *Space Sci. Rev.*, *94* (1-2), 199-214, 2000.

Law, K.S., and W.T. Sturges (Lead Authors), D.R. Blake, N.J. Blake, J.B. Burkholder, J.H. Butler, R.A. Cox, P.H. Haynes, M.K.W. Ko, K. Kreher, C. Mari, K. Pfeilsticker, J.M.C. Plane, R.J. Salawitch, C. Schiller, B.-M. Sinnhuber, R. von Glasow, N.J. Warwick, D.J. Wuebbles, and S.A. Yvon-Lewis, Halogenated very short-lived substances, Chapter 2 in *Scientific Assessment of Ozone Depletion: 2006*, Global Ozone Research and Monitoring Project–Report No. 50, 572 pp., World Meteorological Organization, Geneva, Switzerland, 2007.

Law, R.M., R.J. Matear, and R.J. Francey, Comment On "Saturation of the southern ocean CO_2 sink due to recent climate change," *Science, 319* (5863), 570, 2008.

Le Quéré, C., C. Rödenbeck, E.T. Buitenhuis, T.J. Conway, R. Langenfelds, A. Gomez, C. Labuschagne, M. Ramonet, T. Nakazawa, N. Metzl, N. Gillett, and M. Heimann, Saturation of the Southern Ocean CO_2 sink due to recent climate change, *Science*, *316* (5832), 1735-1738, doi: 10.1126/science.1136188, 2007.

Le Quéré, C., M.R. Raupach, J.G. Canadell, and G. Marland, Trends in the sources and sinks of carbon dioxide, *Nature Geosci.*, *2*, 831-836, doi: 10.1038/ngeo689, 2009.

le Texier, H., S. Solomon, and R.R. Garcia, The role of molecular hydrogen and methane oxidation in the water vapour budget of the stratosphere, *Quart. J. Roy. Meteorol. Soc.*, *114* (480), 281-295, doi: 10.1002/qj.49711448002, 1988.

Lee, H., and A.K. Smith, Simulation of the combined effects of solar cycle, quasi-biennial oscillation, and volcanic forcing on stratospheric ozone changes in recent decades, *J. Geophys. Res.*, *108* (D2), 4049, doi: 10.1029/2001JD001503, 2003.

Lee, J.N., and S. Hameed, Northern Hemisphere annular mode in summer: Its physical significance and its relation to solar activity variations, *J. Geophys. Res*., *112*, D15111, doi: 10.1029/2007JD008394, 2007.

Lee, J.N., S. Hameed, and D.T. Shindell, The northern annular mode in summer and its relation to solar activity variations in the GISS ModelE, *J. Atmos. Sol. Terr. Phys*., *70* (5), 730-741, doi: 10.1016/j.jastp.2007.10.012, 2008.

Leith, C.E., Climate response and fluctuation dissipation, *J. Atmos. Sci.*, *32*, 2022-2026, 1975.

Lenton, A., and R.J. Matear, Role of the Southern Annular Mode (SAM) in Southern Ocean CO_2 uptake, *Global Biogeochem. Cycles*, *21*, GB2016, doi: 10.1029/2006GB002714, 2007.

Lenton, A., F. Codron, L. Bopp, N. Metzl, P. Cadule, A. Tagliabue, and J. Le Sommer, Stratospheric ozone depletion reduces ocean carbon uptake and enhances ocean acidification, *Geophys. Res. Lett.*, *36*, L12606, doi: 10.1029/2009GL038227, 2009.

Li, F., J. Austin, and J. Wilson, The strength of the Brewer-Dobson circulation in a changing climate: Coupled chemistry-climate model stimulation, *J. Clim.*, *21* (1), 40-57, doi: 10.1175/2007.JCLI1663.1, 2008.

Limpasuvan, V., and D.L. Hartmann, Wave-maintained annular modes of climate variability, *J. Clim*., *13*, 4414-4429, 2000.

Lin, P., Q. Fu, S. Solomon, and J.M. Wallace, Temperature trend patterns in Southern Hemisphere high

latitudes: Novel indicators of stratospheric change, *J. Clim*., *22* (23), 2009.

Lorenz, D.J., and E.T. DeWeaver, Tropopause height and zonal wind response to global warming in the IPCC scenario integrations, *J. Geophys. Res.*, *112*, D10119, doi: 10.1029/2006JD008087, 2007.

Lovenduski, N.S., N. Gruber, and S.C. Doney, Toward a mechanistic understanding of the decadal trends in the Southern Ocean carbon sink, *Global Biogeochem. Cycles*, *22*, GB3016, doi: 10.1029/2007GB003139, 2008.

Lu, J., G.A. Vecchi, and T. Reichler, Expansion of the Hadley cell under global warming, *Geophys. Res. Lett.*, *34*, L06805, doi: 10.1029/2006GL028443, 2007.

Lu, J., G. Chen, and D.M.W. Frierson, Response of the zonal mean atmospheric circulation to El Niño versus global warming, *J. Clim.*, *21* (22), 5835-5851, doi: 10.1175/2008JCLI2200.1, 2008.

Lu, J., C. Deser, and T. Reichler, Cause of the widening of the tropical belt since 1958, *Geophys. Res. Lett.*, *36*, L03803, doi: 10.1029/2008GL036076, 2009.

Lynch, A., P. Uotila, and J.J. Cassano, Changes in synoptic weather patterns in the polar regions in the twentieth and twenty-first centuries, Part 2: Antarctic, *Int. J. Climatol*., *26* (9), 1181-1199, 2006.

Madronich, S., and C. Granier, Impact of recent total ozone changes on tropospheric ozone photodissociation, hydroxyl radicals, and methane trends, *Geophys. Res. Lett.*, *19* (5), 465-467, 1992.

Marshall, G.J., A. Orr, N.P.M. van Lipzig, and J.C. King, The impact of a changing Southern Hemisphere Annular Mode on Antarctic peninsula summer temperatures, *J. Clim.*, *19* (20), 5388-5404, doi: 10.1175/JCLI3844.1, 2006.

Matthes, K., Y. Kuroda, K. Kodera, and U. Langematz, Transfer of the solar signal from the stratosphere to the troposphere: Northern winter, *J. Geophys. Res.*, *111*, D06108, doi: 10.1029/2005JD006283, 2006.

McLandress, C., and T.G. Shepherd, Simulated anthropogenic changes in the Brewer-Dobson circulation, including its extension to high latitudes, *J. Clim*., *22* (6), 1516-1540, doi: 10.1175/2008JCLI2679.1, 2009.

McLandress, C., A.I. Jonsson, D.A. Plummer, M.C. Reader, J.F. Scinocca, and T.G. Shepherd, Separating the dynamical effects of climate change and ozone depletion: Part 1. Southern Hemisphere stratosphere, *J. Clim*., *23* (18), 5002-5020, doi: 10.1175/2010JCLI3586.1, 2010.

Mears, C.A., and F.J. Wentz, Construction of the Remote Sensing Systems V3.2 atmospheric temperature records from the MSU and AMSU microwave sounders, *J. Atmos. Oceanic Technol.*, *26* (6), 1040-1056, doi: 10.1175/2008JTECHAI176.1, 2009.

Meehl, G.A., C. Covey, T. Delworth, M. Latif, B. McAvaney, J.F.B. Mitchell, R.J. Stouffer, and K.E. Taylor, The WCRP CMIP3 multi-model dataset: A new era in climate change research, *Bull. Amer. Meteorol. Soc.*, *88* (9), 1383-1394, doi: 10.1175/BAMS-88-9-1383, 2007.

Meehl, G.A., J.M. Arblaster, G. Branstator, and H. van Loon, A coupled air-sea response mechanism to solar forcing in the Pacific region, *J. Clim.*, *21* (12), 2883-2897, doi: 10.1175/2007JCLI1776.1, 2008.

Meehl, G.A., J.M. Arblaster, K. Matthes, F. Sassi, and H. van Loon, Amplifying the Pacific climate system response to a small 11-year solar cycle forcing, *Science*, *325* (5944), 1114-1118, doi: 10.1126/science.1172872, 2009.

Meneghini, B., I. Simmonds, and I.N. Smith, Association between Australian rainfall and the Southern Annular Mode, *Int. J. Climatol.*, *27*, 109-121, doi: 10.1002/joc:1370, 2007.

Meredith, M.P., and A.M. Hogg, Circumpolar response of the Southern Ocean eddy activity to a change in the Southern Annular Mode, *Geophys. Res. Lett.*, *33*, L16608, doi: 10.1029/2006GL026499, 2006.

Miller, R.L., G.A. Schmidt, and D.T. Shindell, Forced annular variations in the 20th century Intergovernmental Panel on Climate Change Fourth Assessment Report models, *J. Geophys. Res.*, *111*, D18101, doi: 10.1029/2005JD006323, 2006.

Monaghan, A.J., D.H. Bromwich, W. Chapman, and J.C. Comiso, Recent variability and trends of Antarctic near-surface temperature, *J. Geophys. Res.*, *113*, D04105, doi: 10.1029/2007JD009094, 2008.

Morgenstern, O., M.A. Giorgetta, K. Shibata, V. Eyring, D.W. Waugh, T.G. Shepherd, H. Akiyoshi, J. Austin, A.J.G. Baumgaertner, S. Bekki, P. Braesicke, C. Brühl, M.P. Chipperfield, D. Cugnet, M. Dameris, S. Dhomse, S.M. Frith, H. Garny, A. Gettelman, S.C. Hardiman, M.I. Hegglin, P. Jöckel, D.E. Kinnison, J.-F. Lamarque, E. Mancini, E. Manzini, M. Marchand, M. Michou, T. Nakamura, J.E. Nielsen, D. Olivié, G. Pitari, D.A. Plummer, E. Rozanov, J.F. Scinocca, D. Smale, H. Teyssèdre, M. Toohey, W. Tian, and Y. Yamashita, Review of the formulation of present-generation stratospheric chemistry-climate models and associated external forcings, *J. Geophys. Res.*, *115*, D00M02, doi:10.1029/2009JD013728, 2010a.

Morgenstern, O., H. Akiyoshi, S. Bekki, P. Braesicke, N. Butchart, M.P. Chipperfield, D. Cugnet, M. Deushi, S.S. Dhomse, R.R. Garcia, A. Gettelman, N.P. Gillett, S.C. Hardiman, J. Jumelet, D.E. Kinnison, J.-F. Lamarque, F. Lott, M. Marchand, M. Michou, T. Nakamura, D. Olivié, T. Peter, D. Plummer, J.A.

Pyle, E. Rozanov, D. Saint-Martin, J.F. Scinocca, K. Shibata, M. Sigmond, D. Smale, H. Teyssèdre, W. Tian, A. Voldoire, and Y. Yamashita, Anthropogenic forcing of the Northern Annular Mode in CCMVal-2 models, *J. Geophys. Res.*, *115* (D00M03), doi: 10.1029/2009JD013347, 2010b.

Mote, P.W., K.H. Rosenlof, M.E. McIntyre, E.S. Carr, J.C. Gille, J.R. Holton, J.S. Kinnersley, H.C. Pumphrey, J.M. Russell, and J.W. Waters, An atmospheric tape recorder: The imprint of tropical tropopause temperatures on stratospheric water vapor, *J. Geophys. Res.*, *101* (D2), 3989-4006, 1996.

Nielsen, J.K., N. Larsen, F. Cairo, G. Di Donfrancesco, J.M. Rosen, G. Durry, G. Held, and J.P. Pommereau, Solid particles in the tropical lowest stratosphere, *Atmos. Chem. Phys.*, *7*, 685-695, 2007.

Notholt, J., B.P. Luo, S. Füeglistaler, D. Weisenstein, M. Rex, M.G. Lawrence, H. Bingemer, I. Wohltmann, T. Corti, T. Warneke, R. von Kuhlmann, and T. Peter, Influence of tropospheric SO_2 emissions on particle formation and the stratospheric humidity, *Geophys. Res. Lett.*, *32*, L07810, doi: 10.1029/2004GL022159, 2005.

Oke, P.R., and M.H. England, Oceanic response to changes in the latitude of the Southern Hemisphere subpolar westerly winds, *J. Clim.*, *17* (5), 1040-1054, 2004.

Olsen, S.C., C.A. McLinden, and M.J. Prather, Stratospheric N_2O-NO_y system: Testing uncertainties in a three-dimensional framework, *J. Geophys. Res.*, *106* (D22), 28771-28784, 2001.

Oltmans, S.J., H. Vömel, D.J. Hofmann, K.H. Rosenlof, and D. Kley, The increase in stratospheric water vapor from balloonborne frostpoint hygrometer measurements at Washington D.C., and Boulder, Colorado, *Geophys. Res. Lett.*, *27* (21), 3453-3456, 2000.

Oman, L., D.W. Waugh, S. Pawson, R.S. Stolarski, and P.A. Newman, On the influence of anthropogenic forcings on changes in the stratospheric mean age, *J. Geophys. Res.*, *114*, doi: 10.1029/2008JD010378, 2009.

Ordóñez, C., D. Brunner, J. Staehelin, P. Hadjinicolaou, J.A. Pyle, M. Jonas, H. Wernli, and A.S.H. Prevot, Strong influence of lowermost stratospheric ozone on lower tropospheric background ozone changes over Europe, *Geophys. Res.*, *Lett.*, *34*, L07805, doi: 10.1029/2006GL029113, 2007.

Pawson, S., K. Labitzke, and S. Leder, Stepwise changes in stratospheric temperature, *Geophys. Res. Lett.*, *25* (12), 2157-2160, 1998.

Perlwitz, J., S. Pawson, R.L. Fogt, J.E. Nielsen, and W.D. Neff, Impact of stratospheric ozone hole recovery on Antarctic climate, *Geophys. Res. Lett.*, *35*, L08714, doi: 10.1029/2008GL033317, 2008.

Peter, T., C. Marcolli, P. Spichtinger, T. Corti, M.B. Baker, and T. Koop, When dry air is too humid, *Science*, *314* (5804), 1399-1402, doi: 10.1126/science.1135199, 2006.

Pezza, A.B., I. Simmonds, and J.A. Renwick, Southern hemisphere cyclones and anticyclones: Recent trends and links with decadal variability in the Pacific Ocean, *Int. J. Climatol.*, *27* (11), 1403-1419, 2007.

Pezza, A.B., T. Durrant, I. Simmonds, and I. Smith, Southern Hemisphere synoptic behavior in extreme phases of SAM, ENSO, sea ice extent, and southern Australia rainfall, *J. Clim.*, *21* (21), 5566-5584, doi: 10.1175/2008JCLI2128.1, 2008.

Pitari, G., E. Mancini, V. Rizi, and D.T. Shindell, Impact of future climate and emission changes on stratospheric aerosols and ozone, *J. Atmos. Sci.*, *59* (3), 414-440, 2002.

Plumb, R.A., and J. Eluszkiewicz, The Brewer–Dobson circulation: Dynamics of the tropical upwelling, *J. Atmos. Sci.*, *56*, 868-890, 1999.

Polvani, L.M., and P.J. Kushner, Tropospheric response to stratospheric perturbations in a relatively simple general circulation model, *Geophys. Res. Lett.*, *29*, doi: 10.1029/2001GL014284, 2002.

Portmann, R.W., and S. Solomon, Indirect radiative forcing of the ozone layer during the 21st century, *Geophys. Res. Lett.*, *34*, L02813, doi: 10.1029/2006GL028252, 2007.

Prinn, R.G., J. Huang, R.F. Weiss, D.M. Cunnold, P.J. Fraser, P.G. Simmonds, A. McCulloch, C. Harth, S. Reimann, P. Salameh, S. O'Doherty, R.H.J. Wang, L.W. Porter, B.R. Miller, and P.B. Krummel, Evidence for variability of atmospheric hydroxyl radicals over the past quarter century, *Geophys. Res. Lett.*, *32*, L07809, doi: 10.1029/2004GL022228, 2005.

Punge, H.J., and M.A. Giorgetta, Net effect of the QBO in a chemistry climate model, *Atmos. Chem. Phys.*, *8* (21), 6505-6525, 2008.

Radko, T., and J. Marshall, Equilibration of a warm pumped lens on a β plane, *J. Phys. Oceanogr.*, *33* (4), 885-899, 2003.

Ramaswamy, V., M.L. Chanin, J. Angell, J. Barnett, D. Gaffen, M. Gelman, P. Keckhut, Y. Koshelkov, K. Labitzke, J.J.R. Lin, A. O'Neill, J. Nash, W. Randel, R. Rood, K. Shine, M. Shiotani, and R. Swinbank, Stratospheric temperature trends: Observations and model simulations, *Rev. Geophys.*, *39* (1), 71-122, 2001.

Ramaswamy, V., M.D. Schwarzkopf, W.J. Randel, B.D. Santer, B.J. Soden, and G.L. Stenchikov, Anthropogenic and natural influences in the evolution of lower stratospheric cooling, *Science*, *311* (5764), 1138-1141, 2006.

Randel, W.J., Variability and trends in stratospheric temperature and water vapor, in *The Stratosphere: Dynamics, Transport and Chemistry*, A Festschrift to Celebrate Alan Plumb's 60th Birthday, American Geophysical Union, in press, 2010.

Randel, W.J., and F. Wu, Biases in stratospheric and tropospheric temperature trends derived from historical radiosonde data, *J. Clim.*, *19* (10), 2094-2104, 2006.

Randel, W.J., and F. Wu, A stratospheric ozone profile data set for 1979–2005: Variability, trends, and comparisons with column ozone data, *J. Geophys. Res.*, *112*, D06313, doi: 10.1029/2006JD007339, 2007.

Randel, W.J., F. Wu, S.J. Oltmans, K. Rosenlof, and G.E. Nedoluha, Interannual changes of stratospheric water vapor and correlations with tropical tropopause temperatures, *J. Atmos. Sci.*, *61* (17), 2133-2148, 2004.

Randel, W.J., F. Wu, H. Vömel, G.E. Nedoluha, and P. Forster, Decreases in stratospheric water vapor after 2001: Links to changes in the tropical tropopause and the Brewer-Dobson circulation, *J. Geophys. Res.*, *111*, D12312, doi: 10.1029/2005JD006744, 2006.

Randel, W.J., K.P. Shine, J. Austin, J. Barnett, C. Claud, N.P. Gillett, P. Keckhut, U. Langematz, R. Lin, C. Long, C. Mears, A. Miller, J. Nash, D.J. Seidel, D.W.J. Thompson, F. Wu, and S. Yoden, An update of observed stratospheric temperature trends, *J. Geophys. Res.*, *114*, D02107, doi: 10.1029/2008JD010421, 2009.

Rao, V.B., A.M.C. do Carmo, and S.H. Franchito, Interannual variations of storm tracks in the Southern Hemisphere and their connections with the Antarctic oscillation, *Int. J. Climatol.*, *23* (12), 1537-1545, doi: 10.1002/joc.948, 2003.

Rayner, N.A., D.E. Parker, E.B. Horton, C.K. Folland, L.V. Alexander, D.P. Rowell, E.C. Kent, and A. Kaplan, Global analyses of sea surface temperature, sea ice, and night marine air temperature since the late nineteenth century, *J. Geophys. Res.*, *108*, 4407, doi: 10.1029/2002JD002670, 2003.

Reed, R.J., and C.L. Vleck, The annual temperature variation in the lower tropical stratosphere, *J. Atmos. Sci.*, *26* (1), 163-167, 1969.

Reichler, T., Changes in the atmospheric circulation as indicator of climate change, in *Climate Change: Observed Impacts on Planet Earth*, edited by T. M. Letcher, Elsevier BV, The Netherlands, ISBN: 978-0-444-53301-2, pp. 145-164, 2009.

Renwick, J., and D. Thompson, The Southern Annular Mode and New Zealand climate, *Water Atmos.*, *14* (2), 24-25, 2006.

Rind, D., D. Shindell, P. Lonergan, and N.K. Balachandran, Climate change and the middle atmosphere. Part III: The doubled CO_2 climate revisited, *J. Clim.* *11* (5), 876-894, 1998.

Rind, D., J. Lean, J. Lerner, P. Lonergan, and A. Leboissitier, Exploring the stratospheric/tropospheric response to solar forcing, *J. Geophys. Res.*, *113*, D24103, doi: 10.1029/2008JD010114, 2008.

Ring, M.J., and R.A. Plumb, The response of a simplified GCM to axisymmetric forcings: Applicability of the fluctuation–dissipation theorem, *J. Atmos. Sci.*, *65* (12), 3880-3898, 2008.

Robock, A., Volcanic eruptions and climate, *Rev. Geophys.*, *38* (2), 191-219, 2000.

Rohs, S., C. Schiller, M. Riese, A. Engel, U. Schmidt, T. Wetter, I. Levin, T. Nakazawa, and S. Aoki, Long-term changes of methane and hydrogen in the stratosphere in the period 1978-2003 and their impact on the abundance of stratospheric water vapor, *J. Geophys. Res.*, *111*, D14315, doi: 10.1029/2005JD006877, 2006.

Rosenlof, K.H., Transport changes inferred from HALOE water and methane measurements, *J. Meteorol. Soc. Japan*, *80* (48), 831-848, 2002.

Rosenlof, K.H., and J.R. Holton, Estimates of the stratospheric residual circulation using the downward control principle, *J. Geophys. Res.*, *98* (D6), 10465-10479, 1993.

Rosenlof, K.H., and G.C. Reid, Trends in the temperature and water vapor content of the tropical lower stratosphere: Sea surface connection, *J. Geophys. Res.*, *113*, D06107, doi: 10.1029/2007JD009109, 2008.

Rosenlof, K.H., S.J. Oltmans, D. Kley, J.M. Russell III, E.-W Chiou, W.P. Chu, D.G. Johnson, K.K. Kelly, H.A. Michelsen, G.E. Nedoluha, E.E. Remsberg, G.C. Toon, and M.P. McCormick, Stratospheric water vapor increases over the past half-century, *Geophys. Res. Lett.*, *28* (7), 1195-1198, 2001.

Roy, I., and J.D. Haigh, Solar cycle signals in sea level pressure and sea surface temperature, *Atmos. Chem. & Phys.*, *10*, 3147-3153, 2010.

Russell, J.L, K.W. Dixon, A. Gnanadesikan, R.J. Stouffer, and J.R. Toggweiler, The Southern Hemisphere westerlies in a warming world: Propping open the door to the deep ocean, *J. Clim.*, *19* (24), 6382-6390, doi: 10.1175/JCLI3984.1, 2006.

Santer, B.D., M.F. Wehner, T.M.L. Wigley, R. Sausen, G.A. Meehl, K.E. Taylor, C. Ammann, J. Arblaster, W.M. Washington, J.S. Boyle, and W. Brüggemann, Contributions of anthropogenic and natural forcing to recent tropopause height changes, *Science*, *301* (5632), 479-483, doi: 10.1126/science.1084123, 2003.

Scaife, A.A., N. Butchart, C.D. Warner, D. Stainforth, W. Norton, and J. Austin, Realistic quasi-biennial

oscillations in a simulation of the global climate, *Geophys. Res. Lett.*, *27* (21), 3481-3484, 2000a.

Scaife, A.A., J. Austin, N. Butchart, S. Pawson, M. Keil, J. Nash, and I.N. James, Seasonal and interannual variability of the stratosphere diagnosed from UKMO TOVS analyses, *Quart. J. Roy. Meteorol. Soc.*, *126* (568), 2585-2604, 2000b.

Scaife, A.A., N. Butchart, D.R. Jackson, and R. Swinbank, Can changes in ENSO activity help to explain increasing stratospheric water vapor?, *Geophys. Res. Lett.*, *30*, 1880, doi: 10.1029/2003GL017591, 2003.

Scherer, M., H. Vömel, S. Fueglistaler, S.J. Oltmans, and J. Staehelin, Trends and variability of midlatitude stratospheric water vapour deduced from the re-evaluated Boulder balloon series and HALOE, *Atmos. Chem. Phys.*, *8*, 1391-1402, 2008.

Schiller, C., J.-U. Grooß, P. Konopka, F. Plöger, F.H. Silva dos Santos, and N. Spelten, Hydration and dehydration at the tropical tropopause, *Atmos. Chem. Phys*., *9*, 9647-9660, doi: 10.5194/acp-9-9647-2009, 2009.

Schultz, M.G., T. Diehl, G.P. Brasseur, and W. Zittel, Air pollution and climate forcing impacts of a global hydrogen economy, *Science*, *302* (5645), 624-627, doi: 10.1126/science.1089527, 2003.

Schwarzkopf, M.D., and V. Ramaswamy, Evolution of stratospheric temperature in the 20th century, *Geophys. Res. Lett.*, *35*, L03705, doi: 10.1029/2007GL032489, 2008.

Scinocca, J.F., M.C. Reader, D.A. Plummer, M. Sigmond, P.J. Kushner, T.G. Shepherd, and A.R. Ravishankara, Impact of sudden Arctic sea-ice loss on stratospheric polar ozone recovery, *Geophys. Res. Lett.*, *36*, L24701, doi: 10.1029/2009GL041239, 2009.

Screen, J.A., N.P. Gillett, D.P. Stevens, G.J. Marshall, and H.K. Roscoe, The role of eddies in the Southern Ocean temperature response to the Southern Annular Mode, *J. Clim.*, *22* (3), 806-818, doi: 10.1175/2008JCLI2416.1, 2009.

Seager, R., M. Ting, I. Held, Y. Kushnir, J. Lu, G. Vecchi, H.P. Huang, N. Harnik, A. Leetmaa, N.C. Lau, C. Li, J. Velez and N. Naik, Model projections of an imminent transition to a more arid climate in Southwestern North America, *Science*, *316* (5828), 1181-1184, doi: 10.1126/science.1139601, 2007.

Seidel, D.J., and J.R. Lanzante, An assessment of three alternatives to linear trends for characterizing global atmospheric temperature changes, *J. Geophys. Res.*, *109*, D14108, doi: 10.1029/2003JD004414, 2004.

Seidel, D.J., and W.J. Randel, Variability and trends in the global tropopause estimated from radiosonde data, *J. Geophys. Res.*, *111*, D21101, doi: 10.1029/2006JD007363, 2006.

Seidel, D.J., and W.J. Randel, Recent widening of the tropical belt: Evidence from tropopause observations, *J. Geophys. Res.*, *112*, D20113, doi: 10.1029/2007JD008861, 2007.

Seidel, D.J., Q. Fu, W.J. Randel, and T.J. Reichler, Widening of the tropical belt in a changing climate, *Nature Geosci.*, *1*, 21-24, doi: 10.1038/nego.2007.38, 2008.

Seidel, D.J., F.H. Berger, H.J. Diamond, J. Dykema, D. Goodrich, F. Immler, W. Murray, T. Peterson, D. Sisterson, M. Sommer, P. Thorne, H. Vömel, and J. Wang, Reference upper-air observations for climate: Rationale, progress, and plans, *Bull. Amer. Meteorol. Soc.*, *90* (3), 361-369, doi: 10.1175/2008BAMS2540.1, 2009.

Semeniuk, K., and T.G. Shepherd, Mechanism for tropical upwelling in the stratosphere, *J. Atmos. Sci.*, *58* (21), 3097-3115, 2001.

Shepherd, T.G., and A.I. Jonsson, On the attribution of stratospheric ozone and temperature changes to changes in ozone-depleting substances and well mixed greenhouse gases, *Atmos. Chem. Phys.*, *8* (5), 1435-1444, 2008.

Sherwood, S., A microphysical connection among biomass burning, cumulus clouds, and stratospheric moisture, *Science*, *295* (5558), 1272-1275, doi: 10.1126/science.1065080, 2002.

Sherwood, S.C., J.R. Lanzante, and C. Meyer, Radiosonde daytime biases and late-20th century warming, *Science*, *309* (5740), 1556-1559, doi: 10.1126/science.1115640, 2005.

Sherwood, S.C., C.L. Meyer, R.J. Allen, and H.A. Titchner, Robust tropospheric warming revealed by iteratively homogenized radiosonde data, *J. Clim.*, *21* (20), 5336-5352, doi: 10.1175/2008JCLI2320.1, 2008.

Shindell, D.T., Climate and ozone response to increased stratospheric water vapor, *Geophys. Res. Lett.*, *28* (8), 1551-1554, 2001.

Shindell, D.T., and V. Grewe, Separating the influence of halogen and climate changes on ozone recovery in the upper stratosphere, *J. Geophys. Res*., *107*, doi: 10.1029/2001JD000420, 2002.

Shindell, D., and G.A. Schmidt, Southern Hemisphere climate response to ozone changes and greenhouse gas increases, *Geophys. Res. Lett.*, *31*, L18209, doi: 10.1029/2004GL020724, 2004.

Shindell, D.T., D. Rind, N. Balachandran, J. Lean, and P. Lonergan, Solar cycle variability, ozone, and climate, *Science*, *284* (5412), 305-308, 1999.

Shindell, D.T., G.A. Schmidt, M.E. Mann, and G. Faluvegi, Dynamic winter climate response to large tropical volcanic eruptions since 1600, *J. Geophys. Res.*, *109*, D05104, doi: 10.1029/2003JD004151, 2004.

Shindell, D.T., G. Faluvegi, R.L. Miller, G.A. Schmidt,

J.E. Hansen, and S. Sun, Solar and anthropogenic forcing of tropical hydrology, *Geophys. Res. Lett*, *33*, L24706, doi: 10.1029/2006GL027468, 2006.

Shine, K.P., M.S. Bourqui, P.M.F. Forster, S.H.E. Hare, U. Langematz, P. Braesicke, V. Grewe, M. Ponater, C. Schnadt, C.A. Smith, J.D. Haigh, J. Austin, N. Butchart, D.T. Shindell, W.J. Randel, T. Nagashima, R.W. Portmann, S. Solomon, D.J. Seidel, J. Lanzante, S. Klein, V. Ramaswamy, and M.D. Schwarzkopf, A comparison of model-simulated trends in stratospheric temperatures, *Quart. J. Roy. Meteorol. Soc.*, *129* (590), 1565-1588, 2003.

Shine, K.P., J.J. Barnett, and W.J. Randel, Temperature trends derived from Stratospheric Sounding Unit radiances: The effect of increasing CO_2 on the weighting function, *Geophys. Res. Lett.*, *35*, L02710, doi: 10.1029/2007GL032218, 2008.

Sigmond, M., J.C. Fyfe, and J.F. Scinocca, Does the ocean impact the atmospheric response to stratospheric ozone depletion?, *Geophys. Res. Lett.*, *37*, L12706, doi: 10.1029/2010GL043773, 2010.

Simmonds, I., and K. Keay, Variability of Southern Hemisphere extratropical cyclone behavior, 1958–97, *J. Clim.*, *13* (3), 550-561, 2000.

Simpson, I.R., M. Blackburn, and J.D. Haigh, The role of eddies in driving the tropospheric response to stratospheric heating perturbations, *J. Atmos. Sci.*, *66* (5), 1347-1365, doi: 10.1175/2008JAS2758.1, 2009.

Solomon, S., R.W. Portmann, and D.W.J. Thompson, Contrasts between Antarctic and Arctic ozone depletion, *Proc. Natl. Acad. Sci.*, *104* (2), 445-449, doi: 10.1073/pnas.0604895104, 2007.

Solomon, S., K.H. Rosenlof, R.W. Portmann, J.S. Daniel, S.M. Davis, T.J. Sanford, and G.-K. Plattner, Contributions of stratospheric water vapor to decadal changes in the rate of global warming, *Science*, *327* (5970), 1219-1223, doi: 10.1126/science.1182488, 2010.

Son, S.-W., L.M. Polvani, D.W. Waugh, H. Akiyoshi, R. Garcia, D. Kinnison, S. Pawson, E. Rozanov, T.G. Shepherd, and K. Shibata, The impact of stratospheric ozone recovery on the Southern Hemisphere westerly jet, *Science*, *320* (5882), 1486-1489, doi: 10.1126/science.1155939, 2008.

Son, S.-W., L.M. Polvani, D.W. Waugh, T. Birner, H. Akiyoshi, R.R. Garcia, A. Gettelman, D.A. Plummer, and E. Rozanov, The impact of stratospheric ozone recovery on tropopause height trends, *J. Clim.*, *22* (2), 429-445, doi: 10.1175/2008JCLI2215.1, 2009a.

Son, S.-W., N.F. Tandon, L.M. Polvani, and D.W. Waugh, Ozone hole and Southern Hemisphere climate change, *Geophys. Res. Lett.*, *36*, L15705, doi: 10.1029/2009GL038671, 2009b.

Son, S.-W., E.P. Gerber, J. Perlwitz, L.M. Polvani, N.P. Gillett, K.-H. Seo, V. Eyring, T.G. Shepherd, D. Waugh, H. Akiyoshi, J. Austin, A. Baumgaertner, S. Bekki, P. Braesicke, C. Brühl, N. Butchart, M.P. Chipperfield, D. Cugnet, M. Dameris, S. Dhomse, S. Frith, H, Garny, R. Garcia, S.C. Hardiman, P. Jöckel, J.F. Lamarque, E. Mancini, M. Marchand, M. Michou, T. Nakamura, O. Morgenstern, G. Pitari, D.A. Plummer, J. Pyle, E. Rozanov, J.F. Scinocca, K. Shibata, D. Smale, H. Teyssèdre, W. Tian, and Y. Yamashita, Impact of stratospheric ozone on Southern Hemisphere circulation change: A multimodel assessment, *J. Geophys. Res.*, *115*, D00M07, doi: 10.1029/2010JD014271, 2010.

Song, Y., and W.A. Robinson, Dynamical mechanisms for stratospheric influences on the troposphere, *J. Atmos. Sci*., *61* (14), 1711-1725, 2004.

Soukharev, B.E., and L.L. Hood, Solar cycle variation of stratospheric ozone: Multiple regression analysis of long-term satellite data sets and comparisons with models, *J. Geophys. Res*., *111*, D20314, doi: 10.1029/2006JD007107, 2006.

SPARC (Stratospheric Processes And their Role in Climate), *SPARC Assessment of Stratospheric Aerosol Properties*, edited by L. Thomason, and Th. Peter, World Climate Research Progam Report 124, SPARC Report 4, WMO/TD-No. 1295, 346 pp., Verrières le Buisson, France, 2006.

SPARC CCMVal, *SPARC Report on the Evaluation of Chemistry-Climate Models*, edited by V. Eyring, T.G. Shepherd, and D.W. Waugh, Stratospheric Processes And their Role in Climate (SPARC) Report No. 5, WCRP-132, WMO/TD-No. 1526, available: http://www.atmosp.physics.utoronto.ca/SPARC, 2010.

Sprintall, J., Long-term trends and interannual variability of temperature in Drake Passage, *Prog. Ocean.*, *77* (4), 316-330, doi: 10.1016/j.pocean.2006.06.004, 2008.

Steig, E.J., D.P. Schneider, S.D. Rutherford, M.E. Mann, J.C. Comiso, and D.T. Shindell, Warming of the Antarctic ice sheet surface since the 1957 International Geophysical Year, *Nature*, *457*, 459-462, doi: 10.1038/nature07669, 2009.

Stenchikov, G., K. Hamilton, R.J. Stouffer, A. Robock, V. Ramaswamy, B. Santer, and H.-F. Graf, Arctic Oscillation response to volcanic eruptions in the IPCC AR4 climate models, *J. Geophys. Res.*, *111*, D07107, doi: 10.1029/2005JD006286, 2006.

Stenchikov, G., T.L. Delworth, V. Ramaswamy, R.J. Stouffer, A. Wittenberg, and F. Zeng, Volcanic signals in oceans, *J. Geophys. Res.*, *114*, D16104, doi: 10.1029/2008JD011673, 2009.

Stevenson, D.S., F.J. Dentener, M.G. Schultz, K. Ellingsen, T.P.C. vanNoije, O. Wild, G. Zeng, M. Anann, C.S. Atherton, N. Bell, D.J. Bergmann, I. Bey,

T. Butler, J. Cofala, W.J. Collins, R.G. Derwent, R.M. Doherty, J. Drevet, H.J. Eskes, A.F. Fiore, M. Gauss, D.A. Hauglustaine, L.W. Horowitz, I.S.A. Isaksen, M.C. Krol, J.-F. Lamarque, M.G. Lawrence, V. Montanaro, J.-F. Müller, G. Pitari, M.J. Prather, S.A. Pyle, S. Rast, J.M. Rodriguez, M.G. Sanderson, H.H. Savage, D.T. Shindell, S.E. Strahan, K. Sudo, and S. Szopa, Multi-model ensemble of present-day and near-future tropospheric ozone, *J. Geophys. Res.*, *111*, D8301, doi: 10.1029/2005JD006338, 2006.

Stolarski, R.S., A.R. Douglass, P.A. Newman, S. Pawson, and M.R. Schoeberl, Relative contribution of greenhouse gases and ozone-depleting substances to temperature trends in the stratosphere: A chemistry-climate model study, *J. Clim.*, *23* (1), 28-42, doi: 10.1175/2009JCLI2955.1, 2010.

Sudo, K., M. Takahashi, and H. Akimoto, Future changes in stratosphere-troposphere exchange and their impacts on future tropospheric ozone simulations, *Geophys. Res. Lett.*, *30* (24), 2256, doi: 10.1029/2003GL018526, 2003.

Takahashi, M., Simulation of the Quasi-Biennial Oscillation in a general circulation model, *Geophys. Res. Lett.*, *26* (9), 1307-1310, 1999.

Terao, Y., J.A. Logan, A.R. Douglass, and R.S. Stolarski, Contribution of stratospheric ozone to the interannual variability of tropospheric ozone in the northern extratropics, *J. Geophys. Res.*, *113*, D18309, doi: 10.1029/2008JD009854, 2008.

Thejll, P., B. Christiansen, and H. Gleisner, On correlations between the North Atlantic Oscillation, geopotential heights, and geomagnetic activity, *Geophys. Res. Lett.*, *30*, 1347, doi: 10.1029/2002GL016598, 2003.

Thomason, L., L.R. Poole, and T. Deshler, A global climatology of stratospheric aerosol surface area density deduced from Stratospheric Aerosol and Gas Experiment II measurements: 1984-1994, *J. Geophys. Res.*, *102* (D7), 8967-8976, 1997.

Thompson, D.W.J., and J.M. Wallace, Annular modes in the extratropical circulation. Part I: Month-to-month variability, *J. Clim.*, *13* (5), 1000-1016, 2000.

Thompson, D.W.J., and S. Solomon, Interpretation of recent Southern Hemisphere climate change, *Science*, *296* (5569), 895-899, 2002.

Thompson, D.W.J., and S. Solomon, Recent stratospheric climate trends as evidenced in radiosonde data: Global structure and tropospheric linkages, *J. Clim.*, *18* (22), 4785-4795, 2005.

Thompson, D.W.J., and S. Solomon, Understanding recent stratospheric climate change, *J. Clim.*, *22* (8), 1934-1943, doi: 10.1175/2008JCLI2482.1, 2009.

Thompson, D.W.J., J.C. Furtado, and T.G. Shepherd, On the tropospheric response to anomalous stratospheric wave drag and radiative heating, *J. Atmos. Sci.*, *63* (10), 2616-2629, 2006.

Thorne, P.W. (editor), Global climate, Chapter 2 in *State of the Climate 2008*, edited by T.C. Peterson and M.O. Baringer, Special Supplement to *Bull. Amer. Meteorol. Soc.*, *90* (8), 196 pp., 2009.

Thorne, P.W., D.E. Parker, S.F.B. Tett, P.D. Jones, M. McCarthy, H. Coleman, and P. Brohan, Revisiting radiosonde upper air temperatures from 1958 to 2002, *J. Geophys. Res.*, *110*, D18105, doi: 10.1029/2004JD005753, 2005.

Tian, W.S., M.P. Chipperfield, and D. Lu , Impact of increasing stratospheric water vapor on ozone depletion and temperature change, *Adv. Atmos. Sci.*, *26* (3), 423-437, doi: 10.1007/s00376-009-0423-3, 2009.

Tie, X.X., and G. Brasseur, The response of stratospheric ozone to volcanic eruptions: Sensitivity to atmospheric chlorine loading, *Geophys. Res. Lett.*, *22* (22), 3035-3038, 1995.

Tromp, T.K., R.-L. Shia, M. Allen, J.M. Eiler, and Y.L. Yung, Potential environmental impact of a hydrogen economy on the stratosphere, *Science*, *300* (5626), 1740-1742, doi: 10.1126/science.1085169, 2003.

Turner, J., S.R. Colwell, G.J. Marshall, T.A. Lachlan-Cope, A.M. Carleton, P.D. Jones, V. Lagun, P.A. Reid, and S. Iagovkina, Antarctic climate change during the last 50 years, *Int. J. Climatol.*, *25* (3), 279-294, doi: 10.1002/joc.1130, 2005.

Turner, J., J.C. Comiso, G.J. Marshall, T.A. Lachlan-Cope, T. Bracegirdle, T. Maksym, M.P. Meredith, Z. Wang, and A. Orr, Non-annular atmospheric circulation change induced by stratospheric ozone depletion and its role in the recent increase of Antarctic sea ice extent, *Geophys. Res. Lett.*, *36*, L08502, doi: 10.1029/2009GL037524, 2009.

Udagawa, Y., Y. Tachibana, and K. Yamazaki, Modulation in interannual sea ice patterns in the Southern Ocean in association with large-scale atmospheric mode shift, *J. Geophys. Res.*, *114*, D21103, doi: 10.1029/2009JD011807, 2009.

Ueyama, R., and J.M. Wallace, To what extent does high-latitude wave forcing drive tropical upwelling in the Brewer-Dobson Circulation?, *J. Atmos. Sci.*, *67* (4), 1232-1246, doi: 10.1175/2009JAS3216.1, 2010.

Ummenhofer, C.C., A. Sen Gupta, and M.H. England, Causes of late twentieth-century trends in New Zealand precipitation, *J. Clim.*, *22* (1), 3-19, doi: 10.1175/2008JCLI2323.1, 2009.

van Loon, H., and G.A. Meehl, The response in the Pacific to the sun's decadal peaks and contrasts to cold events in the Southern Oscillation, *J. Atmos. Solar Terr. Phys.*, *70* (7), 1046-1055, doi: 10.1016/j.jastp.2008.01.009, 2008.

van Loon, H., G.A. Meehl, and D. Shea, Coupled air-sea

response to solar forcing in the Pacific region during northern winter, *J. Geophys. Res*., *112*, D02108, doi: 10.1029/2006JD007378, 2007.

Velders, G.J.M., S.O. Andersen, J.S. Daniel, D.W. Fahey, and M. McFarland, The importance of the Montreal Protocol in protecting climate, *Proc. Natl. Acad. Sci.*, *104* (12), 4814-4819, doi: 10.1073/pnas.0610328104, 2007.

Vera, C., Interannual and interdecadal variability of atmospheric synoptic-scale activity in the Southern Hemisphere, *J. Geophys. Res.*, *108*, 8077, doi: 10.1029/2000JC000406, 2003.

Vernier, J.P., J.P. Pommereau, A. Garnier, J. Pelon, N. Larsen, J. Nielsen, T. Christensen, F. Cairo, L.W. Thomason, T. Leblanc, and I.S. McDermid, Tropical stratospheric aerosol layer from CALIPSO lidar observations, *J. Geophys. Res.*, *114*, D00H10, doi: 10.1029/2009JD011946, 2009.

Vömel, H., D.E. David, and K. Smith, Accuracy of tropospheric and stratospheric water vapor measurements by the cryogenic frost point hygrometer: Instrumental details and observations, *J. Geophys. Res.*, *112*, D08305, doi: 10.1029/2006JD007224, 2007.

Waugh, D., W. Randel, S. Pawson, P. Newman, and E. Nash, Persistence of the lower stratospheric polar vortices, *J. Geophys. Res.*, *104* (D22), 27191-27201, 1999.

Waugh, D.W., L. Oman, P.A. Newman, R.S. Stolarski, S. Pawson, J.E. Nielsen, and J. Perlwitz, Effect of zonal asymmetries in stratospheric ozone on simulated Southern Hemisphere climate trends, *Geophys. Res. Lett*., *36*, L18701, doi: 10.1029/2009GL040419, 2009.

Weinstock, E.M., J.B. Smith, D.S. Sayres, J.V. Pittman, J.R. Spackman, E.J. Hintsa, T.F. Hanisco, E.J. Moyer, J.M. St. Clair, M.R. Sargent, and J.G. Anderson, Validation of the Harvard Lyman-α in situ water vapor instrument: Implications for the mechanisms that control stratospheric water vapor, *J. Geophys. Res.*, *114*, D23301, doi: 10.1029/2009JD012427, 2009.

Weisenstein, D., G. Yue, M. Ko, N.-D. Sze, J. Rodriguez, and C. Scott, A two-dimensional model of sulfur species and aerosols, *J. Geophys. Res.*, *102* (D11), 13019-13035, 1997.

Wetzel, P., A. Winguth, and E. Maier-Reimer, Sea-to-air CO_2 flux from 1948 to 2003: A model study, *Global Biogeochem. Cycles*, *19*, GB2005, doi: 10.1029/2004GB002339, 2005.

White W.B., and Z. Liu, Non-linear alignment of El Niño to the 11-yr solar cycle, *Geophys. Res. Lett.*, *35*, L19607, doi: 10.1029/2008GL034831, 2008.

Wild, O., Modelling the global tropospheric ozone budget: Exploring the variability in current models, *Atmos. Chem. Phys.*, *7* (10), 2643-2660, doi: 10.5194/acp-7-2643-2007, 2007.

Woollings, T., Vertical structure of anthropogenic zonal-mean atmospheric circulation change, *Geophys. Res. Lett.*, *35*, L19702, doi: 10.1029/2008GL034883, 2008.

WMO (World Meteorological Organization), *Scientific Assessment of Ozone Depletion: 2002*, Global Ozone Research and Monitoring Project–Report No. 47, 498 pp., Geneva, Switzerland, 2003.

WMO (World Meteorological Organization), *Scientific Assessment of Ozone Depletion: 2006*, Global Ozone Research and Monitoring Project–Report No. 50, 572 pp., Geneva, Switzerland, 2007.

Wu, S., L.J. Mickley, D.J. Jacob, J.A. Logan, R.M. Yantosca, and D. Rind, Why are there large differences between models in global budgets of tropospheric ozone?, *J. Geophys. Res.*, *112*, D05302, doi: 10.1029/2006JD007801, 2007.

Yin, J.H., A consistent poleward shift of the storm tracks in simulations of 21st century climate, *Geophys. Res. Lett.*, *32*, L18701, doi: 10.1029/2005GL023684, 2005.

Zazulie, N., M. Rusticucci, and S. Solomon, Changes in climate at high southern latitudes: A unique daily record at Orcadas spanning 1903-2008, *J. Clim.*, *23*, 189-196, doi: 10.1175/2009JCLI3074.1, 2010.

Zeng, G., and J.A. Pyle, Changes in tropospheric ozone between 2000 and 2100 modeled in a chemistry-climate model, *Geophys. Res. Lett.*, *30* (7), 1392, doi: 10.1029/2002GL016708, 2003.

Zeng, G., J.A. Pyle, and P.J. Young, Impact of climate change on tropospheric ozone and its global budgets, *Atmos. Chem. Phys.*, *8*, 369-387, 2008.

Zhang, J., Increasing Antarctic sea ice under warming atmospheric and oceanic conditions, *J. Clim.*, *20* (11), doi: 10.1175/JCLI4136.1, 2007.

Zhou, J., and K.-K.Tung, Solar cycles in 150 years of global sea-surface temperature data, *J. Clim.*, *23* (12), 3234-3248, doi: 10.1175/2010JCLI3232.1, 2010.

Zhou, S., M.E. Gelman, A.J. Miller, and J.P. McCormack, An inter-hemisphere comparison of the persistent stratospheric polar vortex, *Geophys. Res. Lett.*, *27* (8), 1123-1126, 2000.

Zhou, T., M.A. Geller, and K. Hamilton, The roles of the Hadley Circulation and downward control in tropical upwelling. *J. Atmos. Sci.*, *63* (11), 2740-2757, 2006.

Zhou, X.-L., M.A. Geller, and M. Zhang, Cooling trend of the tropical cold point tropopause temperatures and its implications, *J. Geophys. Res.*, *106* (D2), 1511-1522, 2001.

Zickfeld, K., J.C. Fyfe, M. Eby, and A.J. Weaver, Comment on "Saturation of the southern ocean CO_2 sink due to recent climate change," *Science*, *319* (5863), 570, doi: 10.1126/science.1146886, 2008.

Zou, C.-Z., M. Gao, and M.D. Goldberg, Error structure and atmospheric temperature trends in observations from the Microwave Sounding Unit, *J. Clim*., *22* (7), 1661-1681, doi: 10.1175/2008JCLI2233.1, 2009.